ABSTRACT

SU, YA-TING. A Systematic Investigation of the Factors that Trigger Thermal Degradation During the Processing of Industrially-Relevant Polymers. (Under the direction of Dr. Russell Gorga and Dr. Melissa Pasquinelli).

Thermal degradation impacted by the presence of oxygen and other impurities as well as the processing conditions has been an issue that needs to be diminished during the formation of polymer products. It not only impacts the physical and mechanical properties of the products, but also often leads to the failure of production lines. An understanding of the molecular mechanisms that underlie thermal degradation can thus lead to the production of polymer materials with enhanced properties and can minimize a waste of resources during production. Two model systems will be used: polypropylene (PP) and polyethylene (PE), in both single and core-sheath bicomponent fiber geometries. The role of thermodynamics on the thermal degradation of polymer systems, including temperature, time, and pressure will be identified. The effects of its local environment, such as the presence of oxygen, water, additives, crystal domains, or impurities will be investigated. Computational simulations will be used to predict potentially hazardous products under particular processing conditions and validate the experimental findings.

A Systematic Investigation of the Factors that Trigger Thermal Degradation During the Processing of Industrially-Relevant Polymers.

by

Ya-Ting Su

A dissertation submitted to the Graduate Faculty of
North Carolina State University
in partial fulfillment of the
requirements for the degree of
Doctor of Philosophy

Fiber and Polymer Science

Raleigh, North Carolina

2015

APPROVED BY:

_____	_____
Russell Gorga Committee co-Chair	Melissa Pasquinelli Committee co-Chair
_____	_____
Behnam Pourdeyhimi	Richard Spontak
_____	
Yaroslava Yingling	

BIOGRAPHY

Ya-Ting Su was born in Kaohsiung, Taiwan 1983. She received her Bachelor's degree in 2005 and Master's degree in 2008, both in Chemical Engineering from National Tsing Hua University. She also did one year research regarding molecular dynamics simulations in the Department of Material Science and Engineering at University Florida. After that, she worked for DuPont Taiwan as an RD engineer for two years. She then received the six sigma green belt after training by performing a research project. She later began her study in the College of Textile of North Carolina State University. Her research focused on thermal degradation of industrial-relevant polymers, bicomponent fibers using both experiments and computational simulations.

ACKNOWLEDGMENTS

I would like to express my great appreciation to my advisors, Dr. Melissa Pasquinelli and Dr. Russell Gorga, who gave me their valuable suggestions and always very supportive on my research. You have been awesome mentors and excellent friends for me. Your advice on both research and career have been priceless for me. I would like to thank my committee members, Dr. Behnam Pourdeyhimi, Dr. Richard Spontak and Dr. Yaroslava Yingling, for your valuable suggestions and insightful comments. I also acknowledge the financial support from the Nonwoven Institute grant number 12-138. The technical supports from the Nonwoven Institute especially the fiber spinning lab led by William Barnes and analytical lab led by Amy Minton are highly appreciated. I also would like to thank the industrial advisors, Dr. Carl Wust from FiberVisions, Dr. Jackie Degroot from Dow Chemical, Ms. Pamela Lawler from BASF, Mr. Logan Hanner from BASF, Dr. Thomas Broth-Nielsen from Fibertex Personal Care, Dr. Barry Wyerman from Janesville Acoustics, Dr. Richard Campbell from Braskem Americas and Dr. Nagendra Anantharamaiah from H&V. You did a fantastic job helping me overcome the difficulties by providing brilliant suggestions and crucial technical supports. I would especially like to thank students from Dr. Gorga's lab, Dr. Pasquinelli's lab and the Nonwoven Institute for the company, discussions and support. I am grateful to Charles Mooney for his help with the SEM. A special thanks to my family and friends who expressed your confidence on me, relieved my anxiety and pushed me to pursue my goal. At the end, I would like to express my appreciation to my beloved husband Chung-Nan and my precious daughter Iris who have been very patient and supportive all the time.

TABLE OF CONTENTS

LIST OF TABLES

LIST OF FIGURES

Chapter 1: Introduction

1.1. Overview of objectives

The properties of fibers greatly depend on the processing conditions. For a period of time during the fiber spinning process before being coagulated into fibers, polymers can experience temperatures that are higher than their melting temperature, thus limiting the degree of thermal degradation during fiber processing is a basic requirement, as the physical and chemical changes induced by thermal degradation are undesirable. For example, if severe thermal degradation happens during melt processing, the molecular weight of the polymer might drop too much to form a fiber. This premature failure usually causes loss by not able to produce any fiber. Once the degradation happens, there might be some by-products formed in the fiber and thus yielding a yellowing appearance. Surface appearance may also change during processing, which is not desirable. In addition, loss of mechanical properties such as tensile strength and elongation to break causes difficulties at later stages of processing and during fiber use.

The goal of this work is to develop a systematic understanding of how processing conditions and environmental conditions impact the thermal degradation of polymer fibers, thus limiting its existence during melt processing. There are many studies in the literature for individual polymers and polymer blends about the mechanisms for thermal degradations, kinetic behavior and stabilizing procedures. However, limited information is available about the thermal degradation of bicomponent fibers. During co-extrusion, the processing temperature and shear viscosity are two key parameters that need to be carefully tuned to produce the best quality fibers. Both polymers are often extruded at the same temperature, and issues can arise when one temperature is too high for one polymer and thus it can degrade while the other is just about to melt. It is possible to co-extrude at separate

temperatures, but there are still problems during coagulation. Shear viscosity is also a key process parameter that is required to be similar during fiber processing, otherwise processing difficulties might cause fiber failure.

The structure of polymer chains has been identified as the key parameter, including the differences among the polymer types, tacticity, molecular weight, molecular weight distributions and the branches types. For example, polypropylene with lower thermal stability has more side groups than polyethylene. Based on previous studies, the local environments also play an important role in thermal degradation, which indicate that oxygen can accelerate thermal degradation while the stabilizers can postpone and limit thermal degradation during melt processing. During melt processing, temperature is the most important parameter that needs to be carefully considered. Melting polymer at temperature higher than degradation temperature can cause tremendous degradation. Furthermore, other processing conditions such as time and pressure can affect thermal degradation.

Both experimental and computational approaches will be used to study thermal degradation during melt processing. So far some of the processing conditions and local environments of individual polymer has been studied and co-sheath fibers will be investigated in the future. Computational simulations will also be performed to understand the mechanisms and predict degradation products.

1.2. Current understanding of thermal degradation in thermoplastic polymers

There are many ways of processing fibers depending on the polymer nature and material process ability. [16,17] Among fiber processes for synthetic polymers, melt processing is the technique that is most frequently used. [18] During the process, the polymer chains might break or form additional bonds with other molecules. Those behaviors are typically called thermal degradation. Thermal degradation happens when the polymer is in the molten state; however, it can also

happen in unsuitable storage environments, which include excessive exposure to UV radiation, moisture and/or heat.

Polymers will encounter four stages during the melt extrusion process including feeding, melting, extruding and drawing (see Figure 1-1). [19] Polyolefin resins, such as polypropylene (PP) and polyethylene (PE) are typically stabilized with compounds to help reduce thermal and thermal oxidative degradation. Polyethylene and polypropylene are two resin types of polyolefins that are commonly used. During the feeding stage, inevitably there will be small amount of air that is trapped or dissolved in the polymer unless a nitrogen blanket is applied. The oxygen can initiate the degradation process by forming polymeric alkyl hydroperoxides with alkyl radicals. The degradation process coupled with oxygen is called thermal oxidation.

After the polymer resin is fed into the extruder, the polymer is conveyed by the screw and begins to melt as a result of the shear between the rotating screw and the barrel. [19] The barrel is heated and the temperature is set in excess of the polymer melt temperature. The high temperature necessary to melt the polymer is also responsible for the thermal degradation. Also, due to the high shear, the polymer can experience “hot spots” where the local temperature could be 50 °C higher than the set operating temperature, which increases the probability for degradation events to occur. Residence time also plays a role since increased time at extrusion temperatures will further exacerbate the degradation mechanism and induce chain cleavage into smaller and smaller fragments.

After the polymer is extruded from spinneret, the temperature of molten polymer is still higher than the melt temperature and thermal oxidation can now occur at the surface. From Carlsson, Garton and Wiles’ research, [20] blanketing the spinneret with nitrogen does not help much since most of the degradation happens in the extruder. During the drawing stage, they also found that free radicals are produced even at high draw rates and drawing temperatures lower than 180 °C.

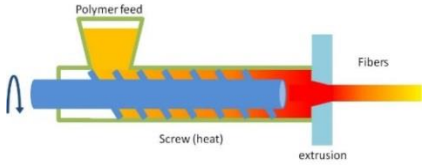

Figure 1- 1: Fiber extrusion process

Even after the fibers are produced, some degradation could occur when storage environments are not suitable (excessive exposure to UV radiation, moisture, heat, and oxygen. [21]This stage of degradation is also called aging and is beyond the scope of this work.

From previous researchers, different polymer materials can undergo different degradation mechanisms. As outlined by Beyler and Hirschler [8], the thermal degradation chemical process may involve one or more of the following reaction mechanisms: 1) random chain scission, in which chain scission happens at a random position along the polymer chain backbone; 2) chain end scission, in which chain scission happens at the end of the polymer chain; 3) chain stripping, in which atoms or side groups which are not part of the polymer backbone are broken; and 4) crosslinking in which bonds are created between neighboring polymer chains.

Thermal degradation during melt-processing is hard to prevent, and the resultant change in properties such as embrittlement and yellowing continue to be a major problem. To control degradation during fiber processing currently, the most effective way is to add a thermal stabilizer. Inert gas blanketing during extrusion and maintaining a low humidity environment will also work to limit thermal degradation.

The elements related to thermal degradation can be categorized as follows (see Figure 1-2): 1) materials (including polymer type, synthesis method, and molecular weight); 2) local environment (oxygen, impurities, additives), 3) process conditions and 4) machinery. These elements will be discussed in turn throughout the remainder of this section.

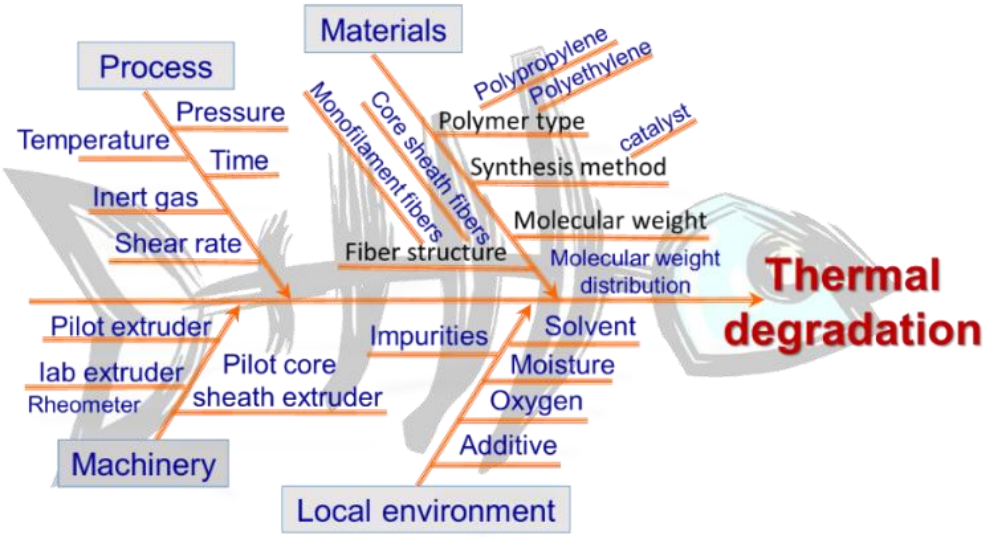

Figure 1- 2: Fishbone diagram of thermal degradation.

1.2.1. Degradations mechanisms in polyethylene and polypropylene

Because of the chemical structure and composition differences for each polymer material, the degradation profile varies. For example, the abundance tertiary carbons in polypropylene are easy to attack by free radical, thus its main mechanism from degradation is chain scission. [22-25]. Double bonds in polyethylene accelerate crosslinking process. [24,26] For polyethylene, degradation mechanism is a competition between chain scissions and crosslinking. Degradation is also a problem for multi-component process mainly because the melting temperatures of polymer are usually different. One polymer might encounter severe degradation while the other polymer just starts to melt at the given temperature. In this work, polyethylene and polypropylene are the target polymers, and their degradation behaviors are discussed.

From the chemical structure view-point, large amount of branching might decrease thermal stability. Previous studies have suggested the order of stability to be HDPE > LDPE > ethylene/propylene copolymer > polypropylene (PP), [27,28] while another studies suggested the stability order of additive-free polymers to be

HDPE > LDPE > LLDPE > polypropylene (PP) [29] Those orders show that with increasing branching, the thermal stability is lowered. For PP, there is no doubt that its stability is lower than PE because there are large amounts of tertiary carbons in the PP chains.

1.2.1.1. Polyethylene (PE)

Thermal degradation of PE was investigated in ambient air which is believed to follow the mechanism [1] shown in Figure 1-3. The initiation steps of degradation are mostly random chain scissions; once radicals are formed, a series of reactions follow, which causes significant molecular weight loss. Based on the densities, type, and branching, polyethylenes are known as high density polyethylene (HDPE), low density polyethylene (LDPE), linear low density polyethylene (LLDPE). Polyethylene can also be categorized by the polymerization method, one is Ziegler PE and the other is metallocene PE. Both the synthesis methods will generate impurities in the form of unsaturated bonds which play an important role in crosslinking and thermal oxidation during degradation. The relatively high concentration of vinyl groups in Ziegler PE suggests that crosslinking might occur during melt-process and cause damage to extruder. [24] There are also double bonds existing in metallocene PE, causing crosslinking at lower processing temperature. [1]

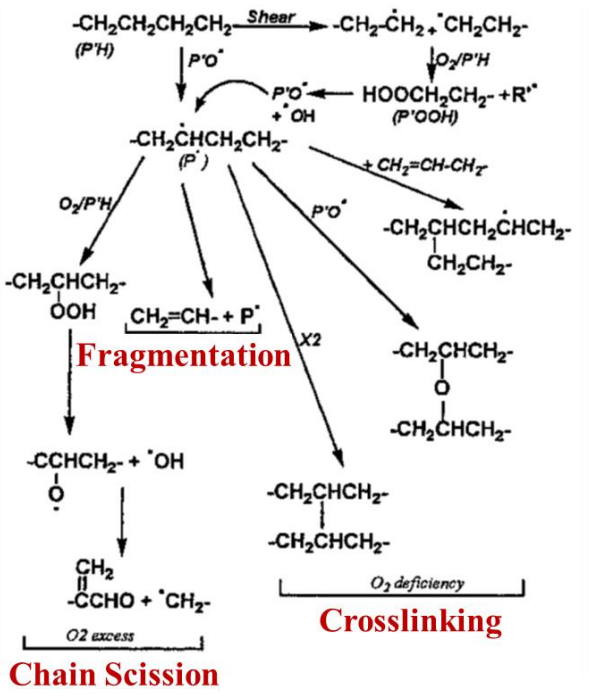

Figure 1- 3: Radical mechanism of the thermal degradation of polyethylene. Taken from Ref. [1].

Severe thermal oxidation of PE was also identified by gas chromatography and a lot of toxic products such as CO and acrolein were found during decomposition. [30] When PE undergoes thermal oxidation at 80-90 °C, more than crosslinking, chain scission occurred [2] as shown in Figure 1-4. Those chain scissions are believed to occur in the non-crystalline part and induce embrittlement. The chain scission here means larger molecules are broken down into polymer fragments. At temperatures higher than 360 °C, the polymer fragments are small enough to escape and be detected.

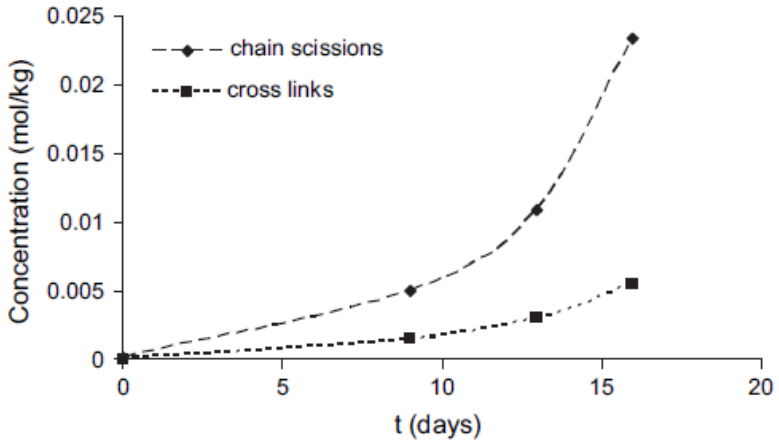

Figure 1- 4: Number of chain scission (n) and crosslinks(x) per mass unit calculated from M_n and M_w values against exposure time. Taken from Ref. [2].

1.2.1.2. Polypropylene (PP)

In a polypropylene chain, half of the carbon atoms in the backbone are tertiary carbons which are prone to attack. Thus the thermal stability of PP is lower than that of PE. The mechanisms are proposed by Kiran and Gillham [25] and corroborated by Bockhorn et al. [31,32]. The initiation is mainly caused by random chain scissions, similar to PE. After bond scission, primary radicals and secondary radical are formed and then rearranged into tertiary radicals. β-scissions then leads to volatile products and a terminated double bond. Polydispersity data are consistent with a homogeneous random chain scission process. [33] Figure 1-5 describes the possible mechanism of thermal degradation of PP.

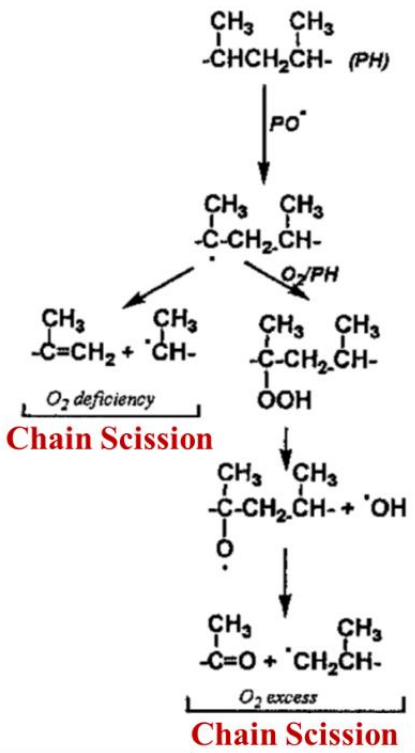

Figure 1- 5: Radical mechanism of the thermal degradation of polypropylene. Taken from Ref. [1].

During thermal oxidation, PP chain scissions also play an important role in the thermal degradation. The loss of mechanical properties and embrittlement is believed to occur during thermal degradation due to breaking of chains, including tie-molecules, which are crystalline regions via and non-crystalline of regions within a semi-crystalline polymer. [22,23]

1.2.1.3. PE/PP blend

In Wong and Lam's [34] research, series of blend products were made from co-rotating twin-screw extruder. From Differential scanning calorimeter (DSC) results, two peaks were shown on every test indicating that PP and PE are basically incompatible. Although PP and PE are incompatible due to viscosity difference [35], the peaks indicating T_m are slightly shifted and the result shows that adding PE has

reduced the T_m of PP. Different PE including HDPE, LDPE and LLDPE are studied in this research and the result from T_m analysis shows that HDPE affects the T_m of PP more than any other PE. Those T_m difference are only ±5 ºC, which might come from mechanism deviation or the deviation of crystal composition in polymer itself. The crystalline morphology of PE/PP blend should be different from PP or PE polymer itself, so we can see some difference.

Thermogravimetric analysis (TGA) was used to determine the weight loss versus time and temperature. [34] TGA was used to determine the weight loss at given temperatures; samples were tested in ambient air atmosphere. Induction time is a useful indication in polymer process, which is defined as the time required at a certain temperature and atmosphere before decomposition becomes measurable, and 5% weight-loss in air condition was used in this research. Due to more side chain groups, LDPE is considered having more open molecules and oxygen can easily penetrate in polymer, which makes LDPE to show lower induction time. The induction time of PP can be improved by adding a small amount of PE. This work also shows that the induction time obeys the Arrhenius equation.

1.2.1.4. Structure effects: Molecular weight, molecular weight distribution, and tacticity

From previous studies, larger molecular weight PE polymer has higher thermal stability in terms of longer induction time. [36] Figure 1-6 indicates the induction times for PP samples with different molecular weight at various temperature. The induction times of m-iPP and ZN-iPP increase sharply up until Mw=20,000 g/mol and Mw=45,000 g/mol, respectively, and then increase more slowly. This indicates that the chain ends concentration can affect the initial steps of thermal oxidation at certain molecular weight. For the ZN-iPP, there were other factors such as catalyst residue and unsaturated bonds; therefore, its induction time at molecular weight around 50,000 does not agree with m-iPP. From Hoang's research [6], they did a series of degradation studies of molecular weight and

molecular weight distribution effects of metallocene-PE. They also found the higher melt flow polymer with higher molecular weight has the better thermal oxidative stability in terms of maintaining the melt flow rate. The other study indicates that larger MW PE chains have found to influence the initial stage of oxidative process during melt-processing while smaller MW PE chains maintain the melt flow rate by reducing the shear of longer chain in the melt state.

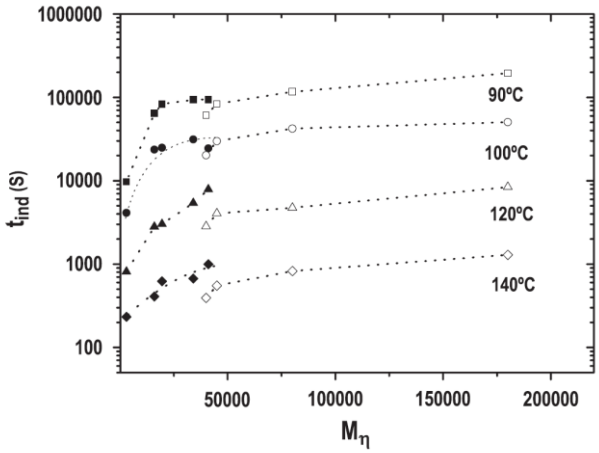

Figure 1- 6: Evolution of induction times for the degradation of m-iPP (solid symbols) and ZN-iPP (open symbols) at various temperature as a function of molecular weight. Taken from Ref. [3].

After metallocene-PP was commercially introduced, the advantages of low catalyst residue and narrow molecular weight distribution made these resins a good choice for spinning application. [37] Different tacticities of m-PP have been studied and their stability decreases as follows: syndiotatic-PP > atatic-PP > isotatic PP. [38] The rate determining reaction of PP degradation is the tertiary hydrogen abstraction, therefore, the oppositely located tertiary hydrogens in the s-PP increase the difficulties of radical transformation and improve its thermal stability. Thermal stability of s-PP has also been validated by the fact that the activation energy of s-PP in air atmosphere is higher than that for i-PP. [39]

1.2.2. Local environment effects: Impurities which are identified as factors that accelerate the degradation rate.

Oxygen, catalyst residues and unsaturated bonds are identified as the most effective factor during melt-processing. [21,40] Others such as moisture, oxygen, nitrogen, acid and other impurities were identified as long-term degradation factors.

1.2.2.1. Oxygen

Peterson et al. [4] revisited the thermal decomposition of PE (MW not provided) and PP (MW=12,000) due to the inconsistency of thermal parameters reported in the literature. From TGA results, they found that PE starts to decompose at ~350 °C under nitrogen gas. In air, a slight increase in mass is detected at ~220 °C indicating thermal oxidation. No noticeable residues were left under both nitrogen gas and air at temperature higher than 550 °C. PP starts to degrade at ~250 °C and no noticeable residues were found after 450 °C. In air, degradation happened at ~180 °C. Figure 1-7 is the TGA data to determine the degradation temperature.

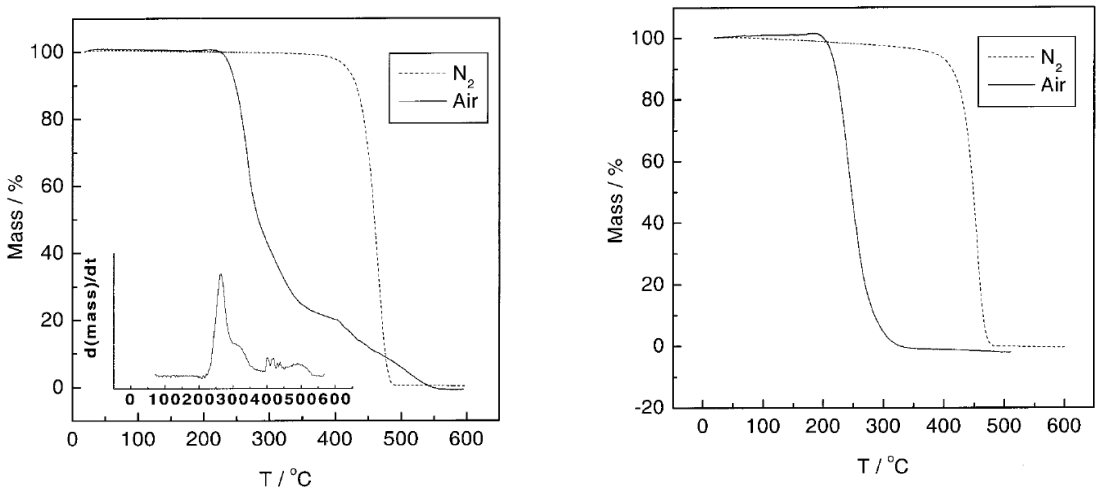

Figure 1- 7: TGA curves for the thermal decomposition in nitrogen (dashed line) and air (solid line). (a) PE, heating rate of 9.2 and 9.0 $Kmin^{-1}$ for nitrogen and air, respectively. Insert plot is derivative graph of mass loss for degradation in air, and (b) PP, heating rate of 9.1 and 8.2 $Kmin^{-1}$ for nitrogen and air, respectively. Taken from Ref. [4].

Gibert and Crespy tested a PP/PE blend from Appryl, Lavera, France (3150 MN 5). TGA were performed with a heating rate 5 ºC/min up to 650 ºC. [5] From TGA curve it was seen that the presence of oxygen accelerated the decomposition temperature from 400 ºC to 375 ºC. A strong exothermic peak in the DTA curve (see Figure 1-8) had been found at around 400 ºC. The IR spectrum of evolved combustible hazes outlined at 427 ºC indicates that those alkenes with alkyl side chains were the main decomposition products. The PE/PP blend was used to evaluate the fire retarded filler, but there is no indication about the PP/PE blend ratio. However, the oxygen effect was verified.

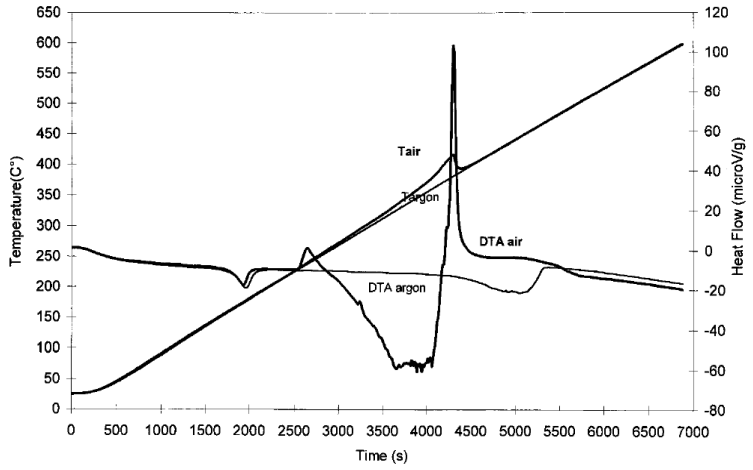

Figure 1- 8: DTA curve and sample temperature of PP/PE copolymer under air and argon. [5]

1.2.2.2. Catalyst effects: unsaturated bonds and catalyst residue in PE

From section II.A.1, the degradation behavior for polyethylene as reflected by the increase or decrease in viscosity depends on the predominance of chain scissions or crosslinking. In the beginning of chain scission process, oxidative scission dominates at lower temperature and high oxygen concentration. As temperature increase, thermal scission dominates. [41] The study has shown that crosslinking happens more at lower temperature while chain scission dominate the degradation behavior at high temperature. [42-44] To understand the different crosslinking behavior during melt-processing, it is crucial to understand the types of unsaturated bonds and their concentrations which vary from different polymerization synthesis methods. Also, the metallic catalyst residue in polymer pellets from synthesis plays a key role during melt-processing.

As for the unsaturation concentration effects, PE with large amount of vinyl bonds tends to crosslink during melt-processing. For example, Philips high density PE (HDPE) [45,46], linear low density PE (LLDPE) [47], metallocene PE (m-PE) [6]

and low density PE (LDPE) [48], they crosslink as the concentration of vinyl group decrease. Philip PE produced more crosslink than Ziegler PE under the same processing conditions [46]. Some PE contains low unsaturation bonds such as Ziegler HDPE [42,49] and hydrogenated, vinyl-free LLDPE do not crosslink. Vinyl bonds play an important role in PE crosslinking while the role of other types of unsaturated bonds such as Vinylidenes and t-vinylenes remains unclear. [50]

The catalyst residue from the polymerization of PE will also accelerate the degradation. The m-PE has been reported to have better thermal stability because of lower catalyst residue concentration. [51,52] For other polymers produced by Ziegler-Natta catalyst, the metal (Titanium, Vanadium, Aluminum and Chromium) and chlorine residue can affect polymer oxidative stability depending on the catalyst used. [7] The fact that the metallocene polymers have lower unsaturation concentration than Z-N polymers is validated by their higher thermal stability. Figure 1-9 indicates how the thermal degradation can be effected by catalyst residues.

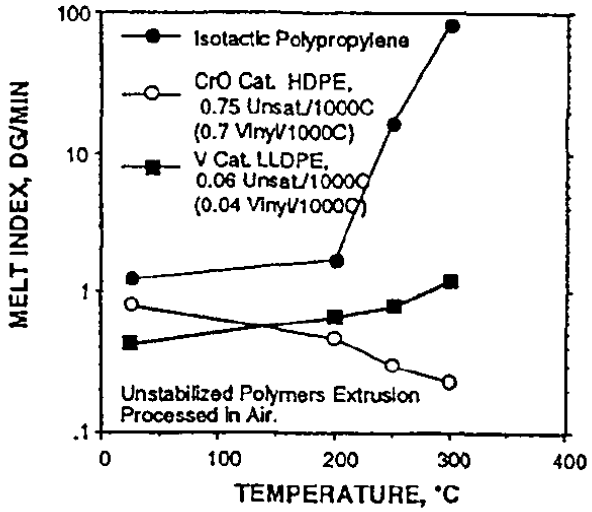

Figure 1- 9: Effect of processing temperature on several polyolefins.

Taken from Ref. [6,7]

1.2.3. Effects of thermal degradation during processing

1.2.3.1. Temperature

Extrusion temperatures are significantly higher than the polymer melting temperature to sufficiently melt the polymer and enable the polymer melt to flow at a reduced viscosity. [50,53,54] During the process, there are several processing conditions such as temperature, resident time, shear stress that will affect thermal degradation. Among them, temperature is the most crucial factor in the process.

The physical changes that occur during thermal degradation are determined by the nature of polymers. [8] Fiber polymers which are categorized as thermoplastic can be softened by heat without irreversible changes, providing an advantage of post processing. This behavior comes from the degree of order in molecular packing, of which the most important is the degree of crystallinity. Figure 1-10 indicates the idealized view of deformation caused by increasing temperature. At the temperature above glass transition temperature (T_g), polymers started to transition to the rubbery state. As temperature goes up to the melting temperature region, the polymers are prepared to flow and ready for meltspun process. This temperature point is also where the thermal degradation starts to occur. During the fiber processing, both T_g and T_m are important process factors that are used to set up the processing conditions. Some polymer materials even do not have the viscosity which allows them to be meltspun since the decomposition happens before melting. The understanding of polymer thermal properties is very important for processing.

The decomposition temperatures (T_d) are affected by the measurement methods and the material nature such as molecular weight and the impurities content. The degradation of polymer usually happens early than T_d and resulting only properties change; the decomposition of polymer occurred after T_d might cause the polymer chain to be seriously damaged and volatile products to be produced. Table 1-1 represents the decomposition temperature of PE and PP from previous researches. [4,55,56]

Table 1- 1: The decomposition temperature reported from previous researches.

Materials	T_d [55] (ºC)*	T_d ($T_{d1\%}$) [56] (ºC)*	T_d [4] (ºC)*
Polyethylene	335-450	217-233 (275-318)	350
Polypropylene	328-410	258 (315)	250

*: Measured by TGA with 10g/min, under nitrogen atmosphere

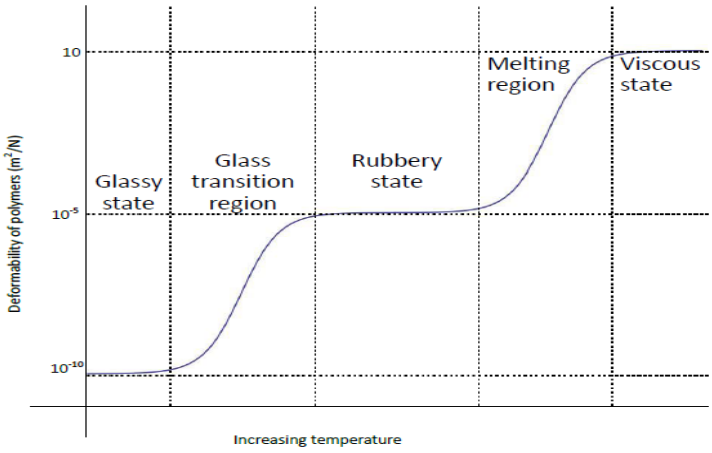

Figure 1- 10: Idealized view of deformation by increasing temperature. [8]

1.2.3.2. Residence time

Past kinetic and mechanical studies about thermal degradation of polymers indicate that time is a crucial parameter; however, not much research has been conducted to study the processing time as a function of degradation. Some studies have elucidated that multiple extrusions deteriorate the performance of polymer. [57-60] Most of the researches are related to polymer recycling and their intention is to

improve the performance of recycled polymer, sometimes by restabilizing polymer. [58]

Qian and coworkers [9] studied the degradation behavior of polypropylene during injection-molding processing. The commercial grade of iPP was processed at 190 °C under various time periods. The carbonyl group defined by Fourier transform infrared spectrum (FT-IR) built up after 40 minutes of degradation. The molecular weight distribution broadened and shifted to lower molecular weight (MW) as degradation time increased. After degradation, the MWD curve can be divided into low MW peak and high MW peak. The low MW peak shifted much faster than high MW shift suggesting that broken polymer chains are easier to continuing breaking. The heterogeneous degradation procedure can be well described with theory developed by Lehrle et al. [61] Other research conducted for m-PE and PP obtained similar results. [6,7] Figure 1-11 gives the details of how MW can be changed by time.

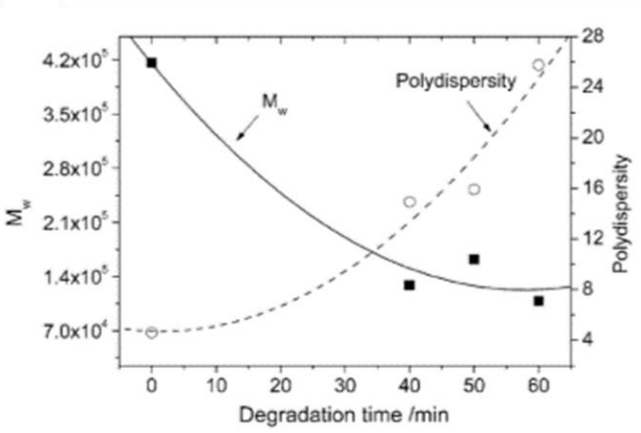

(a)

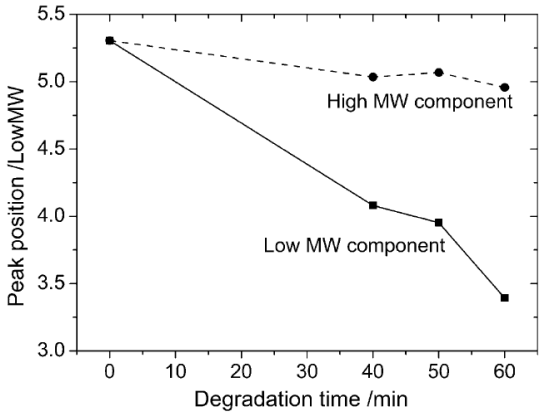

(b)

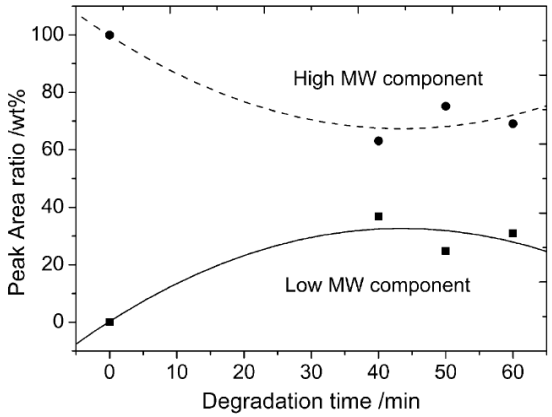

(c)

Figure 1- 11: (a) weight average molecular weight (open circle) and polydispersity (filled square) changes with degradation time, (b) Variation of peak position with degradation time at 190 °C, (c) Variation of peak area with degradation time at 190 °C. Taken from Ref. [9].

1.2.3.3. Shear stress and draw ratio

The effects of shear rate during melt process are usually presented in the form of the heat accumulation at specific area called “hot spot”. [19] Those hot spot accelerate thermal degradation during melt-process. Yamane and White [62] discussed that die-wall induces PP fiber degradation and the degradation can

narrow the molecular weight distribution. However, direct impact from shear stress was suspected and discussed at that time and had not yet been approved. [54] These results confirm the importance of shear as the major source for initiation of free radicals formed by homolytic fission caused via mechanical cleavage of polymer chains. [6]

Carlsson and coworkers reported that during drawing stage free radicals produced by bond ruptures at high draw rate and low draw temperature caused further photo-degradation. [20]

1.2.4. Thermal stabilizers

From previous discussion, oxygen plays a crucial role in terms of accelerating thermal degradation; therefore, antioxidants and stabilizers are added to prevent or inhibit degradation of polyolefin materials during the processing and storage. [1,21,24,63,64] Figure 1-12 indicates how initiators and stabilizers can affect thermal oxidations. Initiators such as oxygen and radicals produced from impurities can accelerate thermal degradation. Stabilizers are compounds that help to prevent polymer from degradation and they are categorized into two groups by their function. One is chain breaking antioxidant which helps retard oxidation during melt-processing, the other is preventive antioxidants which help elongate the polymer shelf life. During process, polymer usually remains at a temperature higher than its degradation temperature for a certain period of time. Adequate amount of antioxidant can postpone the oxidation induction time (OIT); therefore, degradation will be limited during melt-processing. Antioxidants then help to maintain fiber properties such as strength, elongation and tenacity etc. Photo-inhibitors as preventive antioxidants are also added to prevent degradation during storage. The stabilizers and antioxidants have been intensively studied in the past half century, several high quality review papers has been provided.

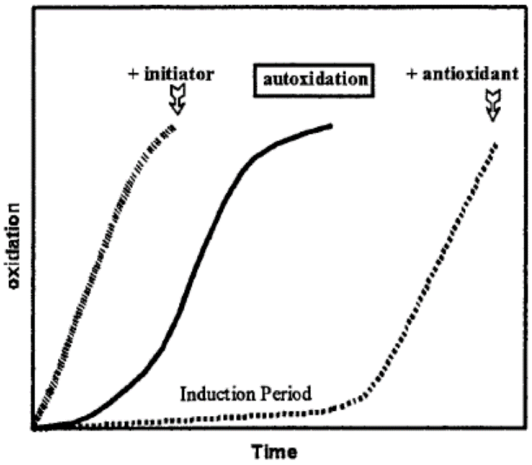

Figure 1- 12: Generalized scheme for changes in autoxidation curve caused by presence of initiators and antioxidants. Taken from Ref. [1].

Typical types of stabilizers can be categorized as 1) phenolic antioxidants, 2) phosphite-type stabilizers and 3) hindered amine light stabilizers (HALS) [64]. Those stabilizers are widely used to protect polymer such as PE and PP pellets from degradation during process and usage. Stabilizer is especially important for PP that has tertiary carbon which is prone to attack therefore has less thermal stability. PE is relatively stable; therefore, less concentration of stabilizers are needed for high density PE. For some applications such as low density PE processed at lower temperature, no antioxidant is even needed.

During the process of preventing the polymers from degradation, the stabilizers themselves might degrade when consuming radicals. [1] Degradation products from phenolic antioxidants and phosphite-type stabilizers are detected while no degradation produces are found for HALS. The HALS is recycled during stabilization of polymers. Hydrolysis of stabilizers which is an undesired side effect can also happen and reduce their capability of protecting the polymer. Table 1-2 gives some examples of stabilizers provided with chemical structures, types and trade names.

1.2.4.1. Phenolic antioxidants

Phenolic antioxidants which also called as chain breaking antioxidants usually attack primary oxidation cycle and prevent polymer chains from further propagation. It can be classified as chain-breaking acceptor antioxidants and chain-breaking donor antioxidant. Chain-breaking donor antioxidants such as Irganox 1076 and Irganox 3114 are scavenging alkyiperoxide (ROO·) radicals at their primary stabilizing steps where hydroperoxides might be produced. In practice, a hydrolysis resistant phosphite as a peroxide decomposer is needed to work as a combination. Chain-breaking acceptor antioxidants such as Irganox 3052 and HP136 deactivate alkyl radicals and work efficiently particularly in oxygen deficient environment. [1]

1.2.4.2. Phosphite and sulfur stabilizers

Phosphite-type and sulfur type stabilizers work well in combination with phenolic antioxidants as melt stabilizers. Phosphites are susceptible to hydrolysis by reacting with hydroperoxides to reduce discoloration. Sulfur stabilizers react with hydroperoxides in a catalyst process which produces sulfur acids and deactivate the free radicals formed.

Table 1- 2: Examples of commercial stabilizers (a) Phenolic antioxidant (b) Phosphite and sulfur type stabilizers. Taken from Ref. [1].

Chemical structure	*Antioxidant*	*Trade name*
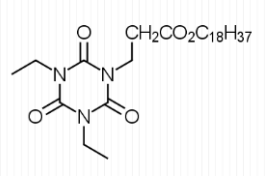	Phenolic antioxidants: chain-breaking acceptor	Irganox 1076
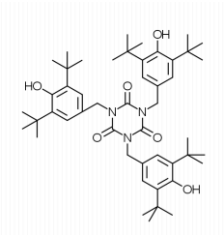	Phenolic antioxidants: chain-breaking acceptor	Irganox 3114
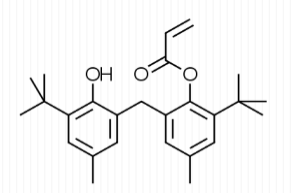	Phenolic antioxidants: chain-breaking donor	Irganox 3052
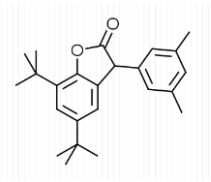	Phenolic antioxidants: chain-breaking donor	HP136
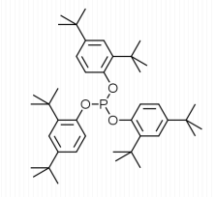	Phosphite type stabilizers	Irgafos 168
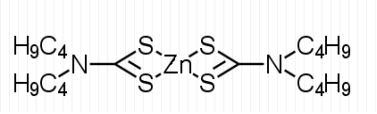	Sulfur type stabilizers	Robec Z bud
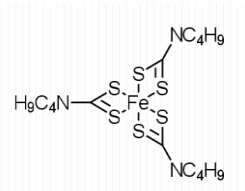	Sulfur type stabilizers	Iron dithiophosphate

1.3. Computational simulations used to study chemical reaction of polymers

The different length scales of materials are presented in Figure 1-13. Fabrics are composed of bunches of fibers (order of mm), often in yarn form, that are combined by weaving or through nonwovens processing. Therefore, the properties of the fabric are influenced by the composition of the individual fibers. Individual fibers (order of μm) are composed of the individual polymer chains (order of nm), and the distinct chemical structure of each polymer results in corresponding properties. Quantum mechanical (QM) calculations and molecular dynamics (MD) simulations are able to predict static and dynamic material properties at the nanoscale, whereas properties at higher scales would need to utilize other approaches such as dissipative particle dynamics simulations or continuum dynamics simulations.

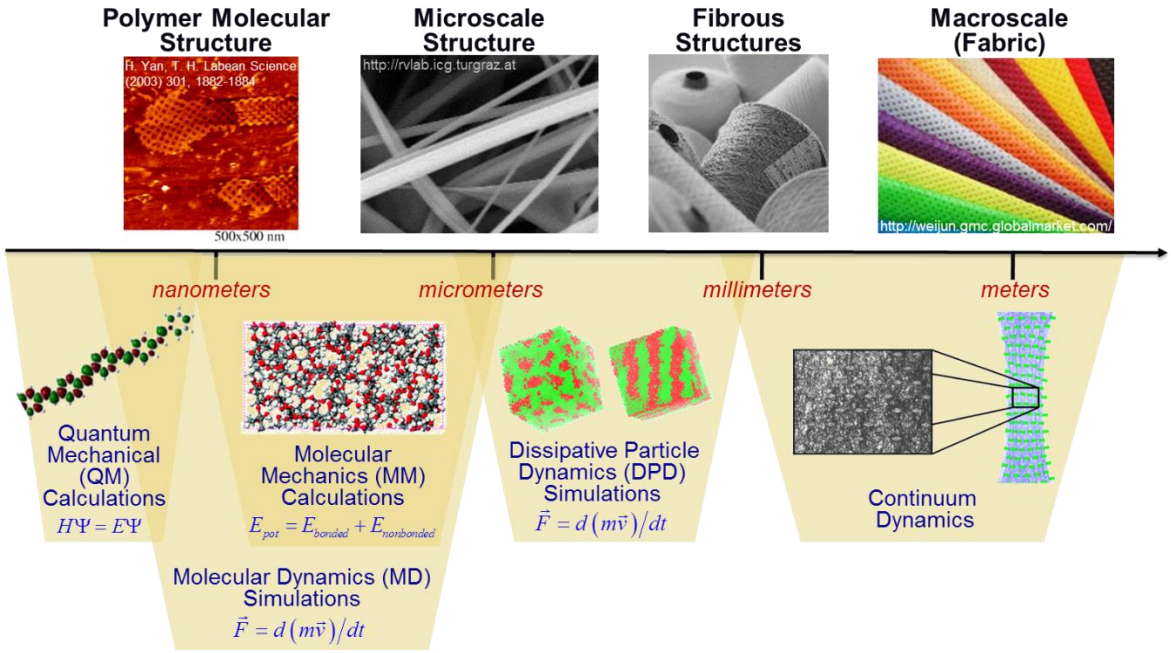

Figure 1- 13: The length scale of materials, mapped onto different simulation approaches across the scales.

To understand the thermal degradation of polymers, both the physical changes and chemical reactions need to be considered at the molecular level. For chemical reactions, such as what occurs during thermal degradation, the most accurate way to investigate the molecular-level details is with QM calculations since it provides a mathematical description of the electronic structure of molecules. [65] QM has been used to study the structural and chemical properties that have been used to construct nuclear magnetic resonance (NMR) and electron paramagnetic resonance. However, the speed of a QM calculation due to the inclusion of so many electronic degrees of freedom makes it impossible to simulate large systems such as polymer fibers. An alternative approximate approach is through the use of molecular mechanics (MM), where the electronic degrees of freedom are included in an average sense per atom type through the use of an empirical force field, and thus

the calculation speed is dramatically increased. Although MM can be used to obtain structural and chemical properties, any property that involves breaking and forming bonds such as what occurs during thermal degradation cannot be investigated with traditional MM force fields. However, a variety of reactive force fields have recently been developed to investigate systems at the MM level that enable bonds to be broken and formed.

To study at the molecular scale the dynamic or non-equilibrium properties such as diffusion processes, the viscosity of a liquid, or the propagation of cracks in crystal materials, molecular dynamics (MD) simulations can be used, which solve Newton's equations of motion to perpetuate the system.[66] MD simulations can be performed by using either QM or MM for the potential energy terms. Dynamical properties can also be calculated with Monte Carlo (MC) simulations, which reduce the computational expense by carrying out of selected important parameters through a stochastic approach; therefore, known mechanisms or kinetic parameters need to be inputted when study in polymer behaviors with MC.

1.3.1. Quantum Mechanics (QM) Calculations

In Quantum mechanics, the electronic degrees of freedom are described by wavefunctions that describe the quantum state of a particle (an electron) and its behavior, the prediction of all observable chemical properties are obtained by solving the Schrödinger equation [65] given by,

$$H\Psi = E\Psi \qquad (1\text{-}1)$$

where H is Hamiltonian operator, Ψ is the wavefunction of the system and E is the energy of the state Ψ. By solving the wavefunction of the system, the properties of the system can be calculated at the quantum or atomic level. However, QM calculations are limited to only a few hundred atoms due to the computational intensity of the calculations since the solution to Eq. III-1 involves the calculation of many double integrals. Simplifications can be made to reduce the computational complexity by substituting some of the double integrals with empirical data from

experiments or higher order QM calculations; these methods are called the semi-empirical approaches. Examples of semi-empirical approaches include PM3 [67,68] and ZINDO [69]. Semi-empirical approaches are only valid for the systems in which they were parameterized.

Density functional theory (DFT) is another QM calculation approach that uses electron density functionals instead of wavefunctions, which enables DFT to provide the ground state properties of a molecular system by investigating the electronic structures of many-body systems. [65] The accuracy of this approach has been validated with molecular orbital theory and experiments. Its applications range from activation energies and bond strengths during organic reactions, optimization of system geometry and molecular polarizabilities.

Usually, activation energy, heat of formation and possible reaction mechanism routes are predicted with QM calculations. The challenge with using QM calculations to investigate possible degradation mechanisms is that the calculations need to be carefully designed and identified before each calculation. In addition, computational limitations make it impossible to calculate large molecules, thus oligomers or model compounds will be designed to represent larger molecules such polymers.

DFT was used to calculate the activation energy of polyglycolide and poly(L-lactide)[70], and the thermal decomposition of a model compound for polyester and polystyrene. [71] The hydrolysis that assisted by water are found to be faster for the glycolyl than the L-lactyl units because the lower energy barrier of the scission of the glycolyl. Tomoyuki and coworkers used the semi-empirical PM3 method to calculate the oxidation of PP by using simplified model compounds to represent the isotactic-PP and syndiotactic-PP.[72] They calculated the activation energy and the heat of formation of four interactions including 1) formation of peroxyl radical, 2) hydrogen atom abstraction by peroxyl radical, 3) decomposition of hydroperoxide, and 4) chain scission reaction. The abstraction reaction from the tertiary hydrogen atom has been determined as the rate-determining step to the relative stability between i-PP and s-

PP because the activation energy of the model compound for s-PP is larger than the model compound for i-PP. A recent DFT study of PP degradation [73], which was validated by experiments, indicates that H-abstraction from a tertiary hydrogen is a minor process in the presence of peroxides in solution, which disagrees with the Tomoyuki study. However, this study was performed at lower temperatures and in solution, and thus the self-termination reaction is favored under these conditions instead of H-abstraction.

1.3.2. Molecular Mechanics (MM) Calculations

In MM calculations, all atoms are treated as spherical particles, where all bonds are treated as springs; the bonded and nonbonded interactions among atoms are stored as potential functions within an empirical force field. [74] The potential energy function contains terms that represent the bonded and nonbonded interactions, described by

$$E_P = E_{bonded} + E_{nonbonded} \quad (1\text{-}2)$$

where the bonded energy is defined as,

$$E_{bonded} = E_{bond} + E_{angle} + E_{dihedral} \quad (1\text{-}3)$$

where E_{bond} , E_{angle} and $E_{dihedral}$ are the bond energy, angle energy and dihedral energy, respectively, and the nonbonded energy is given by,

$$E_{nonbonded} = E_{es} + E_{vdW} \quad (1\text{-}4)$$

where the E_{es} and E_{vdW} are the non-bonded energy of electrostatic energy and van der Waals energy, respectively, between any two atoms in a system.

Classical force fields do not describe bond association or dissociation. However, reactive force fields have also recently been developed to take into account the breaking and forming of bonds during chemical reactions. Based on the review of Faraf and coworkers [75], the reactive force fields that were developed to represent reactive systems can been divided into two categories based on which bond dissociation method was implemented. First, some force fields use a reaction cutoff distance method that has a clear bond distance cutoff point to separate a

bonded state and a nonbonded state; this approach is commonly used in coarse-grained simulations. [76] The empirical reactive force fields use bond order and a radial switching function to smoothly associate the bonds. Commonly used radial switching functions for polymer systems are the Reactive Empirical Bond Order (REBO) potential, [77] which is applicable to carbon-based materials; the Reactive Force Field (ReaxFF) potential, [12] which is a generalized form of REBO that extends to most common elements; and the Reactive Molecular Dynamics (RMD) potential, [78], which is useful for investigating the kinetics of degradation. These REBO and ReaxFF potentials will be described in more detail below and the RMD potential will be elucidated in Section III.C.2 Other potentials such as the charge optimized many body potential [79] were designed for metal systems and thus are not applicable to organic polymer systems.

1.3.2.1. Classical force fields

For the classic force fields, the potential energy is calculated with the interactions between atoms. [65] The potential energy function of class I force fields such as CHARMM [80] and OPLS [81] contains E_{bonded} and $E_{nonbonded}$. To achieve high accuracy when representing the condensed phase system, cross-terms accounting for the bond or angle distortion that caused by nearby atoms are included in the class II force field. An example of a class II force field is the Consistent Valence Force Field (CVFF). [82] Figure 1-14 graphically illustrates the energy terms of CVFF. Energy terms (1) to (5) represent bonded energy, energy terms (6) to (8) represent cross-terms and energy terms (7) and (8) represent the non-bonded energy.

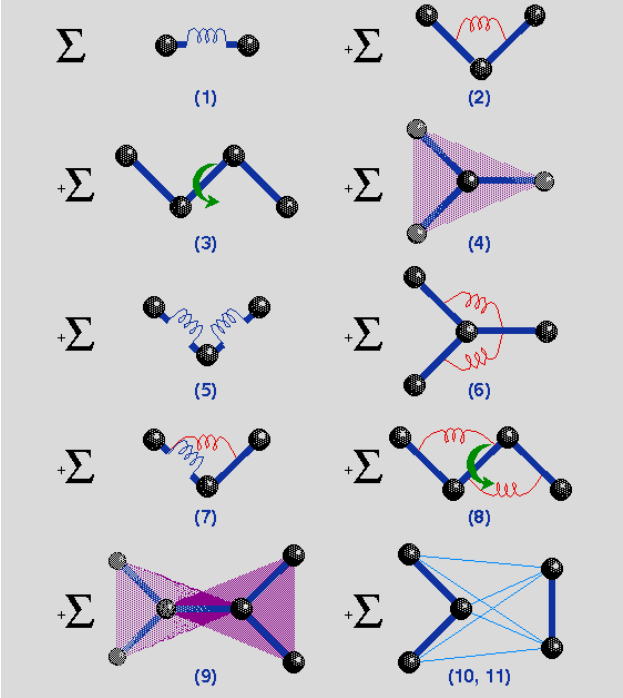

Figure 1- 14: Graphic illustration of terms in CVFF. Taken from Ref. [10].

Coarse-grained force field simplifies large molecules especially biopolymers by focusing on elements of secondary structure. [65] When an entire fragment is highly transferable in a structure such as an entire amino acid in a protein, an interaction site and a potential energy function will be assigned to reduce the redundant calculations. Figure 1-15 represents how the coarse-grained model can be applied to poly(methyl methacrylate) (PMMA) polymer. Those reduced models sacrifice atomistic details in structural analysis; however, the calculation speed can be accelerated significantly since some energy calculations have accomplished.

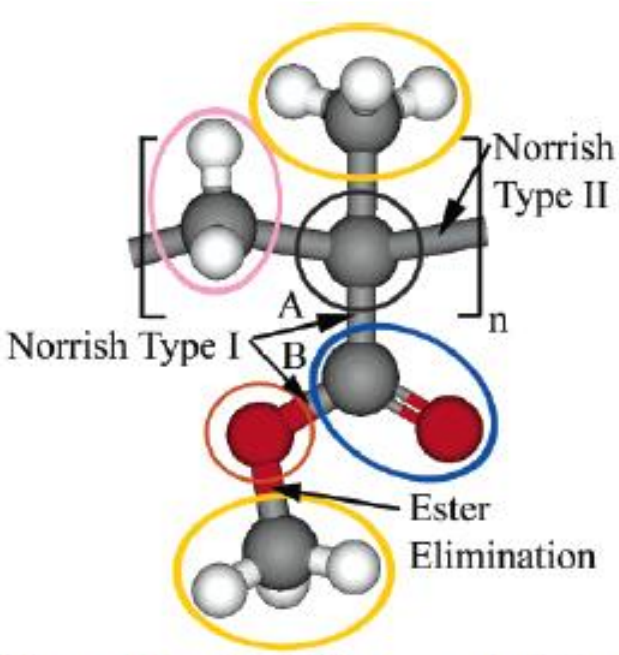

Carbon	Gray
Hydrogen	white
Oxygen	red

Figure 1- 15: Representation of the PMMA coarse-grained model. The ellipses represent approximations for the coarse-grained representation. Taken from Ref. [11]

1.3.2.2. Adaptive intermolecular reactive empirical bond order potential (AIREBO)

The REBO potential was first introduced by Brenner back in 1990. [77] The REBO potential adopted the bond-order-to-bond length concept that exploited the approaches that developed by Abell [83] and Tersoff [84]. It was used to study the reconstruction of diamond [77] and the collision reaction of C60. [85] The second-generation REBO potential for hydrocarbons was then developed to enhance the equilibrium distances, energies and force constants of C-C bonds. [86] The REBO potential treats the electronic degrees of freedom in an empirical manner and the conjugation or hybridization states are derived directly from the geometry, thus it successfully describes the intramolecular interactions in carbon and hydrocarbon

systems. However, this first model did not include a description for intermolecular interactions, which are important for bulk systems such as polymers, liquids and thin films. In addition, an accurate representation of the torsional energy for hindered rotation of single bonds and dihedral angles is also critical when it comes to describing polymer systems. Based on the extended REBO, which includes oxygen parameters [87], the adaptive intermolecular REBO (AIREBO) was developed and it successfully incorporated the nonbonded interactions and torsional energy to study large hydrocarbon systems. [88] The entire energy of AIREBO is given by,

$$E = E^{REBO} + E^{LJ} + E^{tors} \quad (1\text{-}5)$$

where E^{LJ} is the Lennard-Jones potential that describes the dispersion and intermolecular repulsion interactions, E^{tors} represents the torsional interaction around single bonds, and E^{REBO} is the energy composed of covalently bonded pair energies, described by,

$$E = V^R(r) + bV^A(r) \quad (1\text{-}6)$$

where $V^R(r)$ and $V^A(r)$ are the repulsive and attractive pairwise potentials, respectively, which are determined by atoms types and the distance between atoms, and b is the bond-order term that is determined by the Tersoff potential[84].

The REBO and its extended AIREBO potentials have been applied to investigate high energy deposition such as plasma, irradiation and high energy atom bombardment on polymer surfaces. [89-94] For example, the second generation REBO was used to study the mechanism of the interaction of argon ions with polystyrene polymer surfaces, and this study predicted the degree of surface damage with respect to crosslinking and dehydrogenation, the surface roughness, and the initial sputter yields of polymer surface, which had good agreement with experiments. [94] A comparison of the AIREBO and REBO potentials for high energy argon deposition on polystyrene coils that are on top of a silver thin film indicated that the number and the size of fragments resulting from AIREBO were observed to be smaller than the REBO potential because the fragments resulting from the high energy deposition needed to overcome the additional van der Waals interactions.

[90,91] Although the results of both potentials are equally believable, this observation suggests that including a long term interaction can impact the output from chemical reaction simulations. Both the previous studies and another study that investigates high energy Argon deposition on PMMA using AIREBO obtained good agreement from secondary ion mass spectrometry (SIMS) experiments regarding the distribution of fragments after bombardments. [89] AIREBO was also recently used to investigate the irradiation effects in crystal PE and crystal cellulose [95,96], and the main mechanism of UV irradiation for crystal PE and crystal cellulose was predicted to be scissions, whereas the observed degree of crosslinking is quite low for both systems because the UV induced crosslinking usually happened in the amorphous area.

1.3.2.3. Reactive force field (ReaxFF)

ReaxFF is a reactive force field [12] that describes both the physical interactions and chemical reactions of large scale systems. In order to get a smooth transition between the different types of bonds (non-bonds, single, double and triple bonds), ReaxFF applies a relationship between the bond order and the bond length. More specifically, the total system energy (E_{system}) for ReaxFF is given by,

$$E = E_{bond} + E_{over} + E_{under} + E_{val} + E_{pen} + E_{tors} + E_{conj} + E_{vdW} + E_{coulomb} \quad \text{III-7)}$$

where each term is as follows. Just as in a traditional force field, the non-bonded interactions, van der Waals (E_{vdw}) and Coulombic ($E_{Coulomb}$), are calculated between every atom pair, whether bonded or not. The bonding energy (E_{bond}) describes the bond order and the bond energy between atoms. To ensure that the valences for each atom type are controlled, penalty terms are included for when the bond order is larger or smaller than it should be, or over-coordinate (E_{over}) and under-coordinate (E_{under}). For example, carbon should have a bond order of 4, but if the bond order is larger than 4, the E_{over} will be used; if less than 4, E_{under} will be taken into account; For atoms with two double bonds sharing an atom, there is a penalty term (E_{pen}), whereas E_{conj} factors in the contribution of conjugated systems to the molecular

energy. The E_{val} term is for valence angles that is parameterized for all hybridization types for organic atoms, and $E_{torsion}$ is the energy for torsion angles. All connectivity-dependent interactions such as the valence energy (E_{val}) and the torsion angle energy (E_{tors}) are also designed to be bond-order dependent, meaning that when the bond breaks, the energy distribution disappears. Note that the terms E_{bond}, E_{vdW} and $E_{Coulomb}$ are between two atoms, E_{val} is between three atoms, E_{tors} is between four connected atoms, and multi body energies are calculated by E_{over} and E_{under}. In addition, ReaxFF calculates the charges depending on the geometry of the molecule, thus it accounts for polarization effects and thus also differentiates itself from other non-reactive force fields.

Figure 1-16 provides a comparison of the ReaxFF force field as a function of simulation time and system size as compared to two quantum mechanics approaches, DFT and PM3. This graph indicates that the ReaxFF force field is faster than both QM approaches, and is thus practical to simulate the reactivity of large scale systems such as polymers.

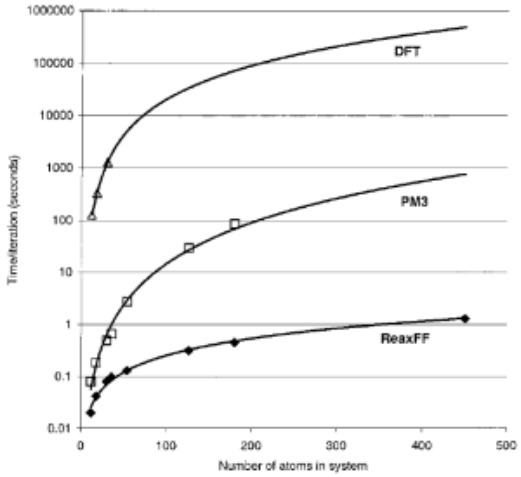

Figure 1- 16: The influence of molecular system size on computer time for two QM approaches, DFT and PM3, and a classical reactive potential, ReaxFF. Taken from Ref. [12].

The thermal decomposition of poly(methylsiloxane) (PDMS) with around 1000 atoms [97] with ReaxFF determined that at a heating rate of 266 K/ps, the onset temperature of PDMS degradation is around 2800 K and the decomposition initiated by Si-C bond cleavage formed CH_3 radicals; they also investigated the effects of several additives such as water, NO_2 and SiO_2 and determined the distribution of products and the temperature-dependent reaction rates. Note that the degradation temperature using ReaxFF will be higher than in reality because the time-scale is different. ReaxFF has been further developed to work for metals and other systems through careful force field parameterization. [12,97-99]

MD simulations with ReaxFF of the effect of fillers such as carbon nanotubes (CNTs) and carbon fibers during the first stage of pyrolysis within a phenol formaldehyde system [100] determined that the primary product is water for all pyrolysis cases, and that the filler effect on the evolution of fragment formation and graphitic precursors can be identified in a low temperature zone (less than 2000 K) but not in the high temperature zone (higher than 2000 K). However, it is difficult to compare their MD results directly with experiments because not only are the time scales of pyrolysis different, but also the structures are not identical. Additionally, the dehydration occurs at 450 K, resulting in crosslinking of polymer chains in experiments but not in MD simulations. A comparison between DFT calculations and ReaxFF regarding the pyrolysis of the same phenolic polymer indicated that the dominant chemical species were similar between both approaches, however the yields of each species were different between the methods. [101] Recent ReaxFF MD simulations demonstrated a simple route to manufacturing of fine CNT fibers by adding a small amount of well-dispersed double wall CNTs can produce an improved structure of CNT fibers.[102]

More recently, the shock compression behavior of PE and poly(4-methyl-1-pentene) [93,103,104]. was studied using density functional theory (DFT), two non-reactive force fields and ReaxFF; ,and the response of weak shocks in both

polymers were predicted to be valid over a large range of densities and pressures when DFT and ReaxFF methods were used, while there are some limits with non-reactive force fields. In addition, the significant dissociation of the poly(4-methyl-1-pentene) in shocked foams which was produced by local heating and hot spot area was observed using ReaxFF simulations; note that the measurement of local temperature and the formation of hot spots around the voids can be observed by MD simulation but not experiments. Dissociations of polymer bonds were then followed by local heating resulting in those hot spots that occurred when the introduced voids collapses. Another research study using ReaxFF elucidated the progress induced by shock wave between the interface of cyclotrimethylene trinitramine (RDX) and hydroxyl-terminated polybutadiene (HTPB), [105] where the shock wave first led to shear relaxation and introduced shear stresses along the interface, then the shear stress caused the energy deposition and significant temperature increase, and finally the polymer bonds broke due to the formation of those hot spots.

The description of the hydrogen bonding between water molecules and a paper-like polymer film was investigated with ReaxFF,[13,106] and the peak modulus was determined when there was about 7% water content between the paper-like polymer films. In addition, the mechanical properties were observed to be controlled by the hydrogen bonds between water molecules and the polymer film; the stiffness increased up to a maximum value of 60 GPa. By tuning the density of the functional groups attached to the polymer film, they were also able to obtain mechanical properties corresponding to the designed structures. Figure 1-17 is the layer geometry of paper-like polymer film and the stress-strain curve after the force applied to the system.

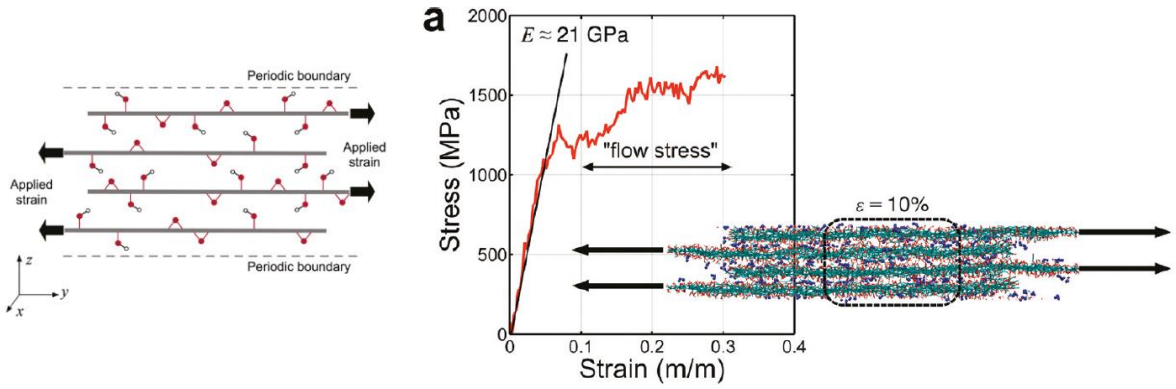

(a) (b)

Figure 1- 17: (a) Multilayer shear model consisting of four sheets of polymer films with 10 Å intervals. Shear was applied to measure the stiffness of the hydrogen-bonded structure in the shear direction. (b) Stress-strain curve for paper-like polymer film with 2.5 wt% water. The inset snapshot was captured at 10% strain. Taken from Ref. [13].

1.3.3. Molecular Dynamics (MD) simulations

Molecular dynamics (MD) simulations are numerically solving the Newton's equations of motion for a system. The general form described by

$$F = ma = \frac{d(mv)}{dt} \tag{1-8}$$

where F is the force, t is time and m and v are the mass and the speed of the atom, respectively.

The potential energies can be calculated in MD either through QM or with classical approaches. QM approaches calculate all the ground, transition and excited states of electrons, and the electronic variables are treated as active degrees of freedom. Therefore the chemical reaction can be represented. Instead of solving the Schrödinger equation like *ab initio* MD simulations, classical MD simulations solve empirical potential equations with selected particular approximations. Classical MD simulations derive properties and trajectories by using

predefined potentials based on empirical data or on independent electronic structure calculations while *ab initio* MD simulations calculate the forces acting on the nuclei from its electronic structure. [107] The potential of classical MD can be summed by two-body, three-body, many-body terms, long-range and short-range interactions. The model potential does not allow bonds to break for non-reactive MD. By carefully tuning the potentials with bond dissociation features, classical MD simulations can now describe chemical reactions as long as the force field has been appropriately parameterized.

1.3.3.1. Quantum MD simulations

By giving a particular approximate solution to the Schrödinger equation, *ab initio* MD simulations allow chemical reactions to take place in the solid phase. Among several approaches, Car-Parrinello MD [108] (CPMD) was used to simulate the pyrolysis of cellulose with 5888 atoms. [109] Simulating fast pyrolysis at 600 °C, levoglucosan was determined as major product that produced from favored mechanism during depolymerization which agrees with experimental findings. Calculating the whole reaction mechanism would be expensive, they decided to determine the free-energy barrier at specific reactions, focusing on ring-opening and depolymerization, to compare with previous calculations [110,111] and experimental results [112]. The results agree with previous calculations well but underestimate with experiment results due to the ignorance of vaporization energies. Furthermore, CPMD also been used to calculate the changes of dissociation free energy and activation barrier for the β-D-glucose condensation reaction. [113]

Another quantum molecular dynamics was used to produce the fragments distribution of polystyrene and polyester. [71] Model compounds were used at the ground state including excited and positive charged states. The semi-empirical molecular orbital calculations were used to obtain the geometry and energy optimization for the initial MD steps. The ratios of charged fragment distributions correspond well to the values obtained from secondary ion mass spectroscopy.

1.3.3.2. Reactive molecular dynamics (RMD) simulations

Nyden and Noid[78] used MD simulations to study the degradation of PE by developing a potential energy function that included 1) a Morse oscillator function to describe two-body interaction, 2) a three-body bending potential energy and 3) the Lennard-Jones potential to describe the torsional motions. The initial step of degradation behavior, bond-dissociation, was identified when the distances between two atoms exceeded 9.5 Å. However, this reactive molecular dynamics (RMD) model only considered one polymer chain, so no intermolecular interactions were being considered. Also the hydrogen-transfer reaction was not considered because of the absence of explicit hydrogen atoms. However, this study suggested that the thermal stability of an individual polymer increases as molecular weight decreases. They revised the model to include a radial switching function to turn off the forces when bonds dissociated due to bending and twisting. [114] New atom types were also introduced to the traditional CVFF force field to represent the β-scission of C-C and C-H bonds. [115] In the beginning, thermal decomposition of simple systems such as PE [116], PP [117] and PP/graphite nanocomposites [115] were studied by RMD and then expanded to PMMA [118] and polyisobutylene [119,120]. The onset temperature of thermal decomposition is much higher if the polymers are less substituted, for example, onset temperature of poly(isobutylene) < PP < PE. The highly coiled conformation of poly(isobutylene) and PP are found during thermal decomposition while PE is much more extended. The coiling is suspected to induce steric strain that cause scissions at lower temperature. Small systems, usually a single chain, are investigated with RMD to study thermal decomposition, even a recent study [121] that combined coarse-grained and RMD to simulate a box of 512 CF_3OCF_3 molecules. However, the simulation size is still smaller than what can be studied with ReaxFF and AIREBO.

1.3.3.3. Coarse-Grained MD simulations

The coarse-grained method (CGMD) reduces the computational load by grouping the unreactive sites into a new site during MD simulations. To simulate chemical reaction involved process such as high energy irradiation or thermal degradation.[76] Some input such as repeat unit molecular weight, bond length of a single repeat unit, characteristic ratios at various degrees of polymerizations, polymer density and the Charlesby-Pinner ratio which defined the crosslinking-scission probability of excited sites are required. [122] By choosing the proper inputs, the simulation results can turn out to match the theoretical and experimental data well.

The coarse-grained method has been used to study the photothermal process of polymers. [11] From known photochemistry and experimental ablation observations, a suitable CG model polymer can be generated. After simulations, the onset of ablation was found to be delayed and the pressure of the system are increased. The pressure relaxation induced by laser was found to be the main mechanism during the onset of polymer ablation. The yield and the composition suggested that the broken bonds in the surface area are caused by photomechanical process instead of photochemical process.

The thermal degradation for a single polymer chain under different conditions has been studied. [123] The particular kind of chain dynamics, over- or under-damped regimes, and the existence of excluded volume interactions between monomers are two major factors that affect the scission kinetics. The chain scission process was found to be better described by first-order reaction. The method can be extended to study a more complex system of bottle-brush polymers. [124] The probability of fragment distribution was found to be sensitive to the degree of steric repulsion; the distribution of fragment sizes at different times agrees well with experimental observations. The measured variables indicated that the bond scission process agrees with first order and zero order reactions.

1.3.3.4. Classic MD simulations

Ian and coworkers [125] reported their study of determining the degradation temperature (T_d) and glass transition temperature (T_g) for polysulphone (PS) and polyethersulphone (PES) by closely monitoring the density changes under isothermal and isobaric conditions (NPT ensemble), which reasonably agreed with experimental data.

1.3.4. Monte Carlo (MC) simulations

Forces, which are the fundamental variables in MD simulations, are calculated at every timestep. However, one way to reduce the heavy calculations is to use Monte Carlo (MC) simulations, whereby only several important properties are selected to carry out through a stochastic approach. Therefore, when performing MC simulations for investigating polymer behaviors, known mechanisms or kinetic parameters need to be identified. After repeated random sampling, numerical results from these simulations are often validated by experimental results. During MC simulations of polymers, the evolution of molecular weight distribution (MWD), randomness of chain breaking [126] and crosslinking density [127,128] can be evaluated.

Chain scissions are the most common mechanism that occurs during thermal degradation and MWD changes can be an indication of this mechanism. Many MC simulations have been conducted to understand how the thermal degradation can be related to the given parameters. In Guaita and coworkers' studies, the degree of polymerization was correlated with the weight loss of the polymer with increasing degradation, which suggested the randomness of chain scissions as a function of time. [129-133] However, another study determined that totally random chain scissions cannot explain the MWD shifts during polymer degradation for linear polymer chains. [126] The preferential scissions of the longest polymer chains have been validated to cause the movement of the MWD peak, a new peak appeared in the MWD chart to accommodate the systematic fragmentation. A more complex

study about the oxidative degradation of PP focused on the effects of the initiation steps as a function of MWD changes. [14] By adjusting the initial concentration and rate constants, and the MWD changes with time predicted from MC simulations are consistent with the results from gel permeation chromatography. The shifts of MWD curves over time were attributed to the degree of structural order and the invasion strength of degrading agents such as oxygen and other impurities. [134] In order to simulate the invasion strength of degrading agents, multiple resistant factors must be created to shield a bond from exposure and the probability determinants must be incorporated. Figure 1-18 indicates the peak of the MWD shifted as reaction time increases.

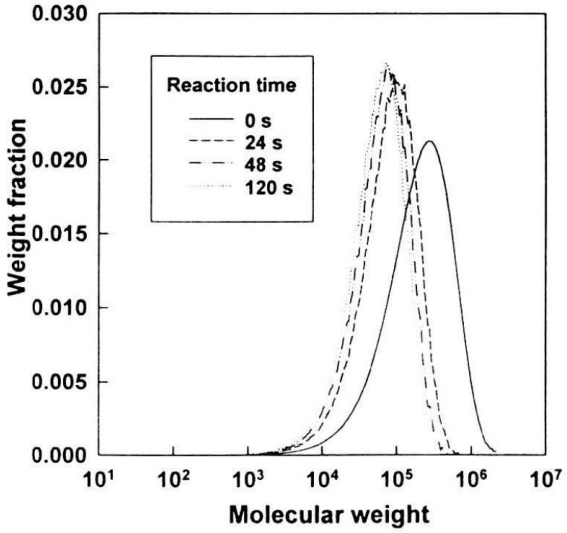

Figure 1- 18: Monte Carlo simulation of the time evolution of MWD.
Taken from Ref. [14].

Not only can chain breaking be predicted by MC simulation, but also is the crosslinking during degradation [127,128]. Staggs proposed a model to simulate random scissions of linear polymers that can accurately validate TGA results and

other MC numerical simulations. [135] Then this population-balance equation was implemented to describe the end-chain scissions and random recombination of PMMA [136,137]; the scission rate and recombination rate agree with TGA results well for the initial stages but not for the long time stages.

The kinetics of mechanisms for both chain scission and crosslinking have been studied using MC simulations. [138-141] The degree of degradation is determined to be highly related to the given rate constant for both linear and highly branched polymers. A more recent depolymerization study of linear polymers indicates that the best model is Avrami equation under isothermal and dynamic modes. [142] The Avrami equation is described by

$$y = \exp[-(k \cdot t)^q] \tag{1-9}$$

Where *y* is the relative mass loss, *k* is effective constant, *t* is time and *q* is the exponent.

MC simulations have also been incorporated with coarse-grained MD simulations as a bridge to provide an insight between experimental and numerical modeling for polymer systems. [15,143-148] Figure 1-19 reveals how the MD and MC simulations are bundled to study the degradation of PMMA. All the inputs are integrated into a MC simulation algorithm and the scheme is demonstrated as follows. In this unique approach, the coarse grain model of PMMA designed to allow chemical reaction[11] has been developed and used to create an integrated setup to investigate the thermal, mechanism and chemical process that might occur during later ablation. The MD simulations used were taken from Kim and coworkers [149] including two-body, three-body and nonbonding intermolecular and intramolecular interaction being described by Morse potential. The reaction pathways, Arrhenius reaction rates and formation energies are predetermined by theoretical, experimental database [150] or computing results using reactive MD[118]. The findings reveal the different pathways of photo energy absorption resulting in various transformations of the system and yield characteristics. The laser energy caused the initial damage along with higher temperature and stress resulted in breaking bonds.

Further propagations caused higher damage in the substrates surface resulting in high yield of fragments. Ablation then caused by phototherrmal and photochemical processes in combination.

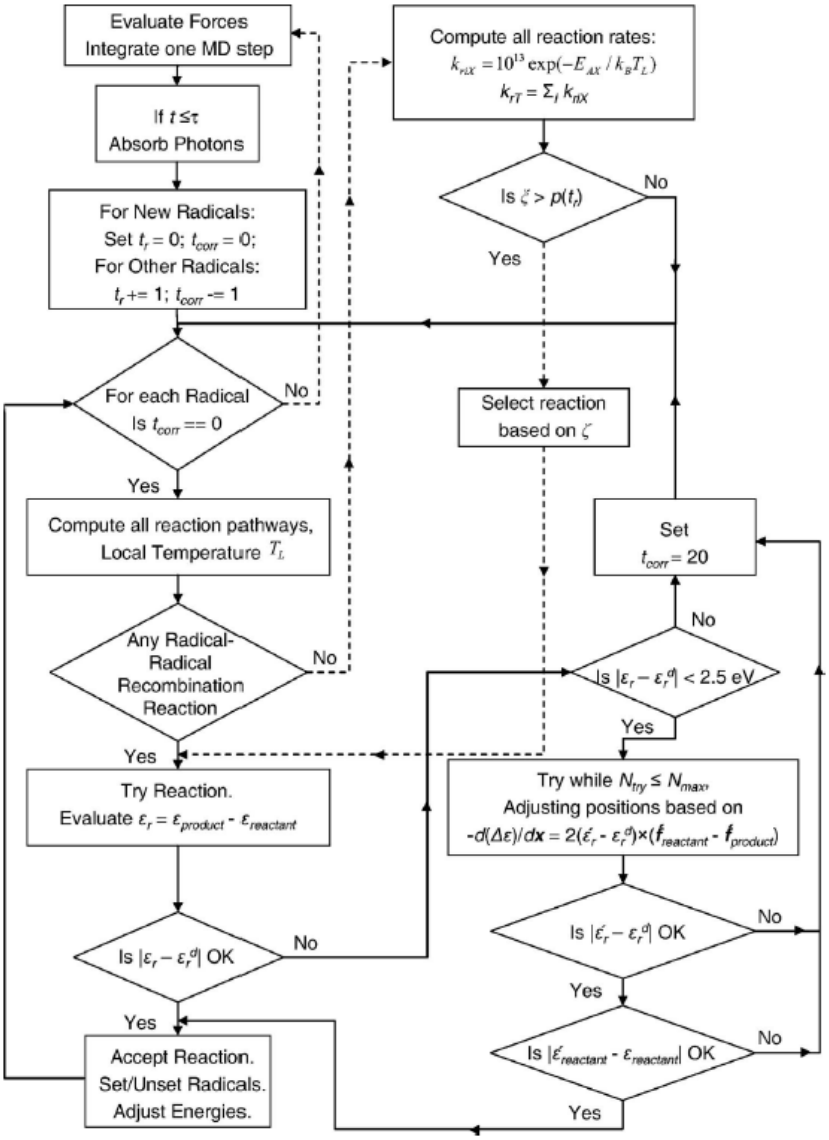

Figure 1- 19: Flow chart of Monte Carlo chemical reaction scheme embedded within the MD simulations. Dashed lines are only for visual clarity. Taken from Ref. [15].

Chapter 2: Use of molecular-dynamic simulations to study the thermal degradation of polyethylene

2.1. Introduction

Thermal degradation of polyethylene (PE) has been intensively studied. [24] Its degradation mechanism is so far known as a competition between chain scissions and crosslinking. Crosslinking is due to the existence of double bonds, which originate during polymerization. PE can be polymerized by either Ziegler catalyst or metallocene catalyst. Both synthesis methods will generate impurities in the form of unsaturated double bonds, which play an important role in crosslinking and thermal oxidation. The relatively high concentration of vinyl groups in Ziegler PE suggests that crosslinking might occur during melt-process and cause damage to the extruder. [24] Double bonds also exist in metallocene PE, causing crosslinking at lower processing temperature. [1]

Thermal degradation of PE in ambient air is also called thermal oxidation. It is believed to follow the mechanism [1] shown in Scheme 1. The initiation steps of degradation are mostly random chain scissions. Once radicals are formed, a series of reactions follow, which cause significant molecular weight loss. At 80-90 °C chain scissions occur more than crosslinking when PE undergoes thermal oxidation, and those chain scissions are believed to occur in the non-crystalline part inducing embrittlement. [2] Chain scission here means larger molecules breaking down into polymer fragments. At temperatures higher than 360 °C, the polymer fragments are small enough to escape and be detected. Toxic products such as CO and acrolein have been identified by gas chromatography during severe thermal oxidation of PE. [30]

To understand the thermal degradation of polyethylene, both physical changes and chemical reactions need to be considered at the molecular level. Here

molecular dynamic (MD) simulations with the ReaxFF force field [12] are used to describe both the physical interactions and chemical reactions of large scale systems. ReaxFF applies a relationship between the bond order and the bond length to get a smooth transition between the different types of bonds (non-bonds, single, double and triple bonds), and calculates the partial atomic charge depending on the geometry of the molecules. This force field has been used to study the thermal decomposition of poly(methylsiloxane) (PDMS) with around 1000 atoms. [97] At a heating rate of 266 K/ps, the onset temperature of PDMS degradation is around 2800 K and the decomposition initiated by Si-C bond cleavage formed CH_3 radicals. Note that the degradation temperature using ReaxFF will be higher than in experiment because the time-scale is different. Other than this thermal decomposition study, ReaxFF has also been used to study the effect of fillers such as carbon nanotubes (CNTs) and carbon fibers during the first stage of pyrolysis within a phenol formaldehyde system [100], the shock compression behavior of PE and poly(4-methyl-1-pentene) [93,103,104], the description of the hydrogen bonding between water molecules and a paper-like polymer film [13,106] and the oxidation of lignin model compounds [151].

In this work, molecular models of PE systems with several compositions are built for high temperature degradation studies. ReaxFF force field has been used to describe the chain scissions of PE chains during degradation process. The molecular weight of polymer systems shift lower as increasing target temperature, the modulus of degraded systems are found to shift lower. Oxygen plays a crucial role during thermal oxidation which has been investigated and its observable mechanisms have been reported. During thermal degradation, oxygen radicals are found to attack polymer chains resulted in early degradation and stable radicals and fragments such as OH radical and H_2O molecules.

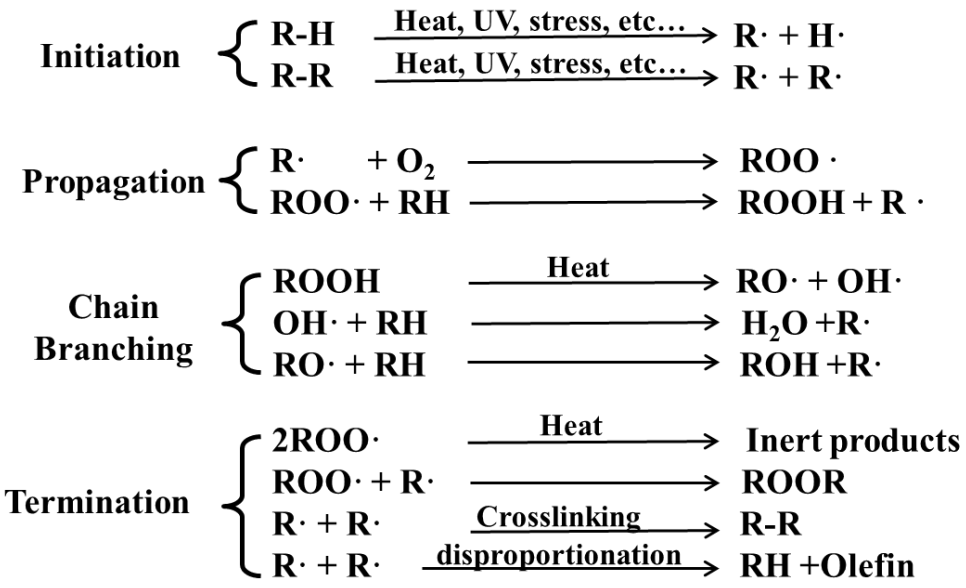

Scheme 2-1: Radical mechanism of the thermal degradation of polyethylene. Adapted from Ref. [1].

2.2. Methodology

As summarized in Table 2-1, we investigated various types of PE systems in this work, which are: pure PE systems with three different chain lengths, a pure PE system with mixed molecular weights, PE systems that contained terminal double bonds, and PE systems that contained oxygen species, and PE systems that contained oxygen species and terminal double bonds. All systems were built to be the same approximate size by atom counts. All simulations were conducted with the Large-scale Atomic/Molecular Massively Parallel Simulator (LAMMPS) software program [152] using the reactive force field, ReaxFF, [153] and the NPT ensemble (constant number of atoms, pressure, and temperature) at 1 atm with an 0.25 fs time step, and were performed at the High Performance Computing Center at NC State University. [154]

Table 2- 1: Details about the composition of each PE system in this study.

System name	Number of repeat units per chain	Number of PE chains per cell	Number of terminal double bonds	Number of O_2 molecules	Number of O• radicals	Wt. % of oxygen
PE10	10	640	0	0	0	0
PE40	40	160	0	0	0	0
PE160	160	40	0	0	0	0
PE-MWD	160	16	0	0	0	0
	40	64	0	0	0	0
	20	64	0	0	0	0
PE40-DB	40	160	160	0	0	0
PE40-O24	40	160	0	24	0	0.4
PE40-O624	40	160	0	624	0	10
PE40-Oa32	40	160	0	0	32	0.3
PE40-DB-O24	40	160	160	24	0	0.4
PE40-DB-O624	40	160	160	624	0	10
PE40-DB-Oa32	40	160	160	0	32	0.3

Preparation of Molecular Models. The polymer systems were built with Accelrys' Material Studio software [10] using the Amorphous Cell module, and then equilibrated in LAMMPS with ReaxFF for 100 ps at 300 K. For the pure PE systems, we chose three different chain lengths: with 10, 40 and 160 units per chain, which we will refer to as PE10, PE40, and PE160, respectively. PE10 contained 10 chains within the molecular model cell, which is then replicated to create a 4x4x4 supercell, resulting in a system with a total of 39,680 atoms. PE40 contained 20 chains in the simulation cell, and PE160 contained 5 chains, which were then both enlarged to a 2x2x2 supercell, resulting in a total of 38,720 and 38,480 atoms, respectively, in each system. Another PE system with mixed molecular weights was built, which we

will refer to as MWD-PE, which contains 64 chains of 10 repeat units, 64 chains of 40 repeat units, and 16 chains of 160 repeat units, resulting in 38,688 atoms.

For investigating the effect of the presence of double bonds in PE and/or oxygen species, we chose the systems with 40 repeat units of PE and 160 total chains in the cell due to proper calculation time and statistically reason. The systems that contained double bonds at both terminal ends of every polymer chain will be referred to as PE40-DB systems. For those that contain either oxygen molecules or oxygen radicals were built by using the Amorphous Cell module in Materials Studio, which randomly distributed the oxygen species in the simulation box. The systems that contain *x* oxygen molecules will be labeled as PE40-O*x*, and those that also contain terminal double bonds will be PE40-DB-O*x*, and those with terminal double bonds and *x* oxygen radicals will be labeled as PE40-DB-O*a*x. During the degradation simulations of PE systems containing oxygen molecules, only unstable fragments with oxygen molecules are found at lower level of O_2 concentration, 24 oxygen molecules in PE40 and PE40-DB. When increasing the O_2 counts to 624, the oxygen radials are formed and interact with polymer chains or fragments which then formed stable fragments. Therefore, 32 oxygen radicals were then added to accelerate the degradation.

MD simulations of polymer degradation. The simulation time (in the order of 10^{-10}-10^{-12} seconds) is short compared to real chemical reaction times. Therefore, high temperatures are needed to accelerate the thermal degradation.

In order to obtain the simulation temperature at which onset of degradation is observed ($T_{d,sim}$), we performed what is called a cookoff simulation, where the temperature of the equilibrated system was set to rise from 300 K to 3800 K in 50 ps (70 K/ps heating rate). Since bond breakages with ReaxFF [153] are defined by bond order, there will be some instances during the simulations where bonds are about to dissociate but it takes an extended period for the bond to truly break; thus, $T_{d,sim}$ is defined as the point at which the polymer chains start to truly break down. We determined that 70 K/ps is an acceptable rate to use by performing a cooking

simulation also at 7 K/ps, where we determined, for example, $T_{d,sim}$ of PE40-DB to be 1750 K under a heating rate 70 K/ps, and 1725 K when the heating rate is lowered to 7 K/ps.

The polymer degradation simulations were applied to PE40 by first raising the temperature from 300 K to the target temperature in 10 ps and then cool down to 300 K in 5 ps. Other polymer degradations are performed by first raising the temperature from 300 K to the target temperature in 10 ps, keep at target temperature for 90 ps and then cool down to 300 K in 10 ps. The output from LAMMPS (bond order and connectivity information is used as input of a C script to analyze the species and numbers of fragments at each time steps. The trajectory is viewed by VMD [155].

Calculate stress-strain curves. These calculations deform the system at a particular strain rate, and the stress response is recorded accordingly for both original system with no heat treatment and degraded system with heat treatment. All systems in Table 2-1 are first cooled down from their target temperature to 300 K before applying the strain, and limited bond breakage is observed during the cooling; we also included systems where no heat treatment is applied (and thus no to very limited degradation). The strain rate for each system was set at 10^{-9} s^{-1}, which was chosen because for strain rates higher than that, we observed an irregular spike in the stress response at low strains along with an increased temperature and additional broken bonds. No or limited bond breakage are found during the formation. To reduce random and temperature-related stress fluctuations that result from applying strains at the atomistic level, the stress is averaged further over a small time interval of 0.125 ps around the desired time point of the stress calculation. The modulus is calculated from 1% strain of the 10^{-9} s^{-1} strain rate.

2.3. Results and discussion

2.3.1. Determination of starting simulation temperature for degradation

We need to identify what temperature that the polymer substrate starts to degrade in the simulations. The onset degradation temperatures summarized in Table 2-2 and blue bars in Figure 2-2 are determined by the cookoff simulation with the temperature rising rate was set to 70 K/ps and starting at 300 K to 3800 K in 50 ps. For the shorter chain substrate, PE10, the polymer chains start to break at 1858 K, and are all cleaved by 3664 K. For the longer chain substrate, PE40, the polymer chains start to break at 1780 K and truly break at 1996 K which set as onset degradation temperature and are all cleaved by 3051 K. For the longest chain substrate, PE160, the polymer chains start to break at 1769 K and are all cleaved by 2688 K. In the beginning stage of bond breaking, the fragments sometimes reformed into the original polymer chain. Not until higher temperatures do the polymer chains remain cleaved. Thus, for all molecular weights, the degradation simulation temperature is around 2000 K. The onset degradation temperatures between those three systems do not change significant. Figure 2-1 are the snapshots taken from cookoff simulations of PE40. As the temperature is raised, small fragments start to appear as larger fragments also break into smaller fragments. However, chains in PE40 are all cleaved early than larger chain length systems. The longer the chain is, the higher the probability the bonds to be attacked. Since the degradation of PE40 happens around a simulation temperature of 2000 K, no fragments are observed at 10 ps (temperature ~1000 K) for both molecular weights. At 20 ps (temperature ~1700 K), some fragments are observed to form and then reform. As the system temperature approaches 2000 K, the fragments form more readily and propagate faster as temperature increases. At higher temperatures, the total number of complete polymer chains starts to disappear very fast coms along with abundance of small fragments. At the end of simulations, the C_2H_4 fragment is observed to

propagate much more than the other fragments. Only the snapshots of PE40 are presented since other systems during cookoff simulations behaves similar.

(a) 0 ps

(b) 20 ps

(c) 30 ps

(d) 35 ps

(e) 40 ps

(f) 50 ps

Figure 2- 1: Snapshots at a series of time steps from the MD simulations for PE40, (a) 0 ps, (b) 20 ps, (c) 30 ps, (d) 35 ps, (e) 40 ps and (f) 50 ps.

Table 2- 2: The observed and normalized onset degradation temperature ($T_{d,sim}$) from cookoff simulations, and the analysis of the degradation MD simulations. The cookoff simulations occurred from 300 to 3800 K in 50 ps, and the degradation simulations occurred from 300 K to target temperature (T_{target}) in 10 ps, then remained at T_{target} for 90 ps and then cooled to 300 K in 10 ps.

	PE10	PE40	PE160	PE-MWD	PE40-DB	PE40-O24	PE40-O624	PE40-Oa32	PE40-DB-O24	PE40-DB-O624	PE40-DB-Oa32
Onset $T_{d,sim}$ (K)	1858	1976	1769	1960	1711	1674	1839	1208	1693	1746	891
$T_{d,sim}$/ $T_{d,sim}^{PE40}$	0.94	1.00	0.90	0.99	0.87	0.85	0.93	0.61	0.86	0.88	0.45
T_{target}	2000	2000	2000	2000	2000	2000	2000	1300	2000	2000	1000
Initial N_{chains}	640	160	40	144	160	160	160	160	160	160	160
Final N_{chains}	584	118	7	95	109	102	101	126	101	106	138
Final % of N_{chains}	91.3	73.8	17.5	66.0	68.1	63.8	63.1	78.8	63.1	66.3	86.3
$N_{species}$ at T_{target}	34	73	91	87	89	88	87	40	98	96	12
Final N_{frag} (excluding O_2/O•)	829	394	337	485	460	478	459	198	473	438	238
Final $N_{ethylene}$	119	161	227	235	206	211	193	3	190	189	0
Final $N_{O2,Orad}$	n/a	n/a	n/a	n/a	n/a	24	619	2	24	620	12
Initial E (GPa)	4.7	10.5	15.4	12.6	12.2	13.4	~0	13.3	10.5	~0	12.5
E at T_{target} (GPa)	~0	~0	~0	~0	~0	~0	~0	~0	~0	~0	~0

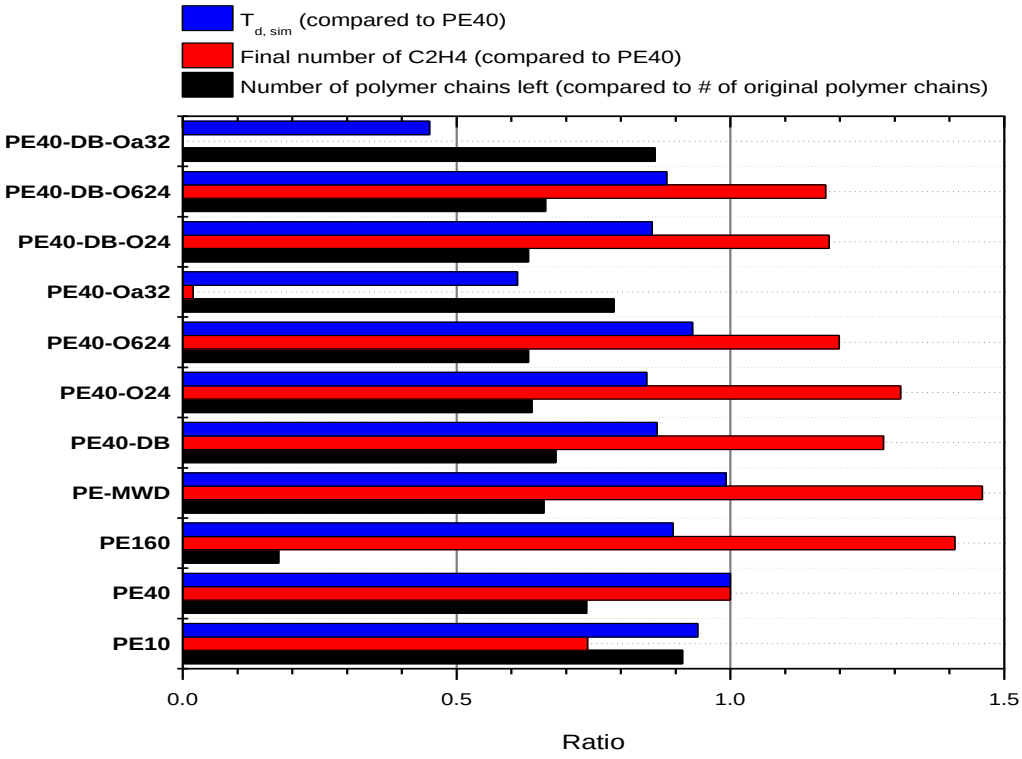

Figure 2- 2: Summary of the degradation MD simulations. Blue bars: percent difference from $T_{d,sim}$ of PE40; Red bars: final numbers of monomer fragments compared to PE40; Black bars: percent of intact polymer chains left at the end of the degradation simulation.

When the compositions of the polymer systems are changed, the onset degration shifted as well. The onset degradation temperature of PE-MWD which is a blend of PE10, PE40 and PE160 chains is similar to PE40. The system with each polymer chains of PE40-DB contains a double bond in the end are found to have lower onset degradation temperature and is less stable then PE40.

To study the effects of the presence of oxygen with simulations, oxygen molecules were added into the molecular model of the polymer systems. Systems

with various oxygen concentrations (0.4 and 10%) were made and tested with cookoff simulations. For the PE system, the onset simulation degradation temperatures decreases if there are oxygen molecules present in the system. For 0.4 wt%, the temperature drops to 1674 K, which is a 302 K drop compared to the pure PE40 system. However, adding up to 10 wt% of oxygen molecules was not observed to decrease the onset degradation temperature further. This observation may be because the 10 wt% of oxygen in the polymer melt might lead to the oxygen molecules interacting more with each other than with PE chains. The 10 wt% of oxygen molecules is also high, considering what is expected to exist during the melting process in reality.

With the present of oxygen molecules, the onset degradation temperatures are lower but not change much. The main interactions are found to occur between oxygen radicals broken from oxygen molecules. Adding oxygen radicals do accelerate the degradation and the onset degradation temperatures are found to significantly lower by 32% and 48% for PE40 and PE40-DB, respectively.

2.3.2. Effect of temperature on degradation and its corresponding modulus

After determined the onset degradation temperature, the PE40 systems are heated up to 5 target temperature, 1000 K, 1500 K, 2000 K, 3000 K, 4000 K in 10 ps and cooled down to 300 K in 5 ps to obtain degraded systems. Those degraded systems are then under the deformation with a strain rate of 10^9 s^{-1}. Table 2-3 are the detail information of PE40 at target temperatures. As the target temperatures get higher, less polymer chains and abundance of fragments can be found. The severe degradation causes large amount of fragments and species. At 4000 K, most of the fragments are further break into smaller fragments thus reduce the number of species found. Figure 2-3 contains the strain-stress curve for the degraded systems. Before degradation, the modulus of PE40 is calculated from the simulations to be 10.5 GPa. The modulus of the degraded systems drops significantly as compared to

the original polymer systems. The modulus of degraded systems at 1000 K and 1500 K are lowed to 3.1 GPa and 1.5 GPa, and dropped to almost 0 after 2000 K. After degraded at a simulation temperature of lower than 1500 K, the number of polymer chains does not change and those larger MW fragments help to maintain the modulus of the systems. However, as the target temperature goes beyond 2000 K, polymer chains break down into very small fragments which reduce the entanglements between polymer chains. There is a noticeable decrease in modulus compared to lower target temperatures.

Table 2- 3: Temperature Effects on PE40. PE fragment analysis as a function of final target simulation temperature and molecular weight. (Heat to target temperature in 10ps)

	PE40				
Target temperature (K)	1000	1500	2000	3000	4000
Actual temperature (K)	1001	1506	1996	3001	3986
Polymer chains left (#)	160	160	155	36	0
Polymer chains left (%)	100%	100%	97%	23%	0%
Total number of species at target temperature (#)	0	0	9	139	108
Total number of fragments at the end of simulation (#)	0	0	165	507	4331
Number of C_2H_4	0	0	0	106	2243
Cool down	From final temperature to 300 K in 5 ps				
Modulus (GPa) (strain rate: 10^9 s^{-1}) PE40: 7.1(1%)	3.1	1.5	0.7	0.6	0.5

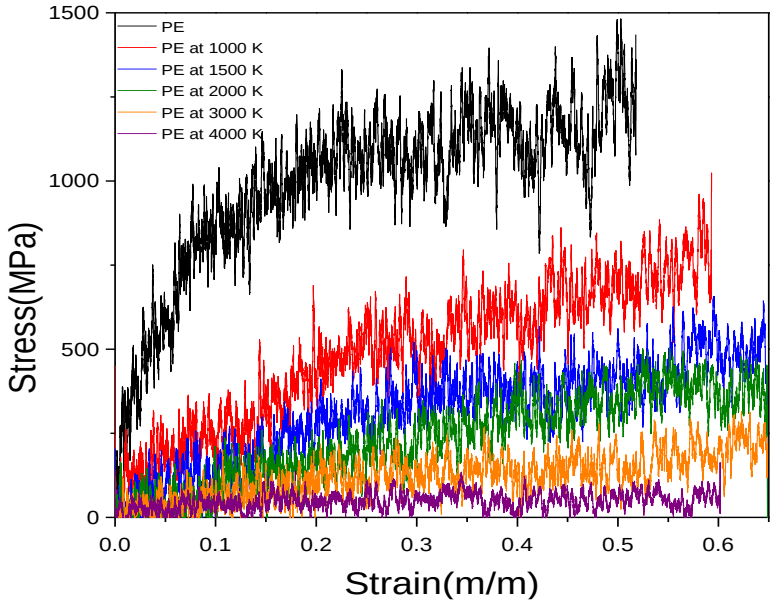

Figure 2- 3: The strain-stress curve for polymer systems of PE40 under stain rate 10^9 $s^{-1.}$

2.3.3. Effect of heating rate on degradation

The degradation of PE40 was observed in cooking simulations to start at around 2000 K, thus the substrate was heated up to 2000 K at different rates and maintained at this temperature for 40 ps. These conditions translate to a temperature rising rate ranging from 170-340 K/ps. The results are summarized in Table 2-4. Even though the temperature remains constant at 2000 K, the PE polymer chains are still breaking, thus there is a decreasing number of polymer chains and increasing number of small fragments. For different temperature rising rates to the target temperature of 2000 K, the rate that the original length PE polymer chains disappear does not change much. From here, the effect of final temperature is larger than the effect of heating rate.

Table 2- 4: PE fragment analysis as a function of molecular weight and of the rate to raising the temperature to 2000 K (and then the system remains at that temperature for 40 ps).

	PE40		
Rate to 2000 K (K/ps)	170	277	340
Polymer strands left (number)	133	135	131
Polymer strands left (percentage)	83%	84%	82%
Total number of species appear during degradation simulation (#)	126	124	127
Total number of fragments at the end of simulation (#)	222	243	233
Number of C_2H_4 at the end of simulation (#)	27	52	42
Final temperature (K)	1997	2007	1994

2.3.4. Effect of molecular weight on degradation.

From the work of Hoang and coworkers [6], metallocene PE with a wide molar mass distribution was determined to have a relatively lower extent of crosslinking and exhibit somewhat greater stability against degradation. Therefore, we are interested in investigating how polymer chains with different molecular weights play a role during thermal degradation.

All the pure PE systems are ran under degradation simulations with a temperature profile of heating to 2000 K in 10 ps, keep for 90 ps and then cool down to 300 K in 10 ps under isothermal and isobaric (NPT) conditions. Certain polymer chains have broken into large fragments during degradation simulations. Those larger fragments are further fall apart into smaller fragments and sometimes into C_2H_4 monomer as degradation time going by. PE160 system contains longest chains

and each chains has highest possibility to be attacked, therefore, less original chains, larger amount of C_2H_4 and higher amount of species are found at the end of degradation simulations. The smallest system, PE10, have 91% of original polymer chains left which is the highest ratio. However, those larger fragments came from original chains became more brittle and break much easier resulting larger quantity of fragments at the end of degradation simulations. Table 2-2 reveals the detail information of each systems after degradation simulations. The red bar and black bar in Figure 2-2 indicate the counts of monomer and the ratio of polymer chains left at the end of degradation simulations, respectively.

A PE-MWD molecular model was built with a distribution of polymer chains (unlike other PE systems which were built with only one length of polymer chains, or a polydispersity of one). There are 16 polymer chains with 160 units per chain, 64 polymer chains with 40 units per chain and 64 polymer chains with 20 units per chain in the PE-MWD system. In the single length PE40 system, the onset degradation simulation temperature is 1996 K at a heating rate of 70 K/ps. For the PE-MWD system, the polymer chains start to break around the same temperature. Among the different molecular weight chains, we observed that the polymer chains with the highest molecular weights disappear faster as compared to polymer chains with smaller molecular weights. Probably because they have less number of chains and have higher possibility being attacked.

2.3.5. Effect of presence of terminal double bonds and/or oxygen species on degradation.

During the production of PE, polymer chains sometime exists residue double bonds. Those double bonds are blamed as the reason of crosslinking. [54] To mimic the effects of double bonds, every polymer chains in PE40-DB contains one double bond in the chain end. The system containing double bonds is less stable then pure

system in terms of less polymer chains left and more monomers appeared after degradation simulation.

To study the fragment propagation in the existence of oxygen molecules, all equilibrated systems were heated up to 2000 K in 10 ps and kept at 2000 K except systems containing oxygen radicals for an additional 90 ps before cooling down to 300 K in 10 ps under isothermal and isobaric (NPT) conditions, and the results are given in Table 2-2. Most of the radicals were observed to result from breaking bonds of polymer chains. Those fragments are sometimes connected to O_2 molecules and form unstable radicals, which disappear within several picoseconds (10^{-12} seconds). Some oxygen molecules in systems with high O_2 loading break down into two oxygen radicals during heating, and those oxygen radicals are then connected to other fragments and form stable radicals such as OH and CH_2O and remain stable until the end of simulation.

From previous analysis of the fragment population for PE-O_2 systems, it takes time and also a high temperature for oxygen molecules to break to interact with polymer chains or fragments and to form stable radicals. Therefore, adding oxygen radicals into the polymer system might be able to accelerate the degradation under oxygen atmosphere. In order to set up the concentration of oxygen radicals, 32 oxygen radicals (0.3 wt%) were added into the PE40 and PE40-DB system.

From the cookoff simulations in Table 2-2, the onset degradation simulation temperatures are found to be 1208 K for the PE system with 32 oxygen radicals. The onset degradation temperature is significantly lower as compared to the pure PE system (1976 K) or the PE system with oxygen molecules (1674 K). Therefore, 2000 K as target temperature will be too high for systems containing oxygen radicals. Thus, the target temperature of the system was raised to 1300 K for PE40-Oa32 and 1000 K for PE40-DB-Oa32. From the fragments analysis, there are more small radicals observed and even H_2O and CO is observable. Since the target temperatures are set only a slightly higher than onset degradation temperature. Less degradation can be found during degradation simulations; however, those oxygen

radicals are much more active than oxygen molecules and attack polymer chains with high efficiency. Figure 2-4 is how oxygen radical interacts and subtracts hydrogen with polymer chains. At 0 ps, the oxygen radical stays near polymer chains. At 17 ps, one hydrogen of polymer chain has been subtracted by oxygen radicals form OH and stays until 52 ps. At 52 ps, the OH radical then obtain another hydrogen from another fragment and form H_2O which last until the end of degradation simulation. For PE40-DB-Oa32, 8 OH and 3 H_2O are found at the end of degradation simulation. Comparing to PE40-Oa32, 6 OH and 10 CH_2O, 1 H_2O are found. Unlike other systems, the systems containing oxygen radicals are found to have less C_2H_4 as residue fragments. The difference comes from lower target temperature and the higher reactivity of oxygen radicals. Lower target temperature causes less bond breakings and high reactivity of oxygen radicals result in more fragments interact with oxygen radicals instead of self-breaking.

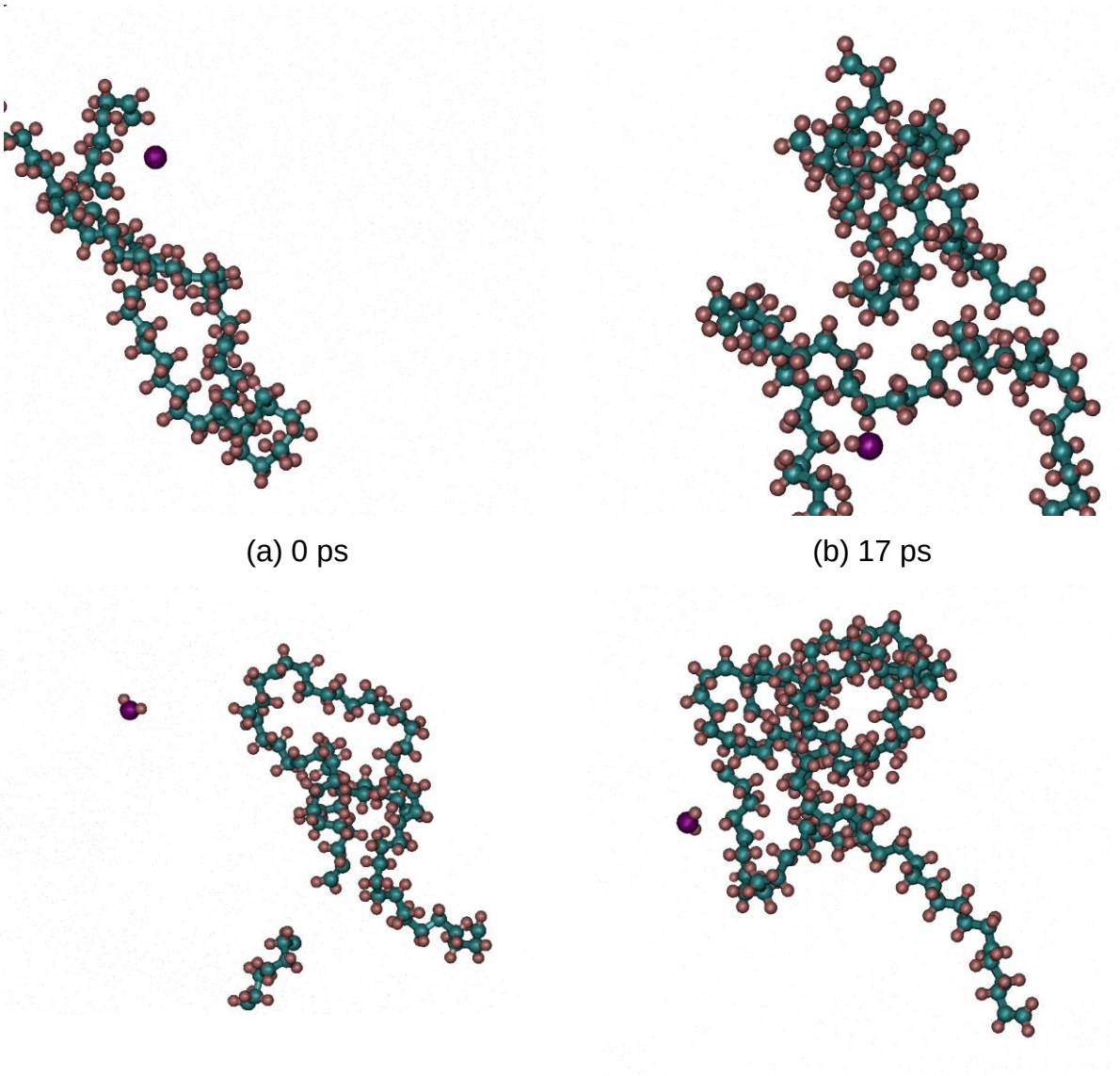

(a) 0 ps (b) 17 ps

(c) 52 ps (d) 109 ps

Figure 2- 4: Snapshots at a series of time steps from the MD simulations for DBPE40-Oa32 from degradation simulations at (a) 0 ps, (b) 17 ps, (c) 52 ps and (d) 109 ps.

To study the modulus changes of each system after degradation, both the original systems and degraded systems are subject to a deformation of strain rate 10^{-9} s^{-1} to

obtain the modulus. As expected, systems with larger Mw chains such as PE160 have higher modulus than systems with smaller Mw chains. Adding small amount of oxygen (~0.3 %) only increase the modulus a little bit. Increasing the oxygen concentration to 10% lowered the modulus to zero. The higher amount of oxygen can cause the loss of entanglement among polymer systems and resulting in zero modulus. After degradation simulations, each system experiences 9-83 % of polymer chain loss which directly deteriorates the modulus. The modulus after degradation become 0 after degradation.

2.4. Conclusions

MD simulations were approved to be able to provide molecular level information during thermal degradation. The chain scission mechanism of polyethylene during thermal degradation, with and without oxygen had been investigated in this research.

Among the processing conditions studied, temperature had the greatest effect to cause bond breaking. For the pure PE system, the onset degradation temperature is around 2000 K in MD simulations. If the system temperature kept a little higher than the onset degradation temperature, simulations indicated that the bonds continued to break, even though the thermal energy of the system didn't change overall.

The study of PE system with different molecular weight distribution revealed that the longer the polymer chain, the easier the bonds will break at lower temperature.

The presence of oxygen can accelerate the thermal degradation, which was described experimentally [30] was confirmed here. Several mechanism that have been proposed, [1] including chains breaking and oxygen attack, also occurred during thermal degradation performed by MD simulation. Due to the limitation of short time scale, oxygen radicals are observed to better describe the mechanism than oxygen molecules.

Chapter 3: Investigation of physical and chemical changes during thermal degradation of polypropylene

3.1. Introduction

Polypropylene (PP) is a commonly used polymer and its thermal degradation has been intensively studied. [7,19,27,54,156] Looking into PP chains, the tertiary carbons in its backbone, which comprises half of the backbone carbon atoms, are prone to attack. Thus the thermal stability of polypropylene (PP) can be challenging during mass production. Its degradation mechanisms have been identified to be initiated mainly by random chain scissions, similar to polyethylene. [25,31,32]. . After bond scission, primary radicals and secondary radical are formed and then rearranged into tertiary radicals, and β-scissions then lead to volatile products and a terminated double bond. Chain scissions that occur during thermal degradation reduce the total molecular weights and broaden the molecular weight distribution. [22,23] The changes of molecular weight distribution caused by thermal oxidation of PP are consistent with a homogeneous random chain scission process. [33] Afterwards, the loss of mechanical properties and embrittlement occur due to breaking of the chains in the tie area, which is the connection area between crystal part and non-crystal part of the polymer. [22,23]

Molecular dynamics (MD) simulations, which solve Newton's equations of motion to perpetuate the system of particles under particular thermodynamic conditions, is a useful tool for investigating polymer systems, including thermal degradation. It can be used to study pure PP properties,[66] since it is quite difficult to do so experimentally.[38] Another advantage of MD simulations is that it can be used to separate out the role of various factors, such as thermodynamics

(temperature, pressure), presence of impurities or additives, or environmental conditions. Additionally, a recent developed force field named reactive force field (ReaxFF) [12] is able to describe both the physical interactions and chemical reactions of large scale systems with an accuracy that can rival quantum chemistry while the computational time is akin to a classical MD simulation. Thus, the factors that trigger the thermal degradation of polymer systems can be investigated with MD simulations using the ReaxFF force field.

In this systematic study, two sets of polypropylene fibers were produced, one from commercial pellets and one from minimally stabilized polypropylene, which are extruded with a monofilament extruder with increasing extrusion temperatures. The molecular weight, rheological properties and mechanical properties of fibers were tested to investigate their differences. Additionally, MD simulations were performed to investigate the molecular details of the degradation process as a function of temperature and existence of oxygen radicals.

3.2. Methods

3.2.1. Materials

Two types of PP, one is pellet type and the other is flake type, are investigated. One is CP360H, supplied by Braskem America and a minimally stabilized PP resin (UPP), provided by Fibervision. For CP360H, the melt index under 446 °F/4.76lb (230 °C/2.16kg) is 36 g/10min provided by manufacturer. Minimally stabilized PP, UPP, supplied by Fibervision and its melt index under 230 °C/2.16kg is 36.1±3.7 g/10min measured by Meltflixer in the extrusion lab of the Nonwoven Institute at North Carolina State University.

3.2.2. Melt spinning process of polymer

To test the degradation behavior of polypropylene, PP fibers were produced using Fuji tester. Fuji tester is a monofilament extrusion with water bath quench; finish was applied before fibers are collected in the Hills testing line. During the trial runs, the extrusion temperatures were systematically increased from 200 °C to

320 °C. Drawn fiber samples were quenched with water bath and applied with finish. Drawn samples with 2.5 drawn rate and free fall samples were collected at a range of extrusion temperatures. Throughput is 10 g/min with single filament extrusion with corresponding bump speed. Samples were named as FJCP###, where ### referred to the extrusion temperature, for CP360H and FJUP### for UPP. Table 3-1 is the detail of process information for collected samples. At the extrusion temperatures of 200 and 210 °C for UPP, it was not able to collect draw sample because of the beating issue. At extrusion temperature higher than 330 °C for UPP, there was oily like product floating on the surface of water quench bath. It is suspected that UPP started to decompose into smaller oligomeric-like molecules thus the trial stopped due to unknown hazard.

Table 3- 1: Settings for the experimental testing

Sample name	*FJCP###*	*FJUP###*
Raw material	CP360H (pellet type)	UPP (flake type)
Extrusion temperature	200-320 °C	200-320 °C
Additional stabilizers	N/A	N/A
Pump speed	2.5	
Residence time	234 seconds	
Throughput	10 g/min	
Quench	Water bath	
Finish	10% larul PP912 @ 15% motor	
Draw conditions (Hills testing line)	Feed roll: 300 rpm @ 45 °C Draw roll: 750 rpm @ 35 °C Relax roll: 745 rpm @ 35 °C	
Draw rate	2.5	
Average diameter of fiber	~20	~14

3.2.3. Rheology analysis

Capillary rheology tests were conducted by a Rosand capillary rheometer manufactured by Malvern Instruments Ltd. A die with 1 mm diameter was used and the barrel length was 290 mm. The temperature was fixed as 230 °C. Due to the fixed barrel length, the testing time varies as a function of shear rate for degradation tests using the capillary rheometer. To simulate long time degradation, lower shear rate must be used (60/s was chosen which was lower than normal processing condition). Shear rate of 300/s which was closer to industrial conditions were used to study the degradation behavior. For all measurements, the pre-heat time were set as 9 minutes to ensure complete melting before analysis. The storage and loss modulus were measured with rotational rheometer by Fibervision, Rheometric Scientific Ares-M with RSI orchestrator software, which were performed in parallel plate geometry, 25 mm diameter of plate at a 2 mm gap. All tests were performed at a temperature of 230 °C and the frequency ranged from 0.1 to 400.

3.2.4. High temperature GPC/SEC (Gel Permeation chromatography/size exclusion chromatography) data

The molecular weight data were obtained from high temperature GPC and measured by Braskem America using Agilent 220 HTGPC with olexis columns. Polymer samples were dissolved in 1,2,4 trichlorobenzene and ran with same solvent at 150°C.

3.2.5. Mechanical tests

Tension was applied to a fiber to measure its tensile-stress response. A 5 N load cell was used. Single filaments with a gage length of 15 mm were drawn until fiber breakage. At least 10 specimens were measured for each fiber samples. After measurements, elongation and tensile strength were obtained.

3.2.6. Methodology for building PP simulation models

All simulations were conducted with the Large-scale Atomic/Molecular Massively Parallel Simulator (LAMMPS) software program [152] using the reactive force field, ReaxFF, [153] and the NPT ensemble (constant number of atoms, pressure, and temperature) at 1 atm with a 0.25 fs time step, and were performed on

the henry2 cluster at the High Performance Computing Center at NC State University. [154]

The molecular model of the amorphous PP system, called PP40, contained 20 chains, where each chain contains 40 units of monomer in the simulation cell which were then both enlarged to a 2x2x2 supercell, resulting in a total of 57,920 atoms. It was built using Accelrys' Material Studio software [10] with the Amorphous Cell module, and then equilibrated in LAMMPS with ReaxFF for 100 ps at 300 K.

3.2.7. MD simulations of polymer degradation

The simulation time (in the order of 10^{-10}-10^{-12} seconds) is short compared to real chemical reaction times. Therefore, high temperatures are needed to accelerate the thermal degradation process.

In order to obtain the simulation temperature at which onset of degradation is observed ($T_{d,sim}$), we performed what is called a cookoff simulation, where the temperature of the equilibrated system was set to rise from 27 °C to 3527 °C in 50 ps (70 °C/ps heating rate). Since bond breakages with ReaxFF [153] are defined by bond order, there will be some instances during the simulations where bonds are about to dissociate but it takes an extended period for the bond to truly break; thus, $T_{d,sim}$ is defined as the point at which the polymer chains start to truly break down.

The polymer degradation simulations were applied to PP40 by first raising the temperature from 300 K to the target temperature in 10 ps, keeping at target temperature for 50 ps and then cooling down to 300 K in 10 ps. The MD simulation trajectory was then analyzed for the species and numbers of fragments at each time steps.

3.2.8. Calculation of stress-strain curves from MD simulations

These calculations are done by deforming the system at a particular strain rate, and then recording the stress response. Stress-strain curves were generated for both the original PP system with no heat treatment and also the degraded system with heat treatment. All systems were first cooled down from their target temperature to 300 K before applying the strain, and limited bond breakage is

observed during the cooling. The strain rate for each system was set at 10^{-9} s^{-1}, which was chosen because for strain rates higher than that an irregular spike in the stress response was observed at low strains along with an increased temperature and additional broken bonds. No or limited bond breakage were found during the deformation. To reduce random and temperature-related stress fluctuations that resulted from applying strains at the atomistic level, the stress was averaged further over a small time interval of 0.125 ps around the desired time point of the stress calculation. The modulus was calculated from 1% strain of the 10^{-9} s^{-1} strain rate.

3.3. Results and discussions

3.3.1. Effects of temperature and shear rate observed from capillary rheometer tests for PP raw materials

Figure 3-1 is the shear viscosity changes measured under constant shear rate and temperature by capillary rheometer. The test duration is based on shear rate selection due to fixed barrel length of capillary rheometer. Lower shear rate of 60/s are performed to study long term degradation which polymer would stay at the barrel temperature at least 100 min. At the fixed temperature of 200 °C and 230 °C, the shear viscosity of both material remained relatively constant, indicating that there is no or limited degradation happening (*ie.* no or limited molecular weight changes). For CP360H, there was a 21% and 42% drop of shear viscosity after 108 minutes at 260 and 280 °C, respectively under 60 /s shear rate. For UPP, there was a 42% and 50% drop of shear viscosity after at 260 °C for 82 minutes and 280 °C for 96 minutes under 60 /s shear rate. As temperature increases up to and higher than 300 °C, the shear viscosity changes even more.

However, the shear rate of extruder that applied by industry ranging from hundreds to several thousands. [157] Considering the barrel length limit, the shear rate was rised up to 300/s and the total observation time was limited around 20 minutes. The shear viscosity at 200 °C and 230 °C remains stable but starts to decrease at 260 °C. For CP360H, there was a 12% and 17% drop of shear viscosity

after 20 minutes at 260 °C and 280 °C, respectively. For UPP, there was a 24% and 43% drop of shear viscosity after 20 minutes while staying at 260 and 280 °C. From Figure 3-1, the decreases in shear viscosity of UPP are faster than for CP360H. As the temperature goes up to 340 °C, UPP loses its 90% shear viscosity (from 125.6 poise to 12.6 poise) and it has almost no shear viscosity at such high temperatures.

There is a sudden decrease in the shear viscosity at 300 °C which indicates that the stabilizers burned out and protected the CP360H from degradation. However, as the temperature is heated up to 340 °C, there is still some more degradation that occurred as chain scissions and causes a drop in the shear viscosity. With no stabilizer protection, UPP has some molecular weight loss as the extrusion temperature increases and the Mw loss speeds up as the temperature increases.

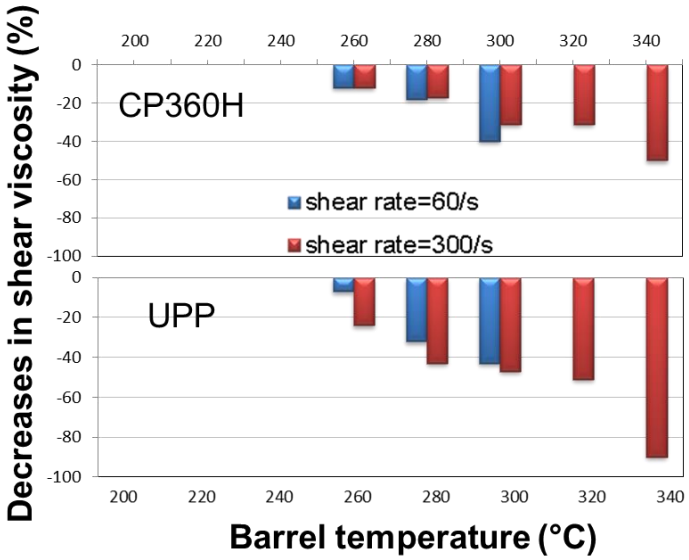

Figure 3- 1 : Degradation test at fixed shear rate, Shear viscosity changes at different shear rate and temperature for PP after the residence time of 20 minutes.

3.3.2. The changes of molecular weight and rheological properties of pilot samples

After identify the degradation behavior of raw PP, a pilot trial has been conducted using Fuji monofilament spinner. Both CP360H and UPP are extruded with changes of extrusion temperature from 200 to 320 °C and cold draw with 2.5 draw ratios. The molecular weights of fiber samples are measured by high temperature GPC and the results are presented in Figure 3-2. The Mw at 200 °C extrusion does not change significantly compared to raw material but decreases as extrusion temperature increases. Not surprisingly, the Mw of UPP decreases faster than CP360H as extrusion temperatures increase. With well stabilized, CP360H can maintain fairly good Mw until 300 °C and drop significant at 320°C.

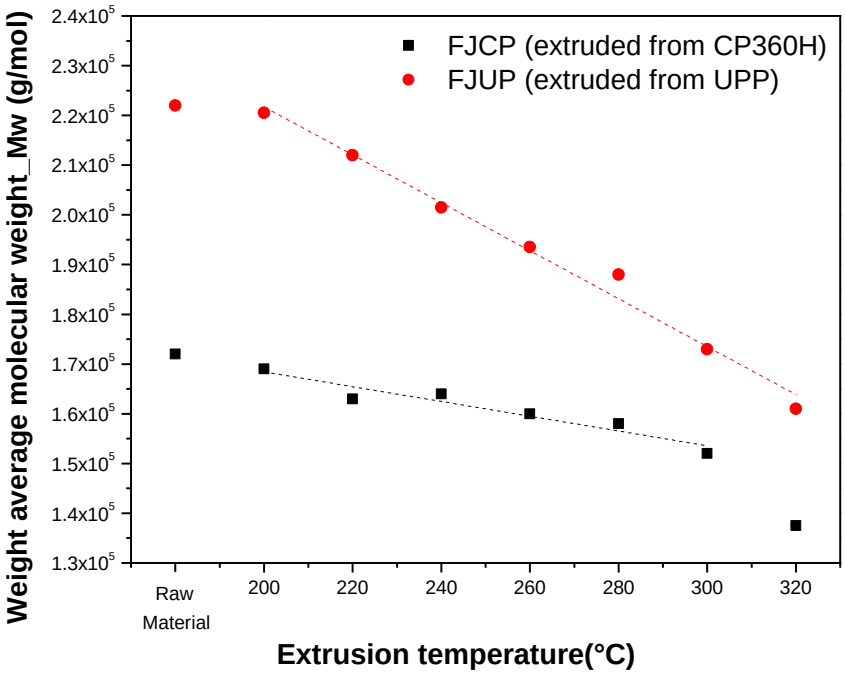

Figure 3- 2 : The weight average molecular weight data of extruded fiber samples as a function of extrusion temperature for CP360H and UPP obtained from high temperature GPC data.

To confirm the effect of molecular weight changes, the PP samples are tested over a low frequency range from 0.01 to 400 rad/s. There is a crossover modulus Gc obtained from crossover point of storage modulus G' and loss modulus G''. Figure 3-3(a) is an examples measured from UPP. The dynamic storage modulus G' represents the elastic modulus of viscoelastic materials while the dynamic loss modulus G'' refers to the dissipated energy. The crossover point of storage modulus (G') and loss modulus (G'') measured from rotational rheometry has found to be an indication of molecular weight reduction. [158,159] Decreasing of molecular weight (Mw) and increasing of molecular weight distribution (MWD) will move the crossover points of G' and G'' to higher frequency value and higher Gc. Higher molecular weight polymer chains are more highly entangled and therefore exhibit more elastic behavior. As the extrusion temperature increases, more chain scissions appear and the entanglements are reduced, followed with less elastic behavior. Therefore, the dynamic storage modulus (G') meets dynamic loss modulus (G'') at higher frequencies.

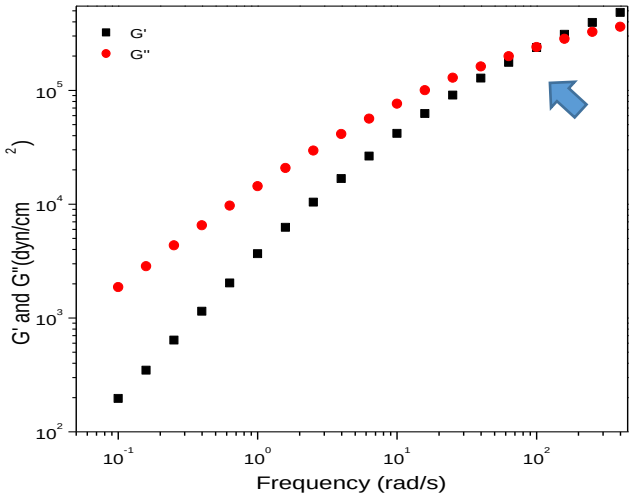

(a)

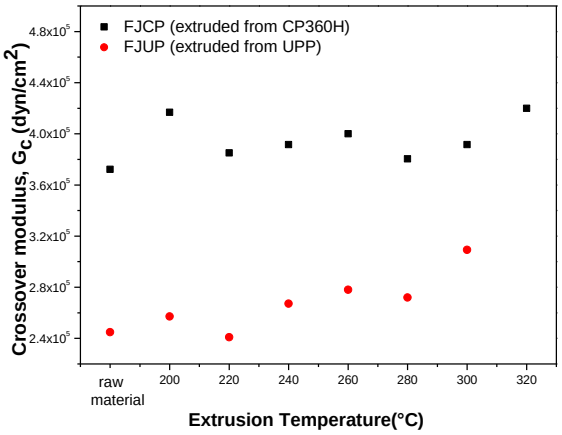

(b)

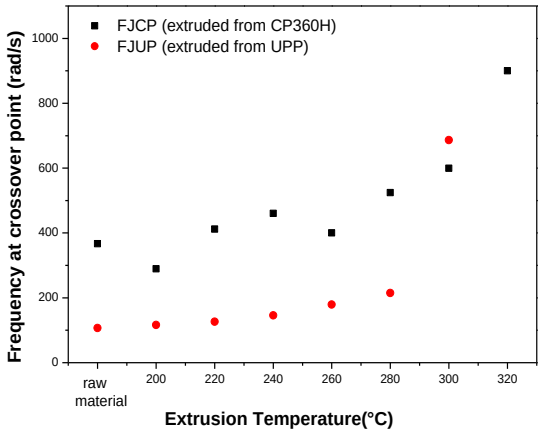

(c)

Figure 3- 3 : (a) Crossover modulus as a function of extrusion temperature obtained from rotational rheometry for UPP. Summary of (b) crossover modulus and (c) frequency at crossover point of extruded fiber samples.

In Figure 3-3 (b) and (c), the crossover modulus and its frequency are plotted as a function of extrusion temperatures to closely look at the degradation effects. The frequencies of crossover points over 400 rad/s are estimated by Controlled-Rheology method (Hercules calculation) [159] due to the crossover points go beyond measurement range. For FJCP, the crossover points at frequency and crossover modulus keep similar up to 300 °C which validate the results from capillary rheometer. For FJUP, the crossover modulus measured by rotational rheometer also validates that the Mw decreases gradually as extrusion temperatures increase.

In the capillary rheology tests for extruded polymer, share rate was fixed as 300/s at 230 °C to study the shear viscosity changes of extruded pilot samples. Figure 3-4 is the shear viscosity changes of CP360H and UPP samples both before and after extrusion at fixed shear rate and temperature. For CP360H, as soon as it is extruded, there is a tremendously drop in shear viscosity. However, there is no obviously difference of shear viscosity between extrusion temperatures from 200 to 300 °C. Not until extrusion temperature at 320 °C, there is another marked decrease. The shear viscosity of UPP drops gradually as extrusion temperature increases and speeds up at higher extrusion temperatures. It has been validated that the shear viscosity can be influenced by Mw and molecular weight distribution. [62] As the molecular weight decreased, the zero shear viscosity increased with 3.4 power for high molecular weight. [160,161] Here we are measuring shear viscosity at 300/s shear rate. Still the shear viscosity of UPP decreases gradually while the Mw of UPP decreases linearly, refer to Figure 3-2. For CP360H, both the shear viscosity and Mw remain at the same level when the extrusion temperatures are lower than 300 °C and drop significantly when the temperature goes to 320 °C.

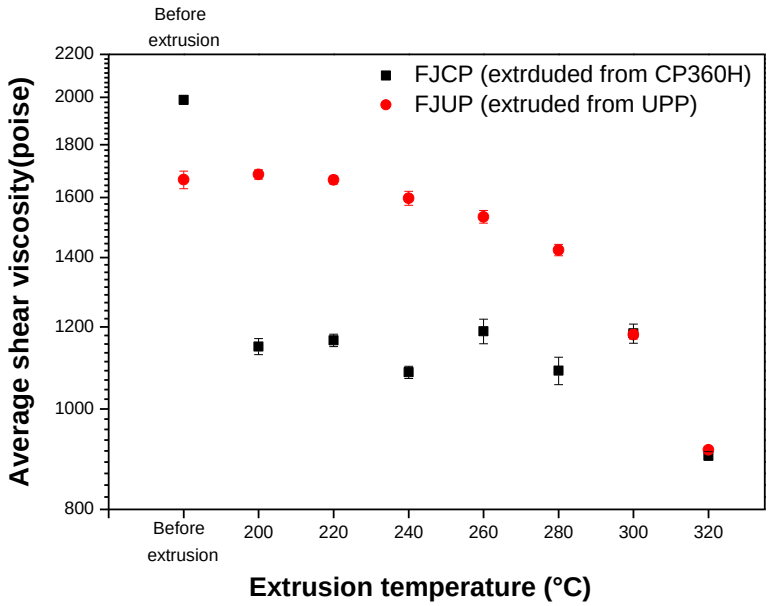

Figure 3- 4 : Average shear viscosity versus extrusion temperature of FJCP and FJUP samples from degradation tests for at 230 °C with 300/s shear rate.

3.3.3. Mechanical properties that are affected by the extrusion temperature

Figure 3-5 are the average mechanical properties of FJCP and FJUP samples extruded from 200 °C to 320 °C. The elongations of FJCP samples reach maximum at extrusion temperature 250 °C and then decrease as extrusion temperatures increase. The trend of tensile strength of FJCP samples decreases as extrusion temperatures increase due to the embrittlement at higher extrusion temperatures.

From previous study, decreasing in shear viscosity of FJUP samples indicates a loss of molecular weight. The broken polymer chains diminish the strength of entanglement in the amorphous area within the test filaments. Elongation and tensile stress at break decrease due to the lowered entanglement and smaller molecular weight. Also, the molecular weights of FJUP fibers are higher

than FJCP fibers; therefore, the tensile strengths of FJUP fibers are higher than FJCP fibers at the same extrusion temperature.

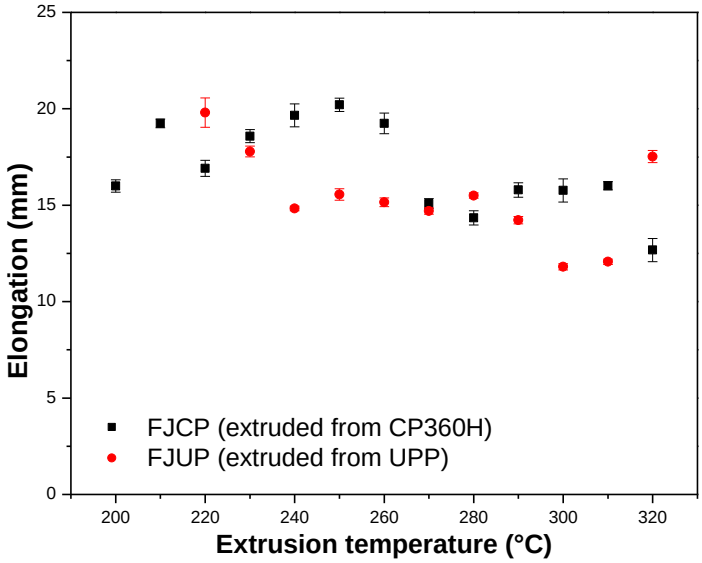

(a)

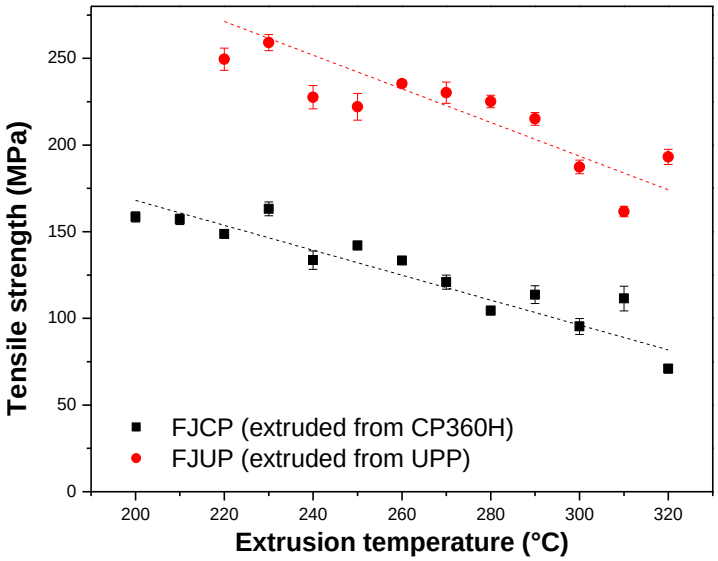

(b)

Figure 3- 5 : Mechanical properties of FJCP fibers (a) elongation and (b) tensile strength.

3.3.4. MD simulations of PP degradation.

To determine the onset degradation temperature, the PP40 system was heated to 3527 °C with a 70 °C/ps heating rate. The onset degradation temperature ($T_{d,sim}^{PP40}$) was defined as the temperature at which the first PP chain is observed to truly break; for PP40, it is 1427 °C.

To investigate how the elevated temperature affects the thermal degradation in term of chains breaking, the PP system was run with several heating-hold-cooling temperature profiles which also are called degradation simulations. Table 3-2 includes the composition of degraded systems and their calculated modulus values from these simulations. Therefore, when degrading PP40 at 0.51 $T_{d,sim}^{PP40}$ and 0.79 $T_{d,sim}^{PP40}$ °C, there is no breaking of polymer chains. As degradation temperature went up to 1.07 $T_{d,sim}^{PP40}$ °C, there is some degradation occurring but there still are 94% of polymer chains left. Polymer chains in the PP40 system which was heated up to 1.35 $T_{d,sim}^{PP40}$ °C are almost gone and lots of small fragments are observed.

Table 3- 2 : Polymer fragment analysis as a function of final target simulation temperature and molecular weight for PP40 system.

	PP40			
Target temperature (°C) $T_{d,sim}^{PP40}$ $T_{d,sim}^{PP40}$ = 1427 °C	0.51	0.79	1.07	1.35
Polymer chains left (number)	160	160	150	7
Polymer chains left (%)	100%	100%	94%	4%
Total number of species at the end of degradation simulation (#)	1	1	26	222
Total number of fragments at the end of simulation (#)	160	160	182	1947
Cool down	From target temperature to 300 K in 10 ps			
Modulus (GPa) @ 1% strain (strain rate: 10^9 s^{-1}) Original PP40: 10.44 GPa	**0.18**	**0.16**	**0.09**	**0.05**

All degraded systems are then deformed with a strain rate of 10^{-9} s^{-1} and the modulus values are calculated at 1% deformation. Figure 3-6 contains the strain-stress curve for the original and degraded systems. Before degradation, the modulus of PP40 is calculated from the simulations to be 10.44 GPa. The modulus of the degraded systems drop significantly when compared to the original polymer system, as expected. The modulus of all degraded systems are pretty low due to the long residence time of remaining at high temperatures. However, there are still differences at each temperature. After degraded at a simulation temperature of 1.07 $T_{d,sim}^{PP40}$, there are still some polymer chains left from the original system and fragments with larger molecular weights (MW). Those larger MW fragments help to maintain the modulus of the system. However, as the target temperature goes up to 1.35 $T_{d,sim}^{PP40}$ °C, all polymer chains break down into very small fragments and there is a decrease in modulus compared to lower target temperatures.

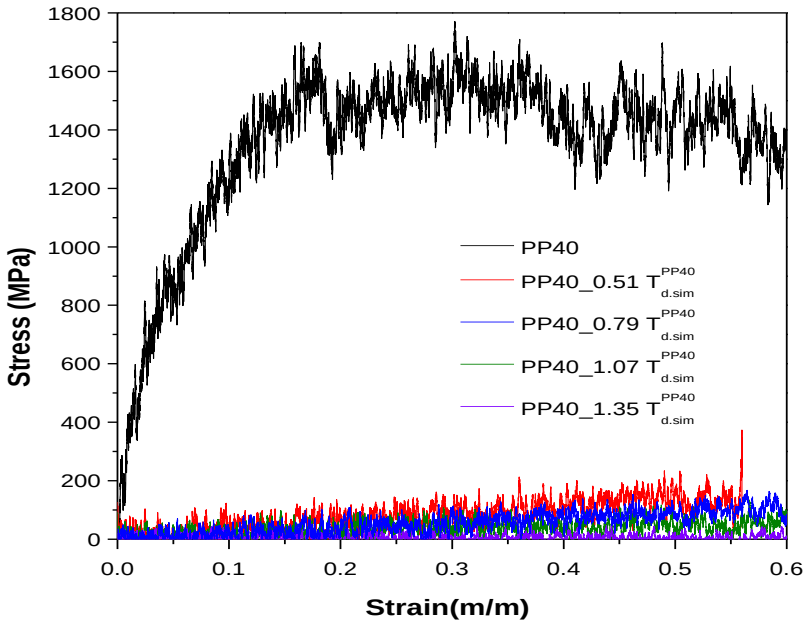

Figure 3- 6 : The simulated strain-stress curves for PP40 under a strain rate of 10^9 (1/s).

To investigate the oxygen effects on PP system, a system compositing from 160 PP40 chains and 32 oxygen radicals was built. The onset degradation temperature ($T_{d,sim}^{PPO}$) was determined as 861 °C after cookoff simulations. Table 3-2 includes the composition of degraded systems and their calculated modulus values from these simulations. There are few breaking of polymer chains when degrading PP_O at 0.5 $T_{d,sim}^{PPO}$ and 0.73 $T_{d,sim}^{PPO}$ °C. As degradation temperature went up to 0.96 $T_{d,sim}^{PPO}$, there is some degradation occurring but the majority polymer chains left. As the system temperatures heated higher than $T_{d,sim}^{PPO}$, the rate of polymer chains disappear much faster lots of small fragments are observed. Due to the high reaction in the system containing oxygen radicals, all the modulus of degraded systems went to zero.

Table 3- 3: Polymer fragment analysis as a function of final target simulation temperature and molecular weight for PP_O system.

	PP_O				
Target temperature (°C) $T_{d,sim}^{PPO}$ $T_{d,sim}^{PPO}$ = 861 °C	0.5	0.73	0.96	1.19	1.43
Polymer chains left (number)	157	158	150	126	123
Polymer chains left (%)	98.1	97.5	93.8	78.8	76.88
Total number of species at the end of degradation simulation (#)	6	5	8	23	44
Total number of fragments at the end of simulation (#)	189	191	191	190	207
Cool down	From target temperature to 300 K in 10 ps				
Modulus (GPa) @ 1% strain (strain rate: 10^9 s^{-1}) Original PP_O: 11.5 GPa	**0.3**	**0.6**	**0.01**	**0.01**	**0**

Figure 3-7 conclude the number of PP chains with original Mw left versus temperatures. At the temperature lower than the onset degradation temperature, most of the PP chains with original Mw survives. Once the temperature heated higher than $T_{d,sim}$ the PP chains with original disappear very fast. These observations reflect the experimental data that there is a critical temperature for PP, depending on the chosen material, where one must not pass the temperature to prevent severe degradation.

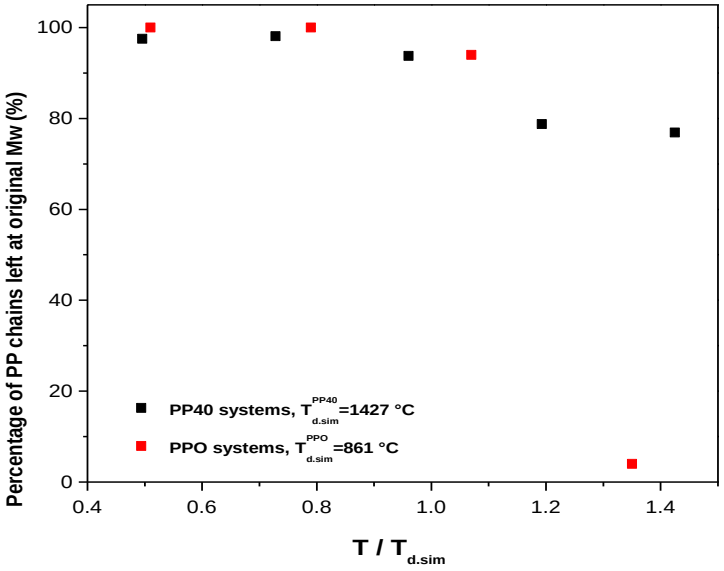

Figure 3- 7: The number of PP chains at original Mw left after degradation simulations of PP systems with and without oxygen radicals.

3.4. Conclusions

Comparing the commercial PP (CP360H) and minimally stabilized PP (UPP), the addition of stabilizers are highly recommended to minimize thermal degradation. From the degradation test of capillary rheology, both higher temperature and higher shear rate accelerate shear viscosity loss of UPP. For CP360H, thermal degradation still occurs at high temperature but shear rate does not effects shear viscosity much like UPP.

Those two PP materials are extruded at various temperatures and drawn to understand the thermal degradation effects on rheological and mechanical properties. Results from high temperature GPC indicate that both polymer experience molecular weight loss. For CP360H with properly stabilized, the slope of the loss of Mw versus extrusion temperature is smoother before extrusion

temperature of 300 °C and drops suddenly beyond that. For UPP, the slope is deeper and the molecular weight losses are more severe than CP360H. The shear viscosity which related to molecular weight validates the findings from High temperature GPC, instead of dropping linearly, the shear viscosity drooped gradually for UPP. For CP360H, shear viscosity only dropped beyond 300 °C for CP360H. The results measured at low frequency by rotational rheometer agree the finding from High temperature GPC and capillary rheometer.

The tensile strengths of drawn fiber are deteriorated by the thermal degradation caused by high extrusion temperature both UPP and CP360H. The elongation changes of CP360H do not significant while the elongations of UPP are lowered as extrusion temperature increases.

The computational simulations results indicate that high temperature will cause the PP chains to break due to its poor thermal stability. Adding oxygen radicals lowered the thermal stability of PP system by 40% indicated that the existence of oxygen radicals did resulted in faster thermal degradation. From the observation of chains breaking, there is a critical temperature that must avoid to prevent severe thermal degradation. Once go beyond the critical temperature which are $\boldsymbol{T_{d,sim}}$ in simulations, 280 °C for CP360H and 220 °C form UPP, noticeable thermal degradation occurred and resulted decreases in Mw and physical properties. PP chains relax during degradation simulations and lose the entanglements of chains that provide the mechanical properties. Therefore, stay at a higher temperature decrease the modulus significantly even though some polymer chains with original molecular weight are still alive.

Chapter 4: The study of chemical reactions during stabilization of polypropylene and its corresponding changes of physical properties

4.1. Introduction

Antioxidants and stabilizers are added to polymer materials to inhibit and limit degradation during processing and storage. [1,21,24,63,64] Thermal degradation during extrusion is caused by heat and is accelerated by oxygen. Degradation usually starts by initiators such as oxygen or radicals resulting from impurities. To protect polymers from degradation stabilizers are usually added, and they are categorized into two groups by their function. The first kind is a chain-breaking antioxidant, which helps retard oxidation during melt-processing. The second kind is a preventive antioxidant, which helps elongate the polymer shelf life. We focus on preventive antioxidants in this research. During the extrusion process, the polymers usually remain at a high temperature for a certain period of time. Thermal degradation occurs if there is not enough antioxidant to postpone the oxidation induction time (OIT), thus to limit degradation during melt-processing. Antioxidants help to maintain fiber properties such as strength, elongation, and tenacity by diminishing thermal degradation.

Three typical types of stabilizers are 1) phenolic antioxidants, 2) phosphite-type stabilizers and 3) hindered amine light stabilizers (HALS) [64]. Those stabilizers are widely used and especially important for PP to prevent thermal degradation during processing and usage. According to the category in Al-Malaika's research [1], phenolic antioxidants usually attack primary oxidation cycle and prevent polymer chains from further propagation. Phenolic antioxidants are also called chain-breaking antioxidants, which can be categorized by their functionality as donors or acceptors.

Chain breaking donors (CB-D), such as Irganox 3114, compete with radicals and prevent hydrogen abstraction from the polymer. A CB-D prevents thermal degradation by donating a hydrogen to react with radicals, and thereby forming stable fragments. A chain breaking acceptor (CB-A), such as Irgastab FS042, reacts with radicals directly to form stable fragments.

To visualize the chemical changes during extrusion that cause thermal degradation, we use molecular dynamics (MD) simulations, which solve Newton's equations of motion to perpetuate the system, to study the interaction between oxygen molecules, stabilizers and polymer chains. [66] The force field applied in this research is called ReaxFF [12]. It is able to describe both the physical and chemical reactions of large-scale systems. Unlike classical MD simulations, which do not incorporate chemical reaction, ReaxFF force field applies a relationship between the bond order and the bond length to get a smooth transition between different types of bonds (not bonded, single, double, and triple bonds). ReaxFF also calculates charges, depending on the geometry of the molecule. Thus, it accounts for polarization effects and differentiates itself from other non-reactive force fields. This force field has been used to study the thermal decomposition of poly(methylsiloxane) (PDMS) [97], the effect of fillers such as carbon nanotubes (CNTs) and carbon fibers during the first stage of pyrolysis within a phenol formaldehyde system [100], the shock compression behavior of polyolefins [93,103,104], the description of the hydrogen bonding between water molecules and a paper-like polymer film [13,106] and the oxidation of lignin model compounds [151].

In the experimental research presented here, two sets of polypropylene fibers with the addition of phenolic and nonphenolic stabilizers were made by extrusion with increasing temperatures. The molecular weight, rheological properties, and mechanical properties of fibers were tested to investigate the stabilizers effects. Additionally, molecular models of PP systems, with oxygen molecules and stabilizers, were built to study high temperature degradation. The ReaxFF force field has been used to describe the chain scission of PP chains and the interaction of

stabilizers during degradation process. Oxygen plays a crucial role during thermal oxidation, and stabilizers are added to prevent oxygen from attacking polymer chains. Both of the interactions have been investigated and its observable mechanisms have been reported.

4.2. Experimental and theoretical (computational) methods

4.2.1. Materials

Minimally stabilized PP, UPP, supplied by Fibervision and its melt index under 230 °C/2.16kg was 36.1±3.7 g/10min measured in the extrusion lab of the Nonwoven Institute at North Carolina State University. Stabilizers added to minimally stabilized PP are supplied by BASF. Irgastab FS301 was a pre-mixed non-phenolic stabilizer containing Irgafos 168, photoantioxidant, and Irgastab FS042, melt stabilizers. One phenolic stabilizer was dry blended with Irgafos 168 and Irganox 3114 to compare the effects of different stabilizers. Their chemical structures were displayed in table 4-1.

Table 4- 1: The chemical structures of stabilizers

Stabilizers trade name:	Irgafos 168	Irganox 3114	Irgastab FS 042
category	Photoantioxidants	Melt stabilizers	Melt stabilizers
Chemical structure	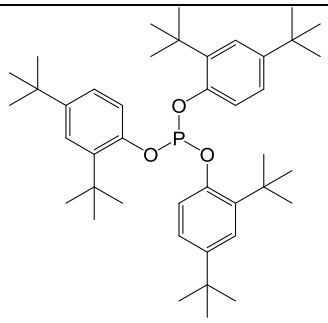	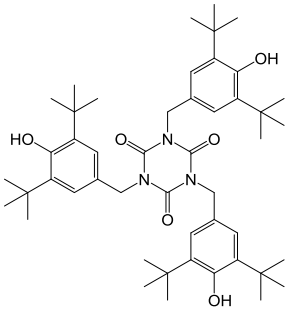	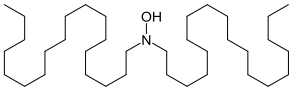

4.2.2. Pilot run for stabilizers added PP

To test the degradation behavior of polypropylene with various stabilizers, PP fibers were produced using Fuji tester. Fuji tester was a monofilament extruder with water bath quench; finish was applied before fibers were collected in the Hills testing line. During the trial runs, the extrusion temperatures were systematically increased from 200 °C to 320 °C. Drawn fiber samples were quenched with water bath and applied with finish. Throughput was 10 g/min with single filament extrusion with 2.5 bump speed. Samples were named as UPP###, where ### refers to the extrusion temperature, for minimally stabilized PP; ph-PP### and nonph-PP### for UPP with addition of phenolic and non- phenolic stabilizers. Table 4-2 was the detail of process information for collected samples. The pump speed was set as 2.5 rpm to collect freefall and draw samples. At extrusion temperature higher than 330 °C, there was oily like product floating on the surface of water quench bath. It was suspected that polymer started to decompose into smaller oligomeric-like molecules thus the trial stopped due to unknown hazard.

Table 4- 2: Settings for the experimental testing

Sample name	UPP	*ph*-PP	*nonph-PP*
Raw material	UPP (flake type)		
Extrusion temperature	220-320 °C		
Additional stabilizers	N/A	Iragfos 168: Irganox I3114=1:1 (0.2% or 0.4%)	Iragstab FS 301 (0.2% or 0.4%)
Pump speed	2.5		
Residence time	234 seconds		
Throughput	10 g/min		
Quench	Water bath		
Finish	10% larul PP912 @ 15% motor		
Draw conditions (Hills testing line)	Feed roll: 300 rpm @ 45 °C Draw roll: 750 rpm @ 35 °C Relax roll: 745 rpm @ 35 °C		
Draw ratio	2.5		

4.2.3. High temperature GPC/SEC (Gel Permeation chromatography/size exclusion chromatography) analysis

The molecular weight data were obtained from high temperature GPC and measured by Braskem America using Agilent 220 HTGPC with olexis columns. Polymer samples were dissolved in 1,2,4 trichlorobenzene and ran in the column with same solvent at 150°C.

4.2.4. Rheology analysis

Rheology tests were conducted using a Rosand capillary rheometer manufactured by Malvern Instruments Ltd. A 1 mm diameter die was used and the barrel length was 290 mm. For all measurements, the pre-heat time were 9 minutes

to ensure complete melting before analysis. Barrel temperature was fixed as 230 °C and Shear rate of 300/s which was closer to industrial conditions were used to study the melt behavior.

The storage and loss modulus were measured by rotational rheometer, Rheometric Scientific Ares-M with RSI orchestrator software, which were performed in parallel plate geometry, 25 mm diameter of plate at a 2 mm gap. All tests were performed at a temperature of 230 °C and the frequency ranges from 0.1 to 400 rad/s.

4.2.5. Mechanical tests

Tension was applied to a fiber to measure its tensile-stress response following ASTM D3822. A 5 N Load cell was used. Single filaments with a gage length of 15 mm were drawn until fiber breakage. At least 10 specimens were measured for each condition. After measurements, tensile strength and elongation were obtained.

4.2.6. Computational settings for addition of stabilizers

Polymer systems were built as an amorphous cell with stabilizers randomly distributed in the simulation box. Each system has 20 polymer chains with 40 repeating units, 4 oxygen radicals and 1 stabilizer (chemical structures are given in Table 4-1). For statistical purposes, we made three different randomized molecular models for each polymer-stabilizer pair. All simulations were conducted with the Large-scale Atomic/Molecular Massively Parallel Simulator (LAMMPS) software program [152] using the reactive force field, ReaxFF, [153] and were performed at the High Performance Computing Center at NC State University. [154] During equilibration, the polymer systems remained at 27 °C for 100 ps under isothermal and isobaric (NPT) conditions. These equilibrated systems are then ready for further simulations.

4.2.7. Computational settings for “cookoff” and degradation simulations

After equilibration, the temperature of the equilibrated systems were set to rise from 27 °C to 2127 °C in 300 ps (7 °C/ps heating rate) to identify the onset degradation temperature; this type of simulation was called a cookoff simulation. [162] The onset degradation temperature was defined as the temperature where the polymer chains start to truly break down. Bond breakings with ReaxFF are defined by bond order; therefore, there will be some instances where bonds were about to dissociate but it took a while for the bond to truly break during the simulations.

During degradation simulations, the system temperature was increased from room temperature to the target temperature with a heating rate 7 °C/ps, and then the system was held at the target temperature for at least 600 ps. The target temperatures were set as 237, 307, 517 and 727 °C for stabilized PP systems.

4.3. Results and discussions

4.3.1. Changes in molecular weight during melting process

Polymer is suspicious to degrade after the melt processing in the form of losing molecular weight. Polypropylene chains are usually truncated during the high temperature processing. In Figure 4-1, the weight average molecular weight (Mw) of PP samples are measured. The molecular wright of UPP lowered after extrusion and dropped monotonically with increasing extrusion temperature.

To diminish the thermal degradation, one phenolic type and one non-phenolic type of melt stabilizers are added. With the addition of phenolic stabilizers, the Mw remains similar and significant drops can only be found at 320 °C with stabilizer loading of 0.2 wt%.

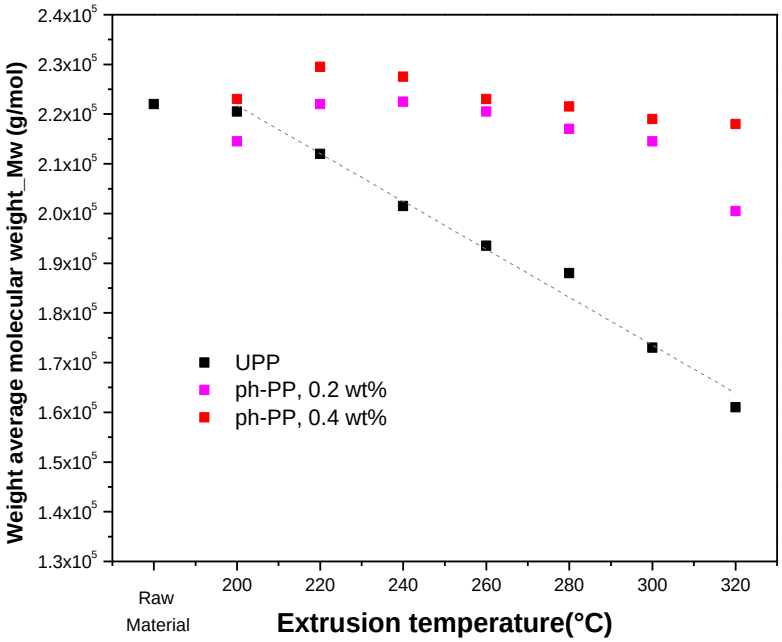

Figure 4- 1: The molecular weight of fiber samples measured by high temperature GPC (HSEC).

4.3.2. Viscosity via capillary rheology tests

Decrease of molecular weight affects viscoelastic behavior of polymer. During the testing of capillary rheometer, the barrel temperature is fixed as 230 °C and the shear rate is fixed 300/s. At the temperature of 230 °C, there should be limited thermal degradation that causes changes in molecular weight. Therefore, the difference in shear viscosity indicates the changes in molecular weight. Figure 4-2 is the average shear viscosity during 20 minutes test measured at 300/s shear rate and 230 °C. The average shear viscosity of UPP, minimally stabilized PP, decreases gradually as extrusion temperatures increase from 200 °C to 320 °C and dropped 45 % at 320 °C. Indicating the molecular weight reduces by thermal degradation when melt processing the UPP. By adding the phenolic stabilizers, the shear viscosities increase a little bit and remain smooth even when the extrusion temperatures go up to 280 °C. The shear viscosity drops only at 300 °C for smaller loading 0.2 wt% while

it remains constant for higher loading 0.4 wt%. However, the nonphenolic stabilizers do not maintain the shear viscosity of PP for both 0.2 and 0.4 wt% loading and its shear viscosity drops in a similar fashion to the UPP. At a extrusion temperature higher than 300 °C, the shear viscosity dropped even more than UPP. From the results, the phenolic stabilizer with proper loading can help prevent thermal degradation of PP during thermal extrusion up to 320 °C.

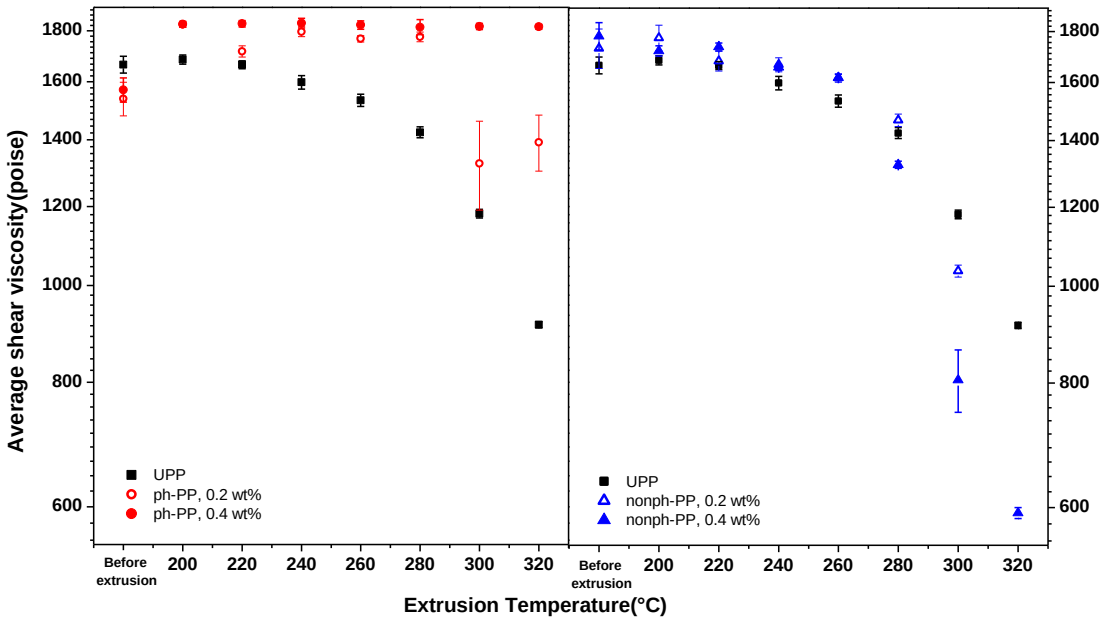

Figure 4- 2: Average shear viscosity during 20 minutes at 300/s shear rate and 230 °C of UPP, ph-PP (phenolic stabilized UPP) and nonph-PP (nonphenolic stabilized UPP). Square black is for UPP, circle is for ph-PP and triangle for nonph-PP with halo symbol is for 0.2 wt% loading while solid symbol for 0.4 wt% loading.

4.3.3. Viscosity via rotational rheology tests

To a more accurate estimation of molecular weight changes, the PP samples are testing over a low frequency range from 0.01 to 100 rad/s by rotational rheometer. There is a crossover modulus Gc obtained from crossover point of storage modulus G' and loss modulus G''. The dynamic storage modulus G' represents the elastic modulus of viscoelastic materials while the dynamic loss modulus G'' refer to the dissipated energy. The crossover points of storage modulus (G') and loss modulus (G'') measured from rotational rheometer have found to be an indication of molecular weight reduction. Detail explanation please refers to Chapter 3.3.2. [158,159]

In Figure 4-3 (a) and (b), the crossover modulus and its frequency are plotted as a function of extrusion temperatures to closely look the degradation effects. The frequencies of crossover points over 400 rad/s are estimated by Controlled-Rheology method (Hercules calculation) [159] due to the crossover points go beyond measurement range. Adding 0.2 wt% of ph-PP stabilizers into UPP successfully limits the thermal degradation up to 280 °C extrusion temperature. Increase the stabilizers loading to 0.4 wt% do help to prevent degradation at all extrusion temperatures studied. However, adding the non-phenolic stabilizers do not significantly help preventing thermal degradation. In fact, both the 0.2 and 0.4 wt% stabilizers loading prompt the MW loss at extrusion temperatures higher than 260 °C. The findings agree with the results observed from capillary rheometry.

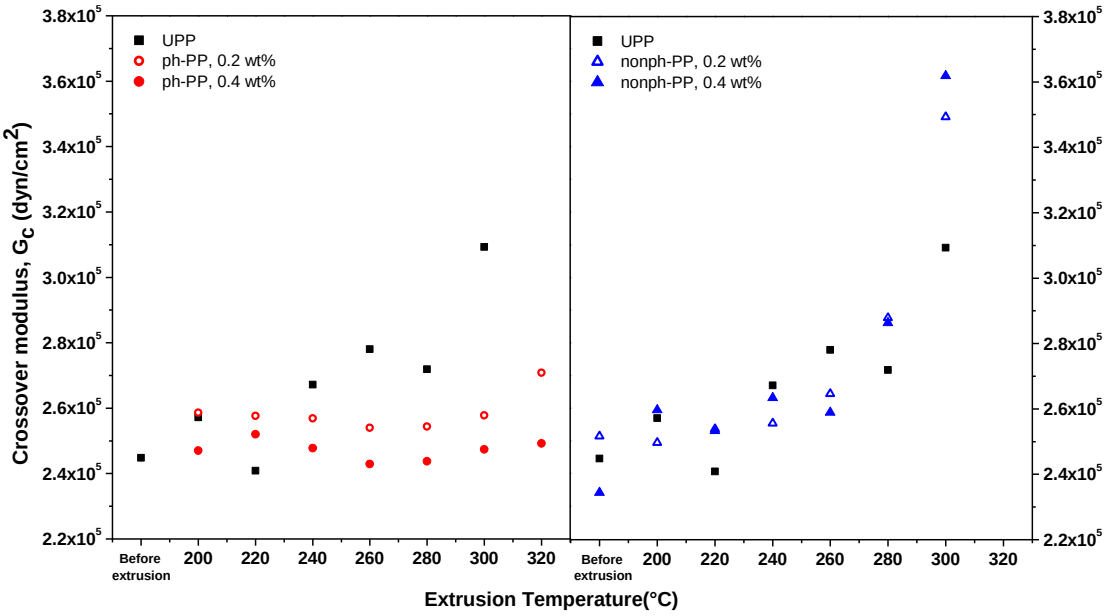

(a)

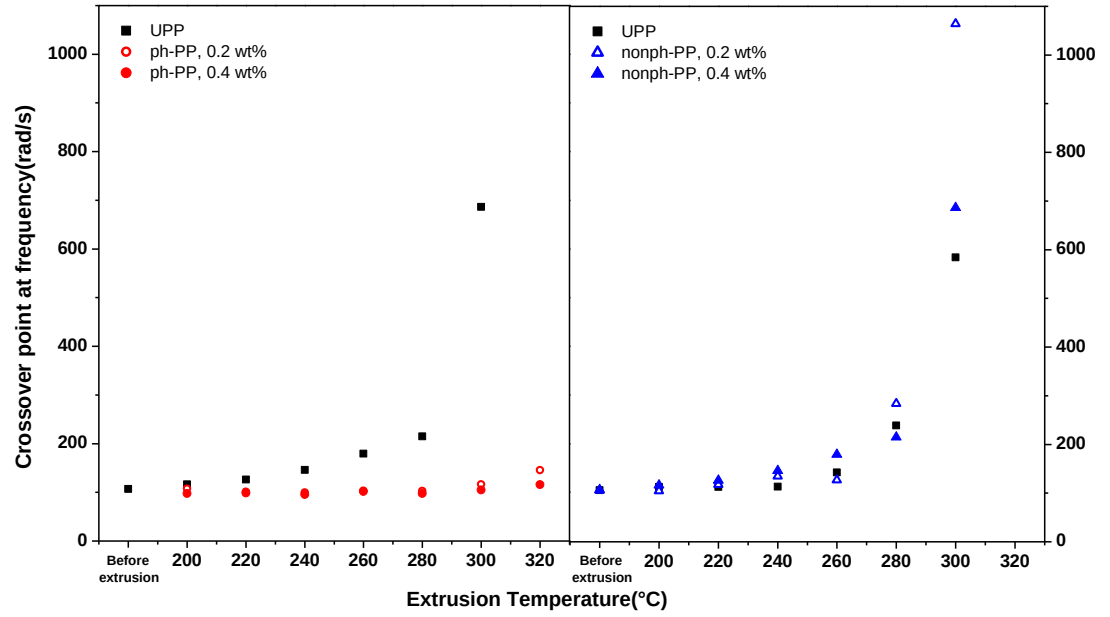

(b)

Figure 4- 3: (a) The crossover modulus (G_c) of minimally stabilized polypropylene (UPP) ,phenolic stabilized PP (ph-PP) and nonphenolic stabilized PP (nonph-PP) and (b) the frequency at the crossover point of G' and G'' for UPP, ph-PP and nonph-PP. Note: The frequency of crossover points over 400 rad/s are estimated by Hercules calculation. Square black is for UPP, circle is for ph-PP and triangle for nonph-PP with halo symbol is for 0.2 wt% loading while solid symbol for

0.4 wt% loading.

4.3.4. Changes in mechanical properties

Figure 4-4 is the data of mechanical properties of PP fibers. The elongations of UPP decrease as extrusion temperatures increase. By adding 0.2 wt% phenolic stabilizers, the elongation of fibers are improved. Even though the elongation decreases a little bit at high extrusion temperatures such as 320 °C, it still remains good enough compared to UPP. By increasing the loading to 0.4 wt%, the elongation of ph-PP at 220 °C goes up to 1.75 ratios compared to UPP. However, the elongation drops quickly as extrusion temperature increases and goes below UPP at 320 °C. The changes of nonph-PP elongation are another story, for both 0.2 and 0.4 wt%, the elongation goes a little bit higher than UPP at temperatures lower than 240 °C but diminished at extrusion temperatures higher than 260 °C. At the same extrusion temperatures, there are more entanglements of fibers for ph-PP because of the larger Mw. Thus, higher elongation will be observed like ph-PP extruded lower than 260 °C and nonph-PP extruded lower than 240 °C. If the chains are breaking, less orientation of polymer chains leads to higher elongation since polymer chains need to be aligned during strain. As the extrusion temperatures increase, there should be less orientation due to more relaxations at higher temperatures; so if the chains are not breaking, then the elongation would be expected to increase with extrusion temperature. From previous section, the molecular weights of fibers at higher extrusion temperature have decreased; therefore, the elongation drops. By adding stabilizers, the chain scissions that usually occurred during melt process are reduced at lower temperature; therefore, the elongations improve at lower extrusion temperatures. As the stabilizers consumed faster at higher temperature and produces more radicals, the elongation decreases faster and sometimes goes below UPP at high extrusion temperatures even with the addition of stabilizers.

The tensile strength is correlated to Mw since larger Mw provides more entanglement which resulted in higher tensile strength. The chain scissions occur in

the tie area causes less entanglements, thus lower tensile strength. Therefore, the tensile strength at break indicated a descending trend for UPP and nonph-PP but fairly flat for ph-PP.

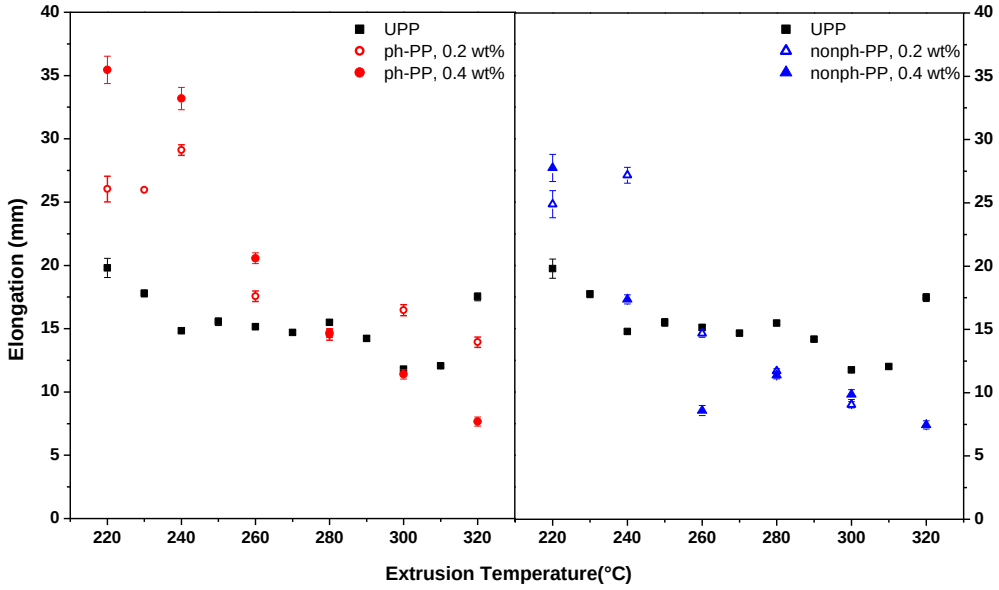

(a)

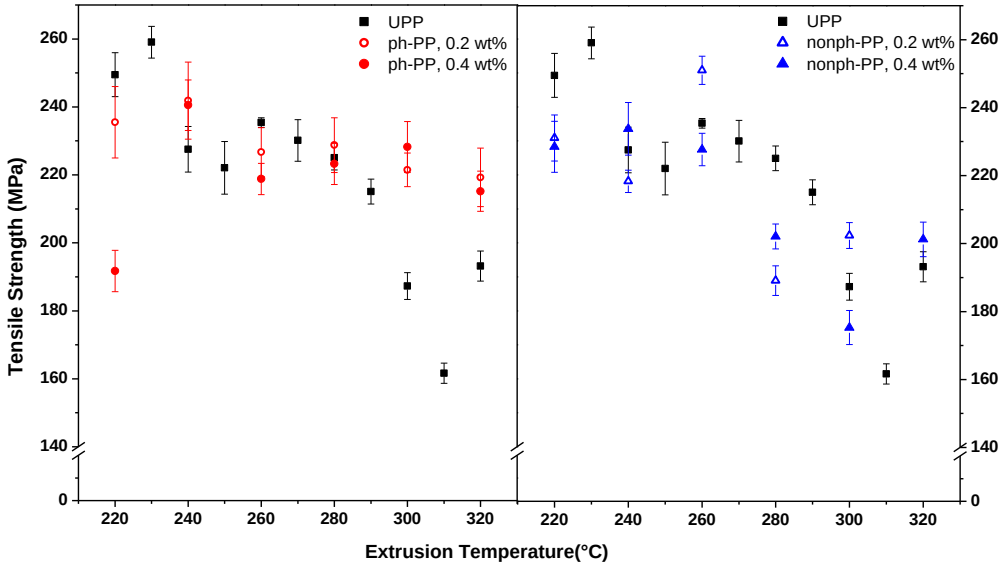

(b)

Figure 4- 4 : Mechanical properties, (a) elongation of minimally stabilized polypropylene (UPP), phnolic stabilized PP (ph-PP)and nonphenolic stabilized PP

(nonph-PP), (b) tensile strength of UPP, ph-PP and nonph-PP.

4.3.5. Chemical changes during melt processing of PP with stabilizer added

MD simulations are used to study the chemical interactions between stabilizers and free radicals during thermal extrusion. Amorphous polymer molecular models were built with stabilizers and oxygen radicals incorporated by using the Materials Studio software. Two stabilizers are investigated (chemical structures in Table 4-1): Irgastab FS042, a non-phenolic stabilizer; and Irganox 3114, a phenolic stabilizer. According to the category in Al-Malaika's research [1], the Irganox 3114 is a chain breaking donor (CB-D) that competes with radicals and prevents hydrogen from being abstracted from the polymer. A CB-D prevents thermal degradation by giving away a hydrogen to react with radicals and forming stable fragments. Irgastab FS042 is a chain breaking acceptor (CB-A). A CB-A reacts with radicals directly and forms stable fragments. The mechanisms are listed in Scheme 1 (a) for Irganox 3114 and Scheme 2 for Irgastab FS042.

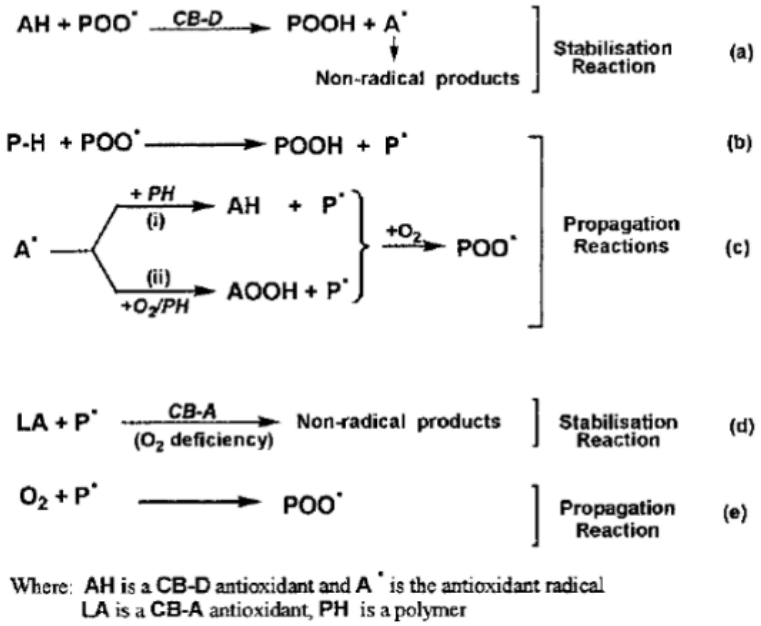

Where: **AH** is a **CB-D** antioxidant and **A** • is the antioxidant radical
LA is a **CB-A** antioxidant, **PH** is a polymer

Scheme 1: Main reactions and competing pathways involved in antioxidant activity that leads to chain breaking. Taken from [1].

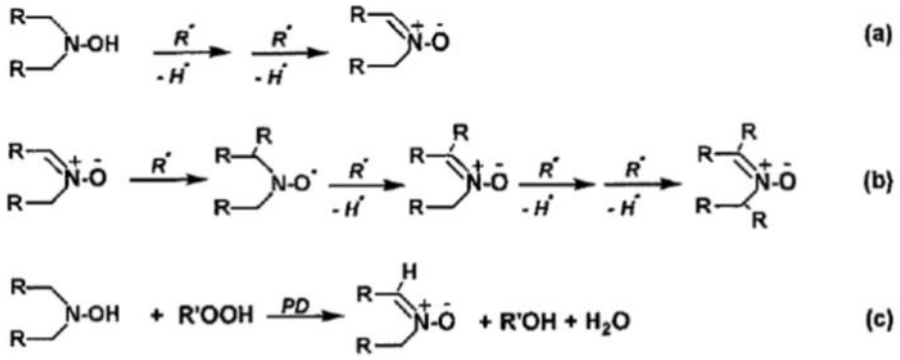

Scheme 2: Chain breaking and peroxidolytic reactions of hydroxylamine antioxidants. Taken from [1].

During the equilibration of the molecular model system, the phenolic systems are observed to not be stable, as the polymer chains or the stabilizer break easily. Comparing the chemical structures of the two stabilizers, Irganox 3114 is more bulky while Irgastab FS 042 is more like a polymer chain. Therefore, there will be more torsion angles surrounding Irganox 3114, and these extra degrees of freedom can cause difficulty during equilibration. For statistical purposes, three amorphous systems of either including Irganox 3114 (ph-PP system a, b and c) or Irgastab FS042 (nonph-PP system a', b' and c') were built and successfully equilibrated.

For reference, the pure system containing 20 polymer chains and 4 oxygen radicals is built and cookoff simulations is run with a heating rate of 7 °C/ps to obtain the onset degradation temperatures which is defined as 524 °C, T_{pure}. While running the cookoff simulations for both stabilized systems, those oxygen radicals in the amorphous systems are trying to attack polymer chains and subtract a hydrogen from the polymer chain to form a OH radical. Those OH radicals will further attack another polymer chain or interact with stabilizer and form a H_2O molecule which is a stable molecule without further propagation possibility. Meanwhile, the stabilizer in

the system is trying to interact with those oxygen radicals as faster as they can. In some cases like system b for ph-PP and systems b and c for nonph-PP, stabilizer is able to interact with oxygen radicals before it attack polymer chains. As temperature increases, other oxygen radicals still are able to attack polymer chains and cause the hydrogen subtraction of the polymer chains. Some oxygen radicals are easier to interact since the systems are randomly built. Figure 4-5 indicates the onset degradation temperatures and stabilizer interaction of each system. The temperature of the first polymer chain attacked to broken by oxygen radical is 502, 582 and 669 °C for the ph-PP system and 239, 522, and 603 °C for the nonph-PP system.

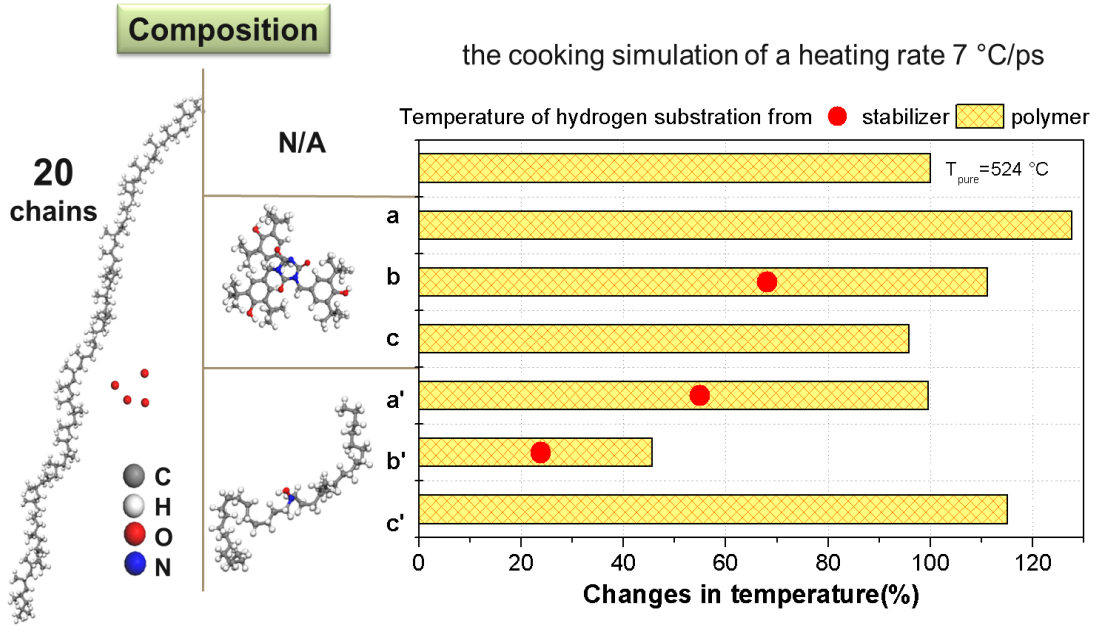

Figure 4- 5: The propagation during cooking simulations of stabilized polypropylene systems

The temperature of the stabilized systems is then raised from room temperature to four different target temperatures of 237, 307, 517 and 727 °C(normalized to 0.45, 0.59, 0.99 and 1.38 T_{pure}, where T_{pure} is 524 °C) with a heating rate of 7 °C/ps and then the systems are kept at that target temperature for more than 600 ps or until all O or OH radicals are consumed. In real systems, polymer is heated up to temperature higher than melting temperature and then stays in the extruder for a certain time before cooled down. The interaction between stabilizers and radicals are summarized in Figure 4-6.

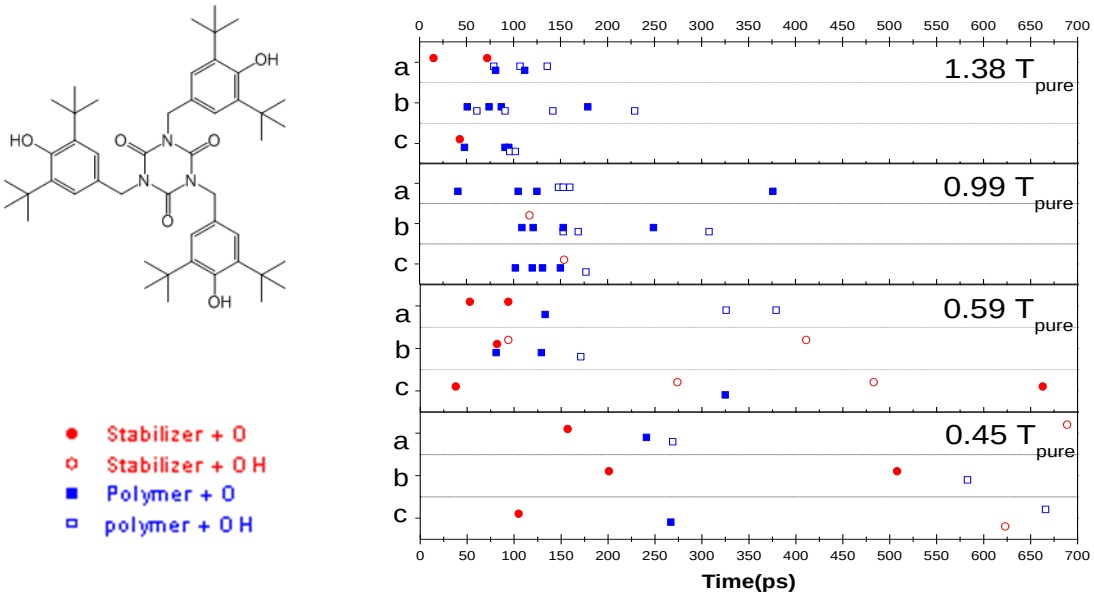

(a)

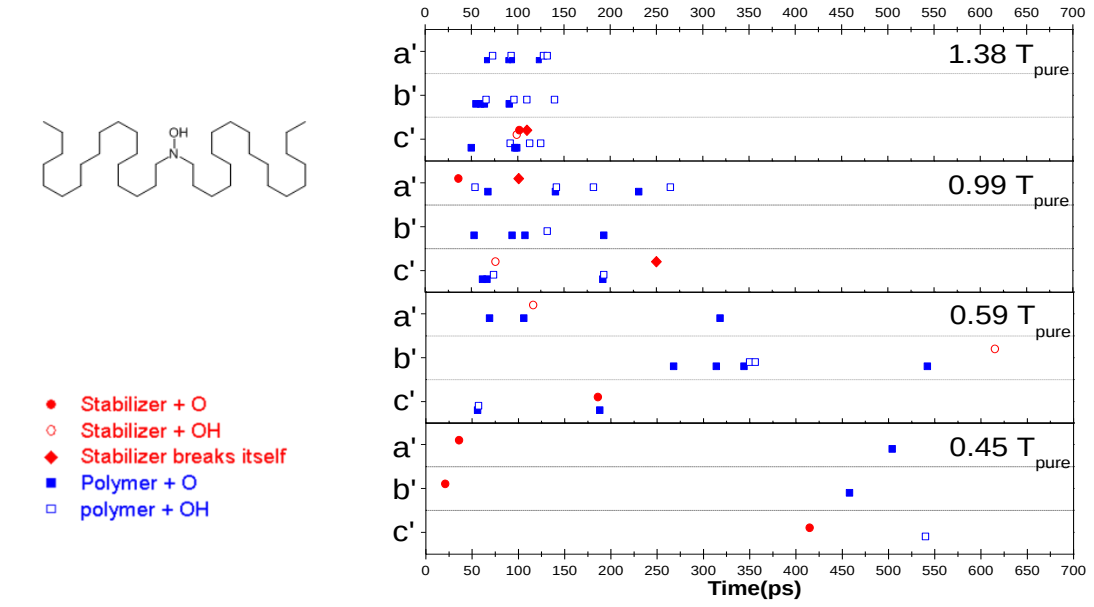

(b)

Figure 4- 6: Summary of radical interactions as a function of simulation time and target temperature (a) phenolic stabilized PP (ph-PP) systems (b) nonphenolic stabilized PP (nonph-PP) systems.

At the lower target temperature of 0.45 T_{pure}, oxygen radicals in the systems do not have enough energy to move and interact very fast; therefore, stabilizers have time to react with radicals, causing a delay in the radicals attacking polymer chains for both stabilizers. Oxygen radicals become more reactive as temperature increase to 0.59 T_{pure}; however, the phenolic stabilizer is still able to interact with radicals. Once the stabilizer is consumed, the radicals then attack polymers chains faster than lower temperature. At those lower temperatures, phenolic stabilizers have higher capability to interact with radicals and stop polymer chains from being attacked which indicates better stabilization than nonphenolic stabilizers.

When the target temperature is 0.99 T_{pure} or 1.38 T_{pure}, polymer chains and radicals move faster and radicals have more energy to attack as many polymer chains as they can reach; most of the radicals were consumed and break polymer chains before they reach the stabilizer, especially at temperature of 1.38 T_{pure}. Draw to a conclusion that stabilizers might be able to prevent thermal degradation at lower temperature. But as temperature goes higher, the reactive radicals still cause more chain breaking.

During the degradation simulations, the phenolic stabilizers are able to interact several times with radical while the non-phenolic stabilizers usually interact only once. The non-phenolic stabilizer sometime breaks itself with the unstable structure after the non-time interaction. The stabilizer in non-phenolic stabilized systems has better capability to stop radicals from attacking polymer chains comparing to phenolic stabilized systems.

4.4. Conclusions

In this study, heat applied to the PP melt during extrusion was found to cause the breakage of polymer chains. The addition of stabilizer can help maintain shear viscosity and mechanical properties after extrusion. Two types of stabilizers were investigated. One was a phenolic type stabilizer that contains 3 benzene rings in its structure, and the other was non-phenolic type with a linear structure. From high

temperature GPC results, the molecular weight of UPP which was minimally stabilized PP decreased linearly. The ph-PP was well stabilized up to 320 °C with 0.4 wt% loading and 280 °C with 0.2 wt% loading. However, the stabilization of nonph-PP was not stabilized as well, the molecular weight dropped gradually as UPP. The crossover modulus measured from rotational rheometry and capillary rheometer tests results validated this observation. The thermal degradation lowered the tensile strength for both systems and the tensile strength of nonph-PP weakened more than for ph-PP. The same trend was also observed by their elongations.

MD simulations were done on a series of molecular models that contained amorphous PP chains with a stabilizer of each type and 4 oxygen radicals. The simulations suggested that at lower temperatures, stabilizers were more able to capture oxygen radicals and prevent polymer chain scissions from happening. Comparing the reactions of stabilizer and oxygen radicals at low temperature (0.45 and 0.59 T_{pure}), the phenolic stabilizers always capture oxygen radicals faster than oxygen radical attacking the chains. The nonphenolic stabilizer did the same thing at lower temperature (0.45 T_{pure}), but it could not protect PP chains at 0.59 T_{pure}. This observation corroborates to experimental results that ph-PP has better stabilized. The oxygen radicals were very active and the polymer chains broke faster as temperature increases; this observation reflect that polymer chains experiences lots chain scissions at higher temperature experimentally.

Chapter 5: Investigation of the thermal degradation of bicomponent fibers comprised of polyethylene and polypropylene (PE/PP)

5.1. Introduction

Bicomponent fibers are widely used and investigated in the nonwoven industry to leverage the advantages of different polymer materials to design particular functionalities. [163,164] Several combinations of major engineering polymers at high-speed melt spinning have been studied, such as polyester/polyethylene (PET/PE) [165], polyester/polypropylene (PET/PP) [166] ,PET/polyamide 6 (PET/PA6) [163]. The mechanical properties of bicomponent fibers are related to take-up speed [165], whereas the structural properties are dependent on the type and composition of the components [163].

The designs of the cross-section are also another way to manipulate the fiber structures to achieve particular properties. Some examples like the segmented-pie design are used to produce nanofiber yarn by splitting the fiber downstream in the production process. [167] Side-by-side fibers can perform as self-crimping fibers because of the different shrinkage properties of the two polymer materials. [168] A core-sheath fiber is built with the core part as one type of polymer and the sheath part as another type of polymer surrounding and fully covering the core. One of the applications for core-sheath fiber is to provide lower thermal bonding temperature during nonwoven web formation. [163] The sheath material can also be chosen from a variety of polymer types to meet industrial needs.

The interfacial adhesion of the two polymer phases within core-sheath fibers plays a crucial role when estimating the value of tensile strength. [163,167,168] The compatibility can be estimated by Flory-Huggins interaction parameter, and the

PE/PP combination has the highest interfacial adhesion value. The interracial fracture energy is also higher for PE/PP compared to other polymer combinations. Although extensive work has been done on the physical properties of core-sheath fibers and their interfacial properties, [163] information is limited about the degradation that occurs particularly at the interface.

The goal of this work is to investigate how the differing extrusion temperatures for the PP and PE phases in core/sheath fibers (where PE is the sheath) impact the degradation in bicomponent fibers, especially at the interface. Experimentally, a systematic study was done where the extrusion temperature of one polymer was fixed and the temperatures of the other polymer were systematically raised to study the degradation behavior. First, the extrusion temperature of PE was fixed at 190 °C to obtain sufficient melting but limited thermal degradation in terms of crosslinking, while the temperature of PP was varied from 220 to 310 °C. Then, the extrusion temperature of PP was fixed at 280 °C and PE was varied from 200 to 270 to investigate the effects of energy transferred to PE. In addition, molecular dynamics (MD) simulations were performed of a PE/PP bicomponent system to reveal molecular level details of what happens to the degradation profile at the interface during the energy transfer during thermal extrusion. These simulations are particularly useful for the PE/PP system since their inherent properties are so close and are thus can be difficult to elucidate their distinct degradation properties by current experimental methods.

5.2. Methodology

5.2.1. Experimental materials

In this research, two commercial polymer pellets of PP and PE were investigated. One was polyethylene, ASPUN 6850, supplied by Dow Chemical, and the other was polypropylene, CP360H, supplied by Braskem America. The melt index of ASPUN 6850 under 190 °C/2.16 kg was 30 g/min based on data sheet

provided by manufacturer. For CP360H, the melt index under 446 °F/4.76 lb (230 °C/2.16 kg) was 36 g/10 min provided by manufacturer.

5.2.2. Extrusion of PE/PP core-sheath fibers

The PP/PE core-sheath fiber was extruded by Tricomponent Spinning Machine but using two extruder for PE and PP, separately. PE was extruded as the sheath of the fiber to provide soft hand and to reduce the temperature when thermal bonding. PP was the core to provide the strength. The ratio of PE/PP in this trial was set as 10%/90%, 30%/70% and 50%/50%, the illustration of fiber cross section was in Figure 5-1. To study the effects of temperature on each polymer, the extrusion temperature of one polymer was fixed and the extrusion temperature of another one changed systematically. Table 5-1 is the summary of setting. First, the extrusion temperature of PE was fixed as 190 °C while the extrusion temperatures of PP were systematically increased from 200 to 310 °C. Then, the extrusion temperature of PP was fixed as 280 °C while the extrusion temperatures of PE were systematically increased from 190 to 270 °C. Air quench was applied before fiber collection. The throughput per hole was 0.8 g/min and there were 36 holes per spinneret making the total throughput of 28.8 g/min. The draw ratio was fixed as 2.5 and each fiber diameter was around 5.8 denier (30 μm).

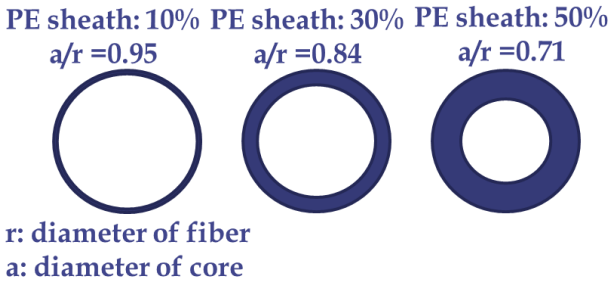

Figure 5- 1: Illustrations of core-sheath fibers with 10%, 30% and 50% PE loading as sheath.

Table 5- 1: Settings for the core-sheath fiber making

Sample name	*PE as sheath*			*PP as core*		
Raw material	ASPUN6850			CP360H		
ratio	10%	30%	50%	90%	70%	50%
First set: Extrusion temperature	190 °C			220-310 °C		
Second set: Extrusion temperature	190-270 °C			280 °C		
Throughput	28.8 g/min for total 36 holes					
Quench	Air					
Finish	applied					
Draw conditions	Feed roll: 495 rpm Draw roll 1: 500 rpm @ 35 °C Draw roll 2: 1000 rpm @ 45 °C Draw roll 3: 1250 rpm @ 45 °C Relax roll: 1240 rpm					
Draw rate	2.5					
Target diameter	5.8 denier (30 μm)					

5.2.3. High temperature thermal gradient interaction chromatography (HT-TGIC)

The high temperature thermal gradient interaction chromatography (HT-TGIC) tests were performed by the Dow Chemical with a commercially available crystallization elution fractionation (CEF) instrument (Polymer char, Spain). A hypercarb column 100 x 4.6 mm (Thermo Scientific) was used to separate the polymer at designed temperature. During the tests, the core-sheath fibers were dissolved with Ortho-dichlorobenzene; PE and PP were separated by different

elution temperatures and their molecular weights and distributions were recorded separately.

5.2.4. Rheology analysis

Rheology tests were conducted using a Rosand capillary rheometer manufactured by Malvern Instruments Ltd. A 1 mm diameter die was used and the barrel length was 290 mm. The temperature was fixed as 230 °C and the shear rate was fixed as 300/s. For all measurements, the pre-heat time were 9 minutes to ensure complete melting before analysis.

5.2.5. Mechanical tests

Tension was applied to a fiber to measure its tensile response. A 5 N load cell was used. Single filaments with a gauge length of 15 mm were drawn until fiber breakage. For statistical purposes, at least 10 specimens were measured for each sample condition. After measurements, tensile strengths and elongations were obtained.

5.2.6. Scanning Electron Microscope (SEM) images

SEM images were taken in the Analytical Instrumentation Facility (AIF) at North Carolina State University (NCSU) using FEI Verios 460L field emission SEM. The detector was Everhart-Thornley detector (ETD) with 1 KV voltage and 13 pA current.

5.2.7. Procedure for building PE/PP bicomponent simulation models

The polymer systems were built with Accelrys' Material Studio software [10] using the Amorphous Cell module. To make a molecular model of the PE-PP bicomponent system, first the individual polymer systems were created by placing 40 PP chains or 60 PE chains in the simulation box using the Amorphous Cell module with both sides confined to create an interface. The system was first equilibrated with ReaxFF at 27 °C for 200 ps under isothermal and isobaric conditions (NPT). After that, walls in z-directions were applied and only x and y directions were set to be periodic to mimic the infinite system along the fiber axis. The system was heated

up to 727 °C for 50 ps and cooled down to 27 °C for 25 ps to ensure that the surfaces of these two polymers created an interface. All simulations were conducted with the Large-scale Atomic/Molecular Massively Parallel Simulator (LAMMPS) software program [152] using the reactive force field, ReaxFF, [153] and were performed at the High Performance Computing Center at NC State University. [154]

5.2.8. MD simulations of polymer degradation

Equilibrated systems were heated up to 2217 °C at a constant heating rate to identify onset degradation temperatures; this type of simulation is called a *cookoff* simulation. The onset degradation temperature was defined as the temperature where the polymer chains start to truly break down. Bond breakings with ReaxFF were defined by bond order; therefore, there will be some instances where bonds are about to dissociate but it takes a while for the bond to truly break during the simulations.

The other type of simulation is called a degradation simulation. Different heating rates are applied to each group of polymer mimicking the bicomponent extrusion where polymers are melted at different temperatures. Once the polymer reached target temperatures, the system then ran at constant volume and constant energy conditions (NVE) for 50 ps. All systems were then cooled down to room temperature. The output from LAMMPS contained the bond order and connectivity information, and was used as input to a C script to analyze the species and numbers of fragments at each time step. The trajectory is visualized with the Visual Molecular Dynamics (VMD) software [155].

5.2.9. Calculation of stress-strain curves from MD simulations

For these calculations, the system was deformed at a particular strain rate, and the stress response was calculated accordingly. All systems were first cooled down from their target temperature to 300 K before applying the strain, and limited bond breakage was observed during the cooling. The strain rate for each system was set at 10^{-9} s^{-1}, which was chosen because for strain rates higher than that, an irregular spike was observed in the stress response at low strains along with an

increased temperature and additional broken bonds. No or limited bond breakage were found during the deformation. To reduce random and temperature-related stress fluctuations that resulted from applying strains at the atomistic level, the stress was averaged further over a small time interval of 0.125 ps around the desired time point of the stress calculation. The modulus was calculated from 1% strain of the 10^{-9} s^{-1} strain rate.

5.3. Results and discussions

5.3.1. Experimental characterization of degradation within PE/PP core-sheath fibers

For the bicomponent fiber, the sheath material uses PE to provide soft hand and lower temperature for thermal-bonding if applicable. The core material uses PP to provide fiber strength. The extrusion temperature of PE was fixed at 200 °C. To study the temperature effects, the extrusion temperatures of PP was systematically increased from 200 °C up to 310 °C which is the maximum temperature of the tri-component spinning machine. The measured temperatures of PP melt after pump were found to be 10-20 °C higher than PP set point while PE melt temperatures were slightly higher but built up as PP set points increase. See Table 5-2 for the measured temperatures of trial run.

Table 5- 2: Measured melt temperatures of polymers near the spinneret.

PE/PP set Point	10% PE sheath (PE/PP)	30% PE sheath (PE/PP)	50% PE sheath (PE/PP)
First set			
190/220 °C	202/231 °C	203/232 °C	204/232 °C
190/240 °C	203/251 °C	203/254 °C	204/254 °C
190/260 °C	203/273 °C	203/275 °C	204/274 °C
190/280 °C	203/293 °C	204/295 °C	204/295 °C
190/300 °C	203/318 °C	204/317 °C	205/316 °C
190/310 °C	205/329 °C	205/327 °C	206/325 °C
Second set			
200/280 °C	214/294 °C	213/294 °C	214/294 °C
210/280 °C	220/294 °C	221/294 °C	223/294 °C
220/280 °C	231/294 °C	232/294 °C	233/294 °C
230/280 °C	240/294 °C	241/294 °C	243/294 °C
240/280 °C	250/294 °C	251/294 °C	253/294 °C
250/280 °C	265/298 °C	265/297 °C	265/296 °C
260/280 °C	272/294 °C	273/294 °C	274/294 °C
270/280 °C	282/294 °C	283/294 °C	284/294 °C

The HT-TGIC was used to study the microstructure of core-sheath fibers, PP and PE are separated by elution temperatures and their molecular weights are recorded individually. This technique invented by the Dow Chemical helps investigating the microstructure a fibers. From Figure 5-2, the average molecular weights of PP gradually decreased as extrusion temperature heated up. From previous study, the commercial PP, CP360H, can be extruded with limited degradation at a temperature lower than 300 °C. Once the extrusion temperature

goes higher than 300 °C, severe thermal degradation along significant drop of Mw and viscosity will be found which is validated again in the HT-TGIC tests. The average molecular weights of PE are similar with some variation across the extrusion temperatures from 220 to 310 °C. Those variations come from its low Mw which affect the sensitivity. Referring to next section, the averages of shear viscosity of the second set are similar across the PE extrusion temperatures from 200 to 270 °C. Therefore, the molecular weights of the fiber samples which PE extruded at 200, 240 and 270 °C and PP extruded at 280 °C are measured. For the second set, the Mw of both PP and PE remains similar across all tested extrusion temperatures of PE.

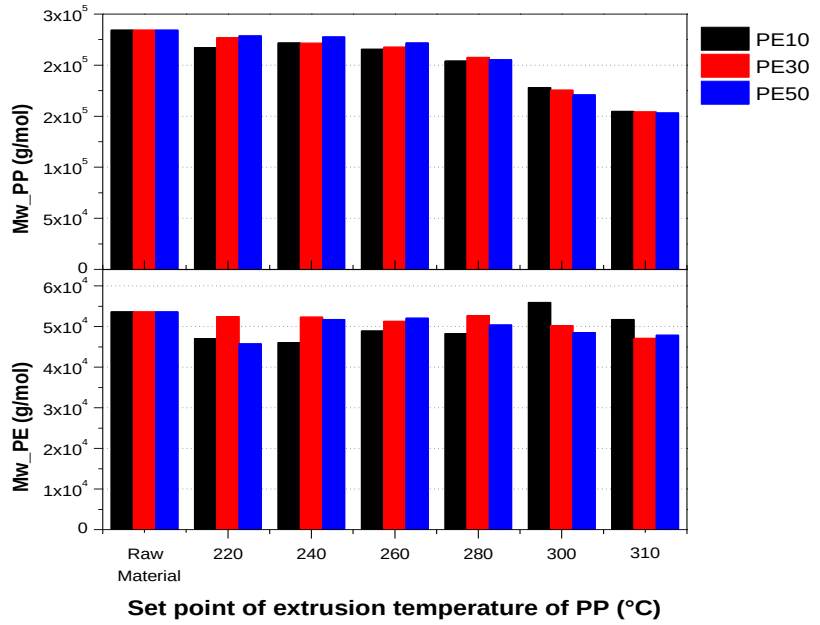

(a)

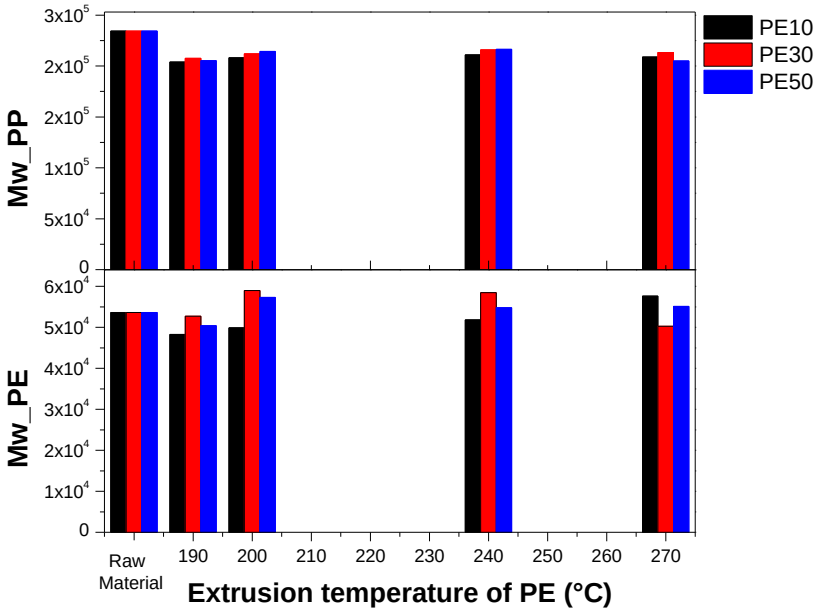

(b)

Figure 5- 2: The molecular weight results from high temperature thermal gradient interaction chromatography for (a) first set with the extrusion temperature of PE fixed as 190 °C and (b) first set with the extrusion temperature of PP fixed as 280 °C.

The thermal degradation of bicomponent fibers can be identified by investigating the average shear viscosity measured by the capillary rheometer at constant shear rate and temperature assuming that the shear viscosity of PE does not change due to fixed extrusion temperature. From Figure 5-3 (a), the average shear viscosities decease gradually as the extrusion temperatures of PP increase and drop quickly above 300 °C. This finding echoes the evidence from previous studies that PP experiences significant degradation at temperature higher than 280 °C. The temperature of PP melt reaches 325 °C when the extrusion temperature of PP set as 310 °C. At that temperature, the shear viscosity drops a lot which indicates that enormous thermal degradation occurred. Among three fibers with different PP core ratio, the shear viscosity of fiber with 90 % PP core are the lowest since it has the largest amount of degraded PP.

From Figure 5-3 (b), the extrusion temperature of PP is fixed as 280 °C which is the highest extrusion temperature with acceptable thermal degradation; the extrusion temperatures of PE increase from 200 to 270 °C. The shear viscosities of this trial do not change significantly indicating that PP is more sensitive to extrusion temperature than PE. After the trial, it takes more time to clean the PE extruder for the second trial than the first trial.

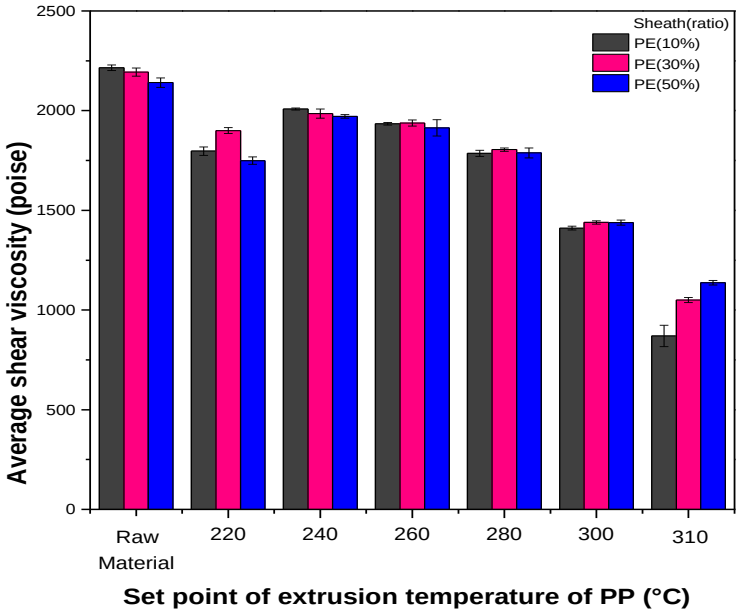

(a)

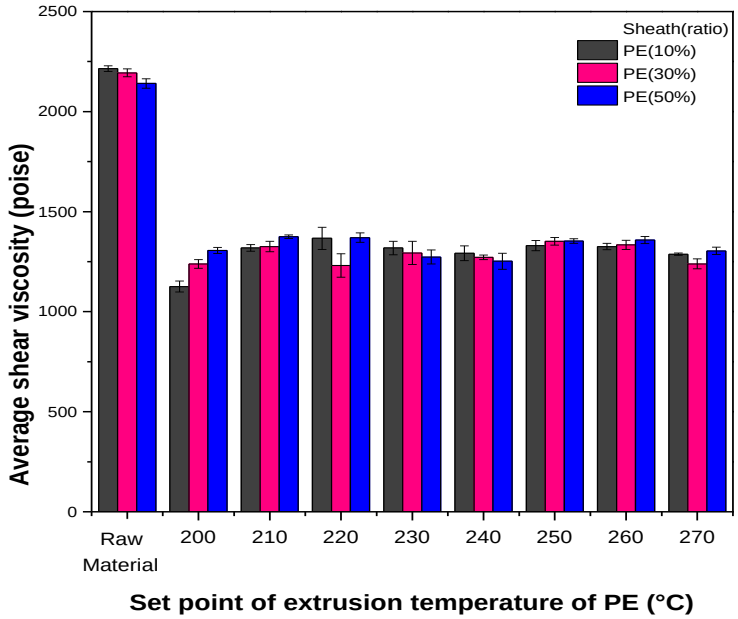

(b)

Figure 5- 3: Average shear viscosity of free fall bicomponent samples measured from capillary rheometer at fixed shear rate of 300 /s of (a) function of PP extrusion temperature and (b) function of PE extrusion temperature.

Figure 5-4 is the selected stress-strain curves from each core-sheath fiber samples. Some dips in the tensile strength are observed during the tensile tests, for example, PE50 at PP extrusion temperature 310 °C (green curve in Figure 5-4 (a)). Those dips come from the defects of the fibers. From Figure 5-4 (b), as extrusion temperature of PP increases, the core-sheath fibers obtain larger elongation and weaker tensile stress for 10 % of PE as sheath.

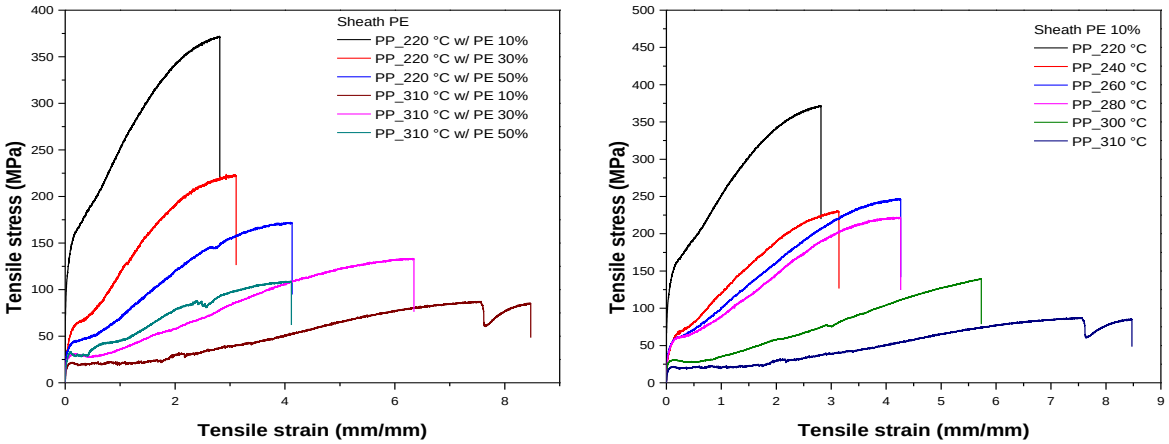

(a) (b)

Figure 5- 4: Stress-strain curves of selected PE/PP core-sheath fibers. (a) Fiber extruded at temperatures of 220 °C and 310 °C for PP and 190 °C for PE. (b) Fiber with 10% ratio as sheath extruded at temperatures from 220 °C to 310 °C for PP and 190 °C for PE.

To understand the surface morphology during tensile progression, SEM images are taken along the fiber after tensile tests. PE is the sheath material. Figure 5-5 includes strain-stress curves of fibers which the extrusion temperature of PE and PP are 270 and 280 °C, respectively. Figure 5-5 (a) are the strain-stress curves referring to Figure 5-5(b)- (f). Figure 5-5 (b) is the original fiber with equally rough surface. During early tensile strain at Figure 5-5 (c), the fiber surface does not

change much and look similar to original fiber. After yield point of Figure 5-5 (d), the fiber starts to appear some regularity with extended trace. Obvious stripes along the extension direction are investigated at the tensile strain of 2.5 like Figure 5-5 (e). When the tensile strain reaches 5.0, ridges which are perpendicular to the strips are found like Figure 5-5 (f). The width of and the distances between the ridges are ~2 μm and its height is ~ 0.3 μm. After failure, the stripes and ridges are still very obvious like Figure 5-5 (g).Tested fibers are relaxed from the high tension after tensile tests, those ridges are the behaviors after relaxation.

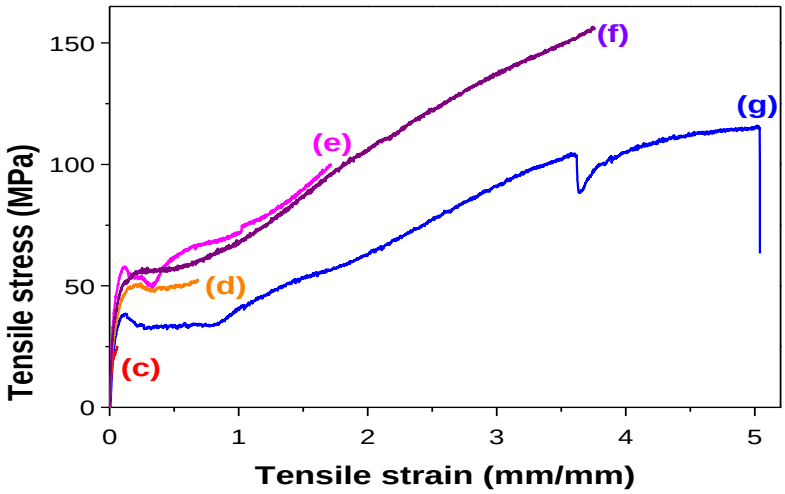

(a)

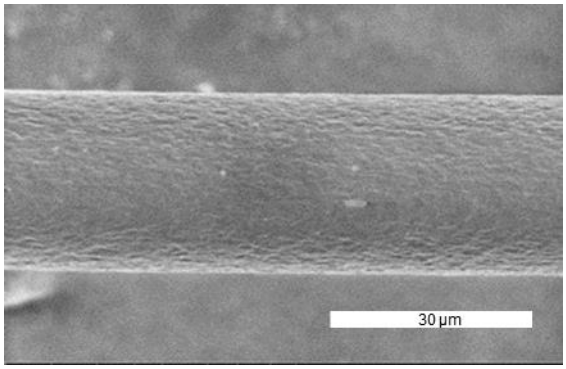

(b)

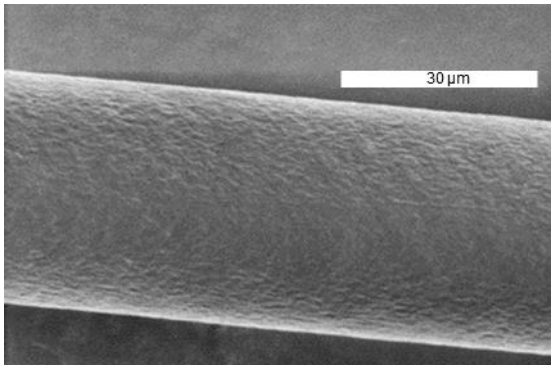

(c)

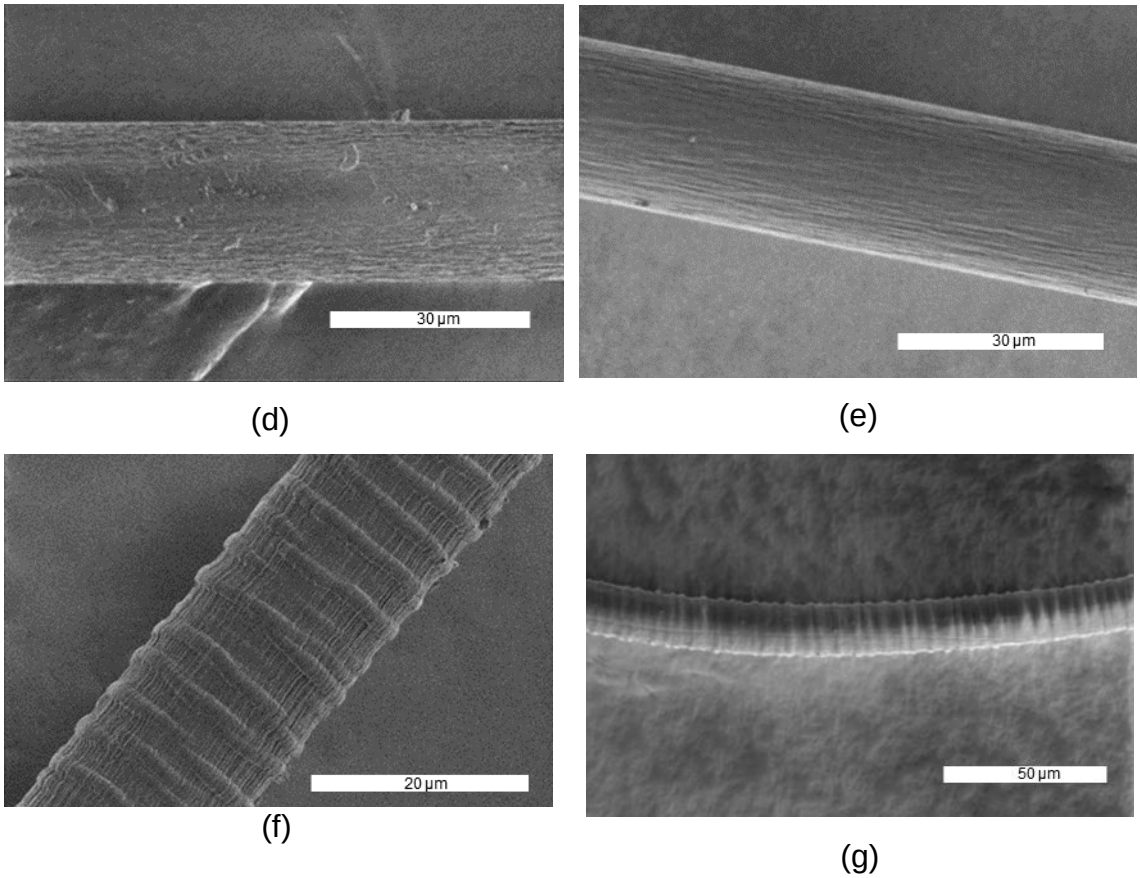

(d) (e)

(f) (g)

Figure 5- 5: Fiber morphology during tensile progression. (a) Strain-stress curves of fiber, (b)-(g) SEM images of fiber surfaces.

We investigate two sets of broken tips for fiber sample which PE sheath extruded at 270 °C and PP extruded at 280 °C. Figure 5-6(a) is their strain-stress curves. At the first set of broken tip Figure 5-6 (b) and (c), the core breaks a little earlier than the sheath and the sheath extends a little bit before it fully breaks. Figure 5-6 (b) indicates the extended PE sheath; the white part of Figure 5-6 (c) is PP core and the gray part is PE sheath. Figure 5-6 (d) is one broken tip of another set and it appears like core has shrunk or the sheath has extended. On the other side of the broken tips, there are some fibrous popped out from the core in Figure 5-6 (e). Other broken fibers with different extrusion temperatures are also investigated. All the SEM

evidences indicate that the PP core breaks earlier than PE sheath, and the PE sheath breaks almost simultaneously with a small extension.

During the tensile tests for all core-sheath fibers, the dips appeared at times. Because the dips might occur several times along one single fiber test, those dips might refer to the defects of the fiber. The dips appear more often when the extrusion temperatures of PE are lower. When searching along the broken fiber along the tensile tests to find the evidence of the dips appeared in blue curve of Figure 5-6 (a) for the fiber sample which PP extruded at 280 °C and PE extruded at 270 °C. There are several small defects along the fiber and a long defect with a length of 243 μm like Figure 5-6 (f). Take a close look at Figure 5-6 (g), the defect causes surface fracture and which might be the reason of the obvious dip appeared when apply a strain on the fiber during the tensile tests.

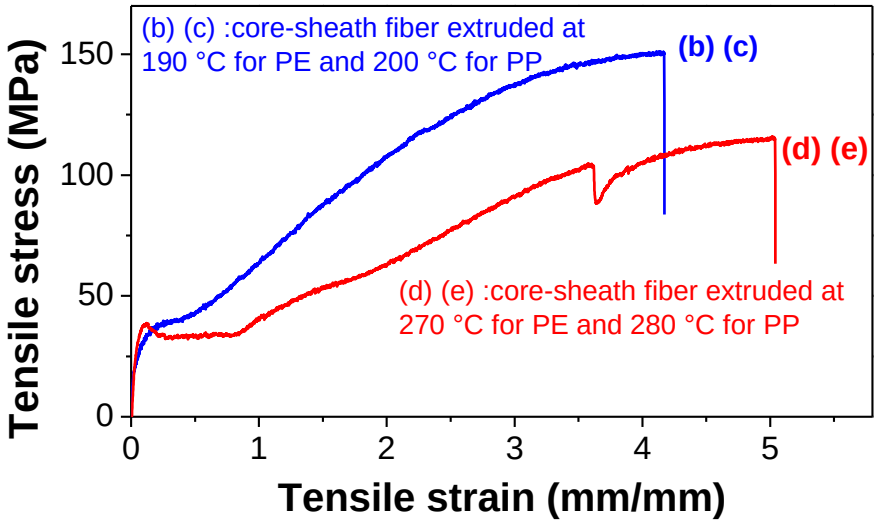

(a)

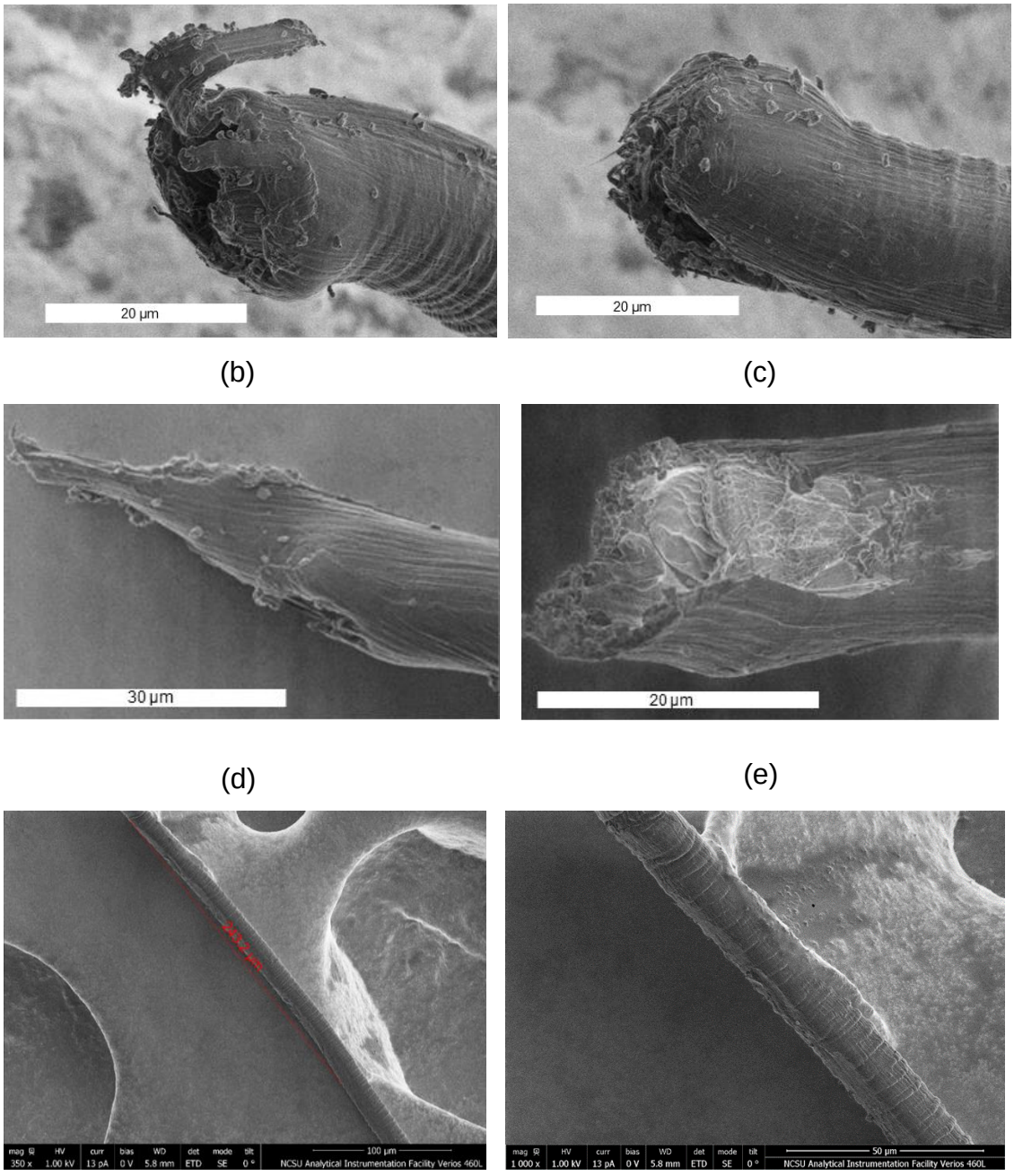

Figure 5- 6: (a) Strain-stress curves of broken fibers, (b)-(e) SEM images of broken tips of fibers after strain, (f)-(g) SEM images along the fiber.

Figure 5-7 (a) and (b) are the averages of the mechanical properties data from all the core-sheath fiber samples. Once the extrusion temperature of PE is fixed, the elongation is increased and the tensile stress is lowered as extrusion temperature of PP goes up no matter what the PE loading is. High extrusion temperatures can result in more disorder of molecular orientation that results in higher extension; however, the tensile strength decreases with lower molecular weight. From Figure 5-7 (b), the tensile stresses of PE50 are lower than PE30 and PE10 indicates that PP contributes more in terms of maintaining the strength of bicomponent fibers. It was also found that the tensile strength of PE10 reduced faster than other two samples. This is another evidence that the PP core supported the tensile strength of core-sheath fiber; therefore, there is a significant decrease of tensile strength when predominate degradation occurred at PP core. And it also explains why the trends of tensile curves of PP extrusion temperatures at 220 °C and 310 °C in Figure 5-4 (a) is different.

If the extrusion temperature of PE changes, the elongation and tensile strength remain similar this elucidates that mechanical properties of core-sheath fiber are less sensitive to extrusion temperatures of PE. Note here that the extrusion temperature of PP is fixed as 280 °C and the mechanical properties seems to be related more to PP core.

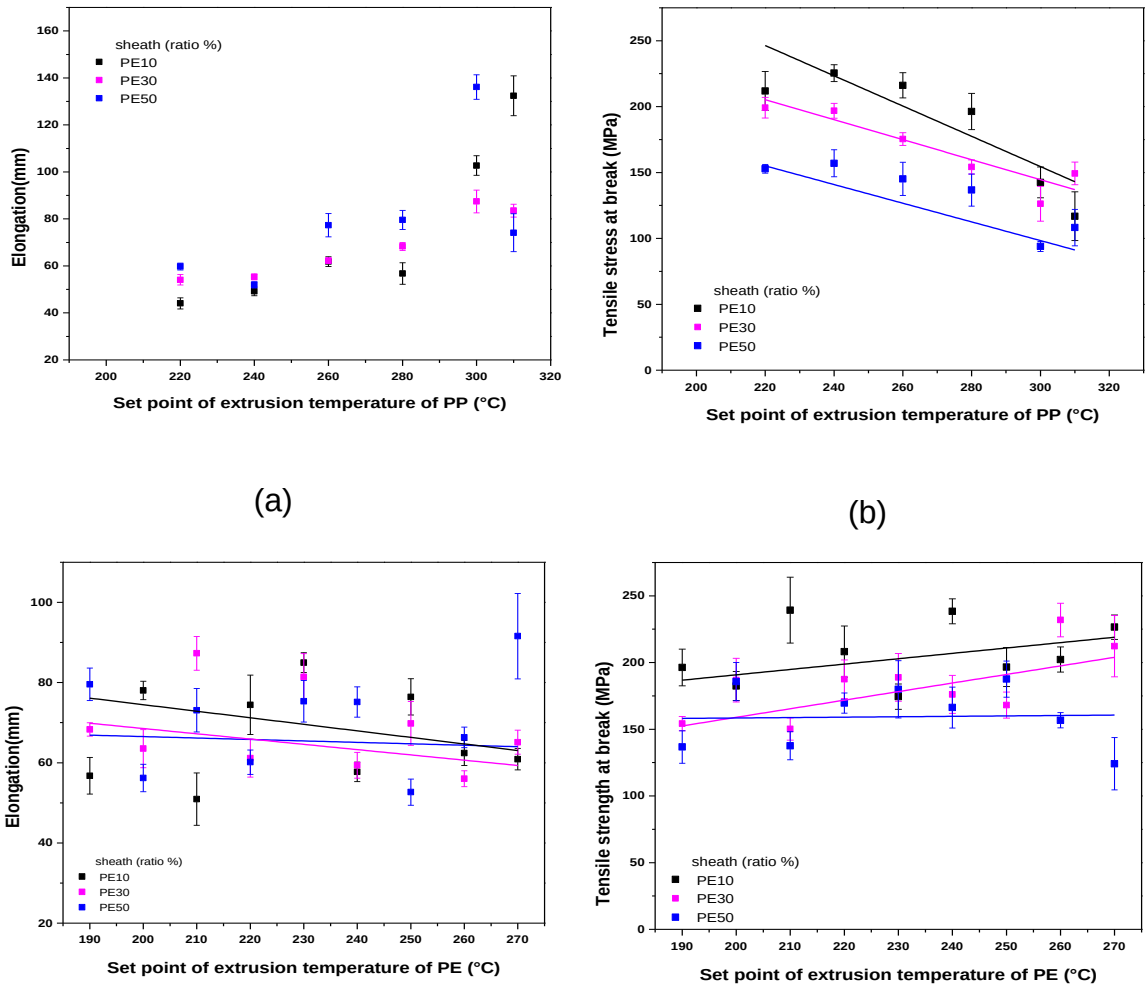

Figure 5- 7: Mechanical properties PE/PP core-sheath fibers: (a) elongation and (b) tensile strength of first set which extrusion temperature of PE fixed as 190 °C, (c) elongation and (d) tensile strength of second set which extrusion temperature of PP fixed as 280 °C. Lines are guides for the eye.

5.3.2. The effect of the interface on the simulated degradation temperature

As mentioned previously, the tensile tests suggest that the PE sheath ruptures easily when contacted with high temperature PP. However, it is challenging to use current techniques such as nano-indentor and birefringence to identify the slightly degradation due the temperature changes, especially at the interface, due to the similar nature of PE and PP. Thus, MD simulations with the ReaxFF force field were performed to investigate the degradation characteristics of each polymer component, particularly as a function of the interface. Note that the degradation temperatures in simulations will be higher than in experiments because of the timescale difference; in other words, we are degrading the system in the picosecond timescale instead of seconds by artificially raising the temperature; this approach has been devised and validated by others, [162]. Thus, temperatures must be viewed in a relative sense instead of absolute sense and have been normalized accordingly.

A molecular model of the PP/PE bicomponent system was built with half of the simulation box containing PP, and the other half containing PE; note that at the nanometer length scale, this representation of the interface is appropriate since the curvature of the core-sheath fiber is on the micron scale. A cookoff simulation was performed after the system was equilibrated to elucidate the temperature at which polymer chains start to break. During the cookoff simulations, PP was observed to start truly breaking at a simulation temperature (set as $T_{d.sim}^{PP}$) of 1577 °C and PE breaks at 1637 °C (set as $T_{d.sim}^{PE}$); these observations also validate that PE has a higher thermal stability than PP. Compared to pure systems, the $T_{d.sim}^{PP}$ increase 10.5% and $T_{d.sim}^{PE}$ decrease 3.9%. When heated up the whole system, the energy can be transferred between polymers. Therefore, the T_{sim}^{PP} increases and $T_{d.sim}^{PE}$ decreases to make $T_{d,sim}$ of two polymers are observed to be similar.

5.3.3. The effect of polymer melt temperatures on interfacial degradation

Since the two polymer components are usually heated at different temperatures during bicomponent fiber extrusion, there can be a temperature gradient when the two polymer materials come into contact in the spin pack, resulting in heat energy being transferred from polymer melt with the higher temperature to the one with a lower temperature. Thus, polymers with a lower thermal stability could severely degrade if the temperature of the other polymer is too high. To investigate these effects, we investigated three different scenarios via degradation simulations where each polymer component is heated (T_{target}) in a different way relative to its onset degradation simulation temperature ($T_{d,sim}$).

For the first scenario, the polymer components were heated such that $T_{target}^{PP} \cong T_{d,sim}^{PP} < T_{d,sim}^{PE}$ and $T_{target}^{PE} < T_{d,sim}^{PP} < T_{d,sim}^{PE}$, as indicated in Figures 5-8(a) and (b). During the heating phase (first 30 ps), Figure 5-8(c) indicates that neither of the polymer systems degraded, thus all of the polymer chains were left intact. During the constant energy phase (30-80 ps), the temperature of PE slightly increased from the heat transferred from PP; however, it is not heated enough to reach $T_{d,sim}^{PE}$, and thus no chains were observed to break in Figure 5-8(c). For PP, even though the temperature does not exceed $T_{d,sim}^{PP}$, there are still some chain breaking observed at later simulation times due to the long term heating.

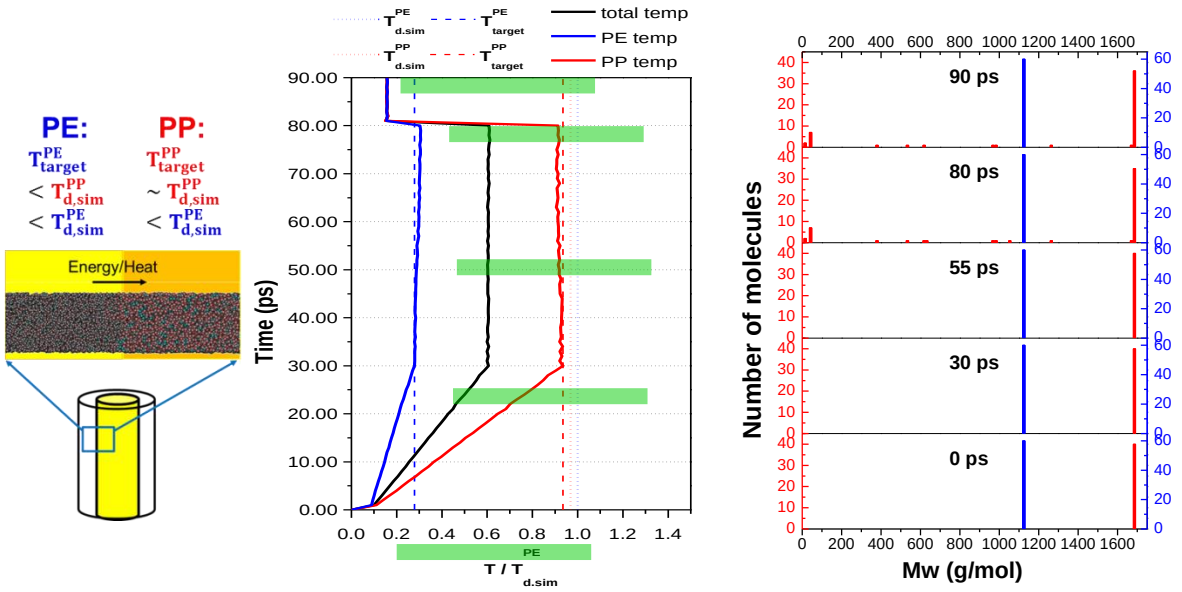

(a) (b) (c)

Figure 5- 8: MD simulations for PE/PP bicomponent systems under the conditions that $T_{target}^{PP} \cong T_{d,sim}^{PP} < T_{d,sim}^{PE}$ and $T_{target}^{PE} < T_{d,sim}^{PP} < T_{d,sim}^{PE}$; (a) a schematic of the energy transfer occurring at the interface, (b) the temperature as a function of time during the degradation simulations for the entire system (black), PP (red), and PE (blue), and (c) the molecular weight distribution for fragments from PP (red) and PE (blue) at the time points annotated by green boxes in (b).

For the second scenario, as indicated in Figures 5-9(a) and (b), we investigated what will happen if the temperature of PP is heated beyond $T_{d,sim}$ for both PP and PE but keeping PE below both $T_{d,sim}$; in other words, $T_{target}^{PP} > T_{d,sim}^{PE} > T_{d,sim}^{PP}$ and $T_{target}^{PE} < T_{d,sim}^{PP} < T_{d,sim}^{PE}$. In Figure 5-9(c), as the temperature of PP reaches $T_{d,sim}^{PP}$ during its heating phase, as expected degradation of PP is observed, and the degree of degradation increases significantly with long term heating at this high temperature. For PE, a slight amount of heat energy is transferred from PP and

thus its temperature is slightly higher than T_{target}^{PE} in Figure 5-9(b); however, since it is still much lower than $T_{d,sim}^{PE}$, no chains are observed to break in Figure 5-9(c), even after extended heating.

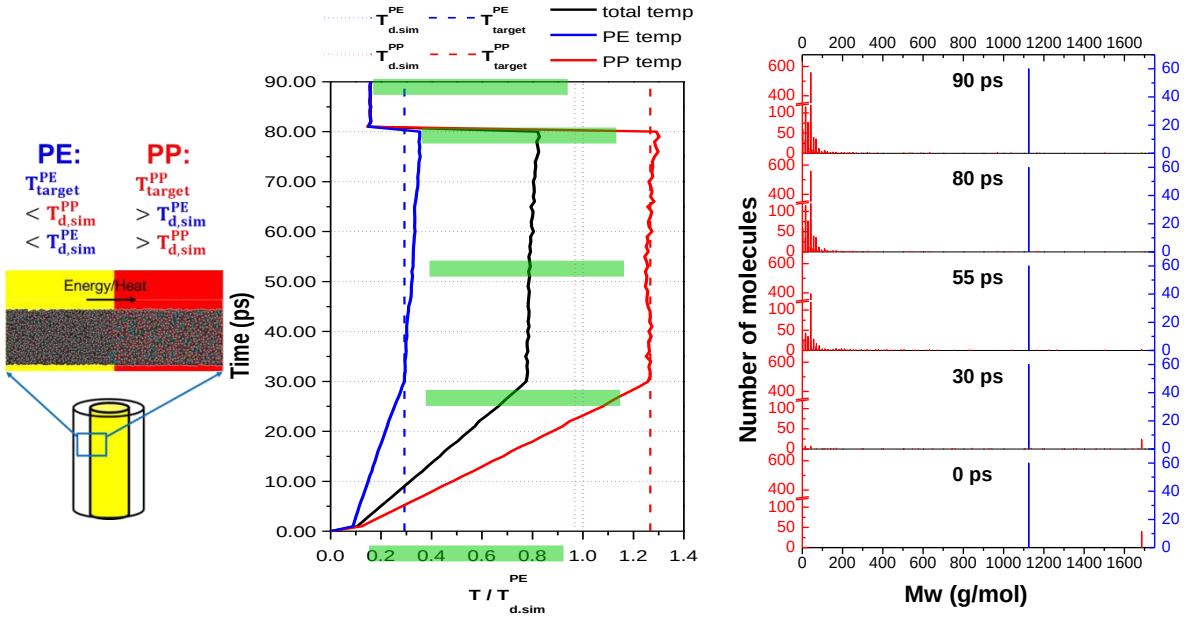

(a) (b) (c)

Figure 5- 9: Same as Figure 5- 8, but for PE/PP bicomponent systems under the conditions that $T_{target}^{PP} > T_{d,sim}^{PE} > T_{d,sim}^{PP}$ and $T_{target}^{PE} < T_{d,sim}^{PP} < T_{d,sim}^{PE}$.

For the third scenario, as indicated in Figures 5-10(a) and (b), we investigated what will happen if the temperature of PP is heated beyond $T_{d,sim}$ for both PP and PE, and also heating PE close to its degradation temperature; in other words, $T_{target}^{PP} > T_{d,sim}^{PE} > T_{d,sim}^{PP}$ and $T_{target}^{PE} \cong T_{d,sim}^{PP} < T_{d,sim}^{PE}$. From Figure 5-10(b), once the temperature of PE is heated to $T_{target}^{PE} \cong T_{d,sim}^{PE}$ and $T_{target}^{PP} > T_{d,sim}^{PP}$ (around 30 ps), as the system energy is maintained (constant total energy), the temperature of PE increases due to the energy transferred from the PP, thus its temperature becomes greater than $T_{d,sim}^{PE}$. As a consequence of that rise in temperature, the PE

chains are observed in Figure 5-10(c) to start to degrade at this stage (55 ps) in addition to the PP chains.

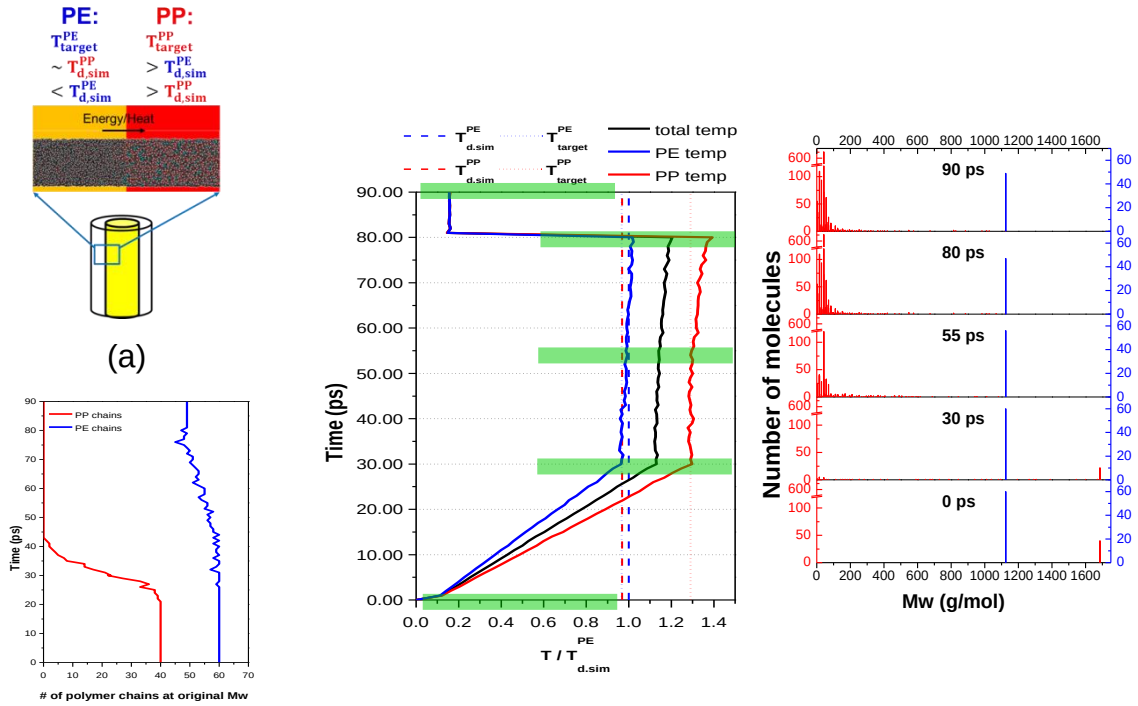

Figure 5- 10: Same as Figure 5- 8, but for PE/PP bicomponent systems under the conditions that $T_{target}^{PP} > T_{d,sim}^{PE} > T_{d,sim}^{PP}$ and $T_{target}^{PE} \cong T_{d,sim}^{PP} < T_{d,sim}^{PE}$. Also included in (d) is a graph of the number of polymer chains left at the original Mw as a function of time for both PP and PE.

The elastic modulus was also predicted of each of these systems after the degradation simulations by appling a constant strain and calculating its correponding stress, and the results are given in Figure 5-11. The simulated modulus of the original undegraded system is 14.4 GPa. For the first scenario where $T_{target}^{PP} \cong T_{d,sim}^{PP} < T_{d,sim}^{PE}$ and $T_{target}^{PE} < T_{d,sim}^{PP} < T_{d,sim}^{PE}$, the modulus drops by 10%. For the

second scenario where $T_{target}^{PP} > T_{d,sim}^{PE} > T_{d,sim}^{PP}$ and $T_{target}^{PE} < T_{d,sim}^{PP} < T_{d,sim}^{PE}$, all of the PP chains are ruptured thus there are a lot of fragments but the PE chains are all still intact, and the modulus drops by 28%. For the third scenario when both the temperature of PP and PE are high, in other words, $T_{target}^{PP} > T_{d,sim}^{PE} > T_{d,sim}^{PP}$ and $T_{target}^{PE} \cong T_{d,sim}^{PP} < T_{d,sim}^{PE}$, the modulus drops by 37%. The results suggest that the amount of chains within the system with high Mw can yield a higher modulus of bicomponent systems.

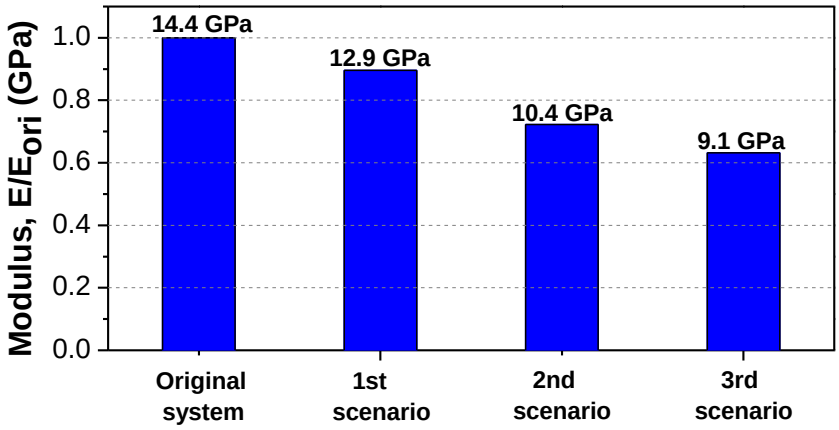

Figure 5- 11: Modulus of degraded systems from simulations, E_{ori} is the modulus of original system.

5.4. Conclusions

Two sets of core-sheath fibers were made using the trico spinning machine. The sheath material was chosen as PE to provide a soft hand and lower thermal bonding energy, and the core material was chosen as PP to provide better mechanical properties. One set of fibers were extruded with fixed extrusion temperature of PE as 190 °C and the extrusion temperature of PP was systematically increased from 200-310 °C. The PP pellets were chosen from commercial pellets with suitable stabilization packaging, which can be operated at extrusion temperatures lower than 300 °C. Therefore, the molecular weight of PP

gradually decreased as extrusion temperature increased and dropped significantly when the extrusion temperature was higher than 280 °C. The shear viscosities of the core-sheath fibers decreased as expected. The mechanical properties such as elongation increased due to less order of molecular orientation and the tensile strength decreased due to lower molecular weight.

Another set of core-sheath fibers were made with a fixed extrusion temperature of PP of 280 °C to study the effects of high contact temperature to PE at the spin pack. The extrusion temperature of PE ranged from 200 to 270 °C. The shear viscosity and mechanical properties such as elongation and tensile strength remained similar, which indicates that the properties of fibers are less sensitive to the extrusion temperature of PE.

During the tensile tests, there are dips that appear in the stress-strain curves at times and occur more at higher extrusion temperatures. SEM images revealed changes of the surface morphology for the core-sheath fibers; the stripes along the strain direction appear as the strain passes yield point and ridges perpendicular to the strain direction appear at higher strain and remain until the fiber breaks. The SEM images of broken tips indicate that the PP core breaks only a little earlier than PE sheath, and that the PE sheath extends a little bit to warp the PP core. Searching along the fiber, many defects were observed and there are big defects at the PE surface that might cause the dips along the tensile test.

The energy transfer between the interfaces of core-sheath fiber has been investigated at the molecular level with MD simulations. Each polymer component was heated to their own target temperatures and the temperature changes and degradation profile are observed as the heat energy is transferred across the interface. The energy transferred from the PP with high temperatures will increase the bulk temperature of PE. However, the energy transfer will only accelerate the chain scissions of PE when it is closer to its degradation temperature.

Chapter 6: Summary and future outlook

The goal of this work was to perform a comprehensive, systematic investigation using both simulations and experiments of the factors that trigger thermal degradation of PE and PP fibers, as well as PP/PE core-sheath bicomponent fibers. This work is significant because it provides guidance on how the process conditions can be manipulated to reduce thermal degradation during processing and thus yield reliable products. The differences of polymer materials and the local chemical environments were also investigated to understand their correlation and effects on thermal degradation. Molecular dynamics (MD) simulations are an excellent tool to complement the experiments for investigating thermal degradation because they can produce molecular-level details as a function of simulation time such as the onset degradation temperature (T_{onset}) and reaction mechanisms and products, as well as predict the effects of thermal degradation on the elastic modulus of the system. The MD simulations can also be used to separate out various factors that affect thermal degradation, such as the temperature, or the presence of double bonds, oxygen, or additives such as stabilizers.

The results for PE indicate that the degradation behavior depends on its conditions. From the MD simulations, T_{onset} of systems containing oxygen were predicted to decrease by 39% relative to the pure PE system. By analyzing the fragments that were produced, systems containing oxygen can produce CHO or H_2O, indicating that a chemical reaction between PE and oxygen radicals occurred. The modulus loss of the degraded systems was predicted from the MD simulations to be tremendous because of the severe degradation.

For PP, commercial PP pellets and minimally stabilized PP flakes were compared in the experiments. We determined that the commercial PP pellets can limit thermal degradation to acceptable levels up to 280 °C, but degraded unacceptably at higher temperatures. When noticeable degradation occurred, the

molecular weight (Mw) and shear viscosity dropped an accordingly significant amount. For minimally stabilized PP flakes, thermal degradation happened gradually and its related Mw and shear viscosity decreased gradually. The tensile strength of both PP materials decreased linearly, which is the same trend as their Mw. The simulation results indicate that there is a critical temperature called onset degradation temperature $T_{d,sim}$ for each polymer material. The breakings of polymer chains are not obvious at temperature lower than $T_{d,sim}$, and the chain breakings became significant once beyond the $T_{d,sim}$ and faster as temperature increases. This observation also validated the experimental results that PP has a high threshold where the thermal degradation can be limited. Therefore, adding stabilizer is crucial for PP because it limits thermal degradation during processing.

A detailed investigation of the role of a phenolic versus non-phenolic stabilizers was also performed. Samples were created where each type of stabilizer was added to the minimally stabilized PP flakes at both 0.2 wt% and 0.4 wt% loading. As indicated by changes in Mw, shear viscosity and crossover modulus, adding phenolic stabilizer at both 0.2 wt% and 0.4 wt% can limit thermal degradation up to 300 °C and 340 °C, respectively. The elongation values of phenolic stabilized PP were higher at lower extrusion temperatures and the tensile strength values of such were better as compared to minimally stabilized PP. However, the properties of adding nonphenolic stabilizers did not change. To investigate the molecular level interaction during stabilization, several molecular models were built that contain PP chains, oxygen radicals and stabilizers, and MD simulations were performed to investigate the effects of heating. Analysis of the MD simulation trajectory illustrated how the stabilizers in the system prevent the oxygen radicals from attacking the polymer chains during heating. At high temperatures, stabilizers can capture the oxygen radicals before they attack the polymer chains, and thus prevent the chains from breaking. However, degradation in terms of chain scissions occurred at very early stages of heating at higher temperature, especially temperatures higher than T_{onset}.

For PP/PE core-sheath fibers, it is critical to choose an appropriate temperature for each material; not only should the thermal degradation temperature of each material be considered, but also the temperature effects to the adjacent materials since heat energy is likely to transfer across interfaces. Thus, core-sheath fibers were extruded, with PE as sheath and PP as core, to investigate their thermal degradation behavior as a function of extrusion temperatures of each phase. The Mw and shear viscosity results indicated that PP degraded at temperatures higher than 300 °C; it was not obvious from the experiments whether PE degraded when temperatures were high. During tensile testing, kinks were observed in the stress-strain curve when either PE or PP was extruded at higher temperatures. We suspect that the dips arise from defects within the PE sheath when it was unable to share the load. Since the chemical nature of PP and PE are so similar, it is challenging to distinguish experimentally the degradation profile of each phase at the interface in bicomponent fibers, but MD simulations can make this distinction. From the MD simulations of the degradation of bicomponent PP/PE systems, more chains scissions occurred when the T_{target} of PE was close to T_{onset} and the T_{target} of PP was higher than T_{onset}. In other words, the simulation results indicate that the energy transferred from the PP to PE phase, resulting in the PE portion being heated up and thus accelerating the thermal degradation of that phase.

For future work, studying different combinations of core-sheath fiber would be beneficial. Several combinations of core-sheath fibers and different cross-section designs have been tried to meet the specific needs of industry. However, there are limited studies conducted especially to understand thermal degradation. The proper extrusion temperatures of commonly used industrial polymer materials are sometimes distinct. Therefore, there might be some areas where one polymer will be in contact with the other polymer at a temperature higher than its onset degradation temperature during bicomponent and tricomponent extrusion, which might cause severe thermal degradation at interfaces and result in deteriorated properties in the

finished products. By understanding the changes during fiber formation and their corresponding properties, it is possible to find suitable operational windows.

MD simulations with a ReaxFF force field have been validated to be able to study both the chemical reaction and physical changes during the thermal degradation. By manipulating the processing parameter individually, it is possible to find out the bottleneck parameters that cause the deteriorated properties and failure. From here, it will be more efficient for troubleshooting and improving the process capability of bicomponent fibers. Furthermore, ReaxFF is a convincing method to study the interaction with polymer systems such as the polymer interactions in an acid or base solution and the controlled degradation via peroxide cracking. Complex systems such as bicomponent fibers or the addition of small molecules such as additives or impurities can also be simulated.

REFERENCES

[1] Al-Malaika, S. Oxidative Degradation and Stabilisation of Polymers. Int. Mater. Rev. 2003, 48, 165-185.

[2] Fayolle, B.; Colin, X.; Audouin, L.; Verdu, J. Mechanism of Degradation Induced Embrittlement in Polyethylene. Polym. Degrad. Stab. 2007, 92, 231-238.

[3] Gómez-Elvira, J.M.; Tiemblo, P.; Elvira, M.; Matisova-Rychla, L.; Rychly, J. Relaxations and Thermal Stability of Low Molecular Weight Predominantly Isotactic Metallocene and Ziegler–Natta Polypropylene. Polym. Degrad. Stab. 2004, 85, 873-882.

[4] Peterson, J.; Vyazovkin, S.; Wight, C. Kinetics of the Thermal and Thermo-Oxidative Degradation of Polystyrene, Polyethylene and Poly(Propylene). Macromol. Chem. Phys. 2001, 202, 775-784.

[5] Gibert, J.; Cuesta, J.; Bergeret, A.; Crespy, A. Study of the Degradation of Fire-Retarded PP/PE Copolymers using DTA/TGA Coupled with FTIR. Polym. Degrad. Stab. 2000, 67, 437-447.

[6] Hoang, E.M.; Allen, N.S.; Liauw, C.M.; Fontan, E.; Lafuente, P. The Thermo-Oxidative Degradation of Metallocene Polyethylenes: Part 2: Thermal Oxidation in the Melt State. Polym. Degrad. Stab. 2006, 91, 1363-1372.

[7] Foster, G.; Wasserman, S.; Yacka, D. Oxidation Behavior and Stabilization of Metallocene and Other Polyolefins. Angew. Makromol. Chem. 1997, 252, 11-32.

[8] Beyler, L.,Craig; Hirschler, M.,Marcelo. Thermal decomposition of polymers. In SFPE Handbook of Fire Protection Engineering, third ed.; Beyler, L.,Craig, Ed., 2001, pp. 1–110.

[9] Qian, S.; Igarashi, T.; Nitta, K. Thermal Degradation Behavior of Polypropylene in the Melt State: Molecular Weight Distribution Changes and Chain Scission Mechanism. Polymer Bulletin 2011, 67, 1661-1670.

[10] Accelrys Software Inc. Discovery Studio Modeling Environment, Release 4.0, San Diego. 2013.

[11] Yingling, Y.; Garrison, B. Coarse-Grained Model of the Interaction of Light with Polymeric Material: Onset of Ablation. J Phys Chem B 2005, 109, 16482-16489.

[12] van Duin, A.; Zybin, S.; Chenoweth, K.; Han, S.; Goddard, W.A. Reactive Force Fields Based on Quantum Mechanics for Applications to Materials at Extreme Conditions. Advances in Computational Methods in Sciences and Engineering 2005, Vols 4 A & 4 B 2005, 4A-4B, 1109-1113.

[13] Compton, O.C.; Cranford, S.W.; Putz, K.W.; An, Z.; Brinson, L.C.; Buehler, M.J.; Nguyen, S.T. Tuning the Mechanical Properties of Graphene Oxide Paper and its Associated Polymer Nanocomposites by Controlling Cooperative Intersheet Hydrogen Bonding. ACS Nano 2012, 6, 2008-2019.

[14] Huang, C.; Tzoganakis, C.; Duever, T. Monte-Carlo Simulation of Peroxide Initiated Degradation of Polypropylene. Polymer Reaction Engineering 1995, 3, 43-63.

[15] Prasad, M.; Conforti, P.F.; Garrison, B.J. Coupled Molecular Dynamics-Monte Carlo Model to Study the Role of Chemical Processes during Laser Ablation of Polymeric Materials. J. Chem. Phys. 2007, 127, 084705.

[16] Handbook of Technical Textiles.; CRC Press; Woodhead Pub. Ltd., in association with The Textile Institute: Boca Raton Fla.]; Cambridge, England, 2000.

[17] Progress in Polymer Degradation and Stability Research.; Nova Science Publishers: New York, 2008.

[18] Fourné, F. Synthetic Fibers : Machines and Equipment, Manufacture, Properties: Handbook for Plant Engineering, Machine Design, and Operation.; Hanser/Gardner Publications: Cincinnati, OH, 1999.

[19] Norman S. Allen. Degradation and Stabilisation of Polyolefins.; Applied Science Publishers; Sole distributors in the USA and Canada, Elsevier Science Pub. Co: London ; New York; New York, NY, USA, 1983.

[20] Carlsson, D.J.; Garton, A.; Wiles, D.M. Weatherability of Polypropylene Monofilaments - Effects of Fiber Production Conditions. J Appl Polym Sci 1977, 21, 2963-2978.

[21] White, J.; Turnbull, A. Weathering of Polymers - Mechanisms of Degradation and Stabilization, Testing Strategies and Modeling. J. Mater. Sci. 1994, 29, 584-613.

[22] Fayolle, B.; Audouin, L.; Verdu, J. Oxidation Induced Embrittlement in Polypropylene - a Tensile Testing Study. Polym. Degrad. Stab. 2000, 70, 333-340.

[23] Gijsman, P.; Hennekens, J.; Vincent, J. The Mechanism of the Low-Temperature Oxidation of Polypropylene. Polym. Degrad. Stab. 1993, 42, 95-105.

[24] Al-Malaika, S. Perspectives in Stabilisation of Polyolefins. Long-Term Properties of Polyolefins 2004, 169, 121-150.

[25] Kiran, E.; Gillham, J. Pyrolysis Molecular Weight Chromatography - New Online System for Analysis of Polymers .2. Thermal-Decomposition of Polyolefins - Polyethylene, Polypropylene, Polyisobutylene. J Appl Polym Sci 1976, 20, 2045-2068.

[26] Robert T. Johnston, Evelyn J. Morrison. Thermal Scission and Cross-linking during polyethylene melt processing. In Polymer Durability : Degradation, Stabilization, and Lifetime Prediction.; Roger L. Clough, editor, Norman C. Billingham, editor, Kenneth T. Gillen,editor., American Chemical Society. Division of

Polymer Chemistry., Billingham, N.C. and Gillen, K.T., Eds.; American Chemical Society: Washington, DC, 1996, pp. 651.

[27] Setnescu, R.; Jipa, S.; Osawa, Z. Chemiluminescence Study on the Oxidation of several polyolefins—I. Thermal-Induced Degradation of Additive-Free Polyolefins. Polym. Degrad. Stab. 1998, 60, 377-383.

[28] Audouinjirackova, L.; Verdu, J. Chemiluminescence of Hydrocarbon Polymers. J. Polym. Sci. Pol. Chem. 1987, 25, 1205-1217.

[29] Gugumus, F. Thermooxidative Degradation of Polyolefins in the Solid State: Part 5. Kinetics of Functional Group Formation in PE-HD and PE-LLD. Polym. Degrad. Stab. 1997, 55, 21-43.

[30] Paabo, M.; Levin, B. A Literature-Review of the Chemical Nature and Toxicity of the Decomposition Products of Polyethylenes. Fire Mater. 1987, 11, 55-70.

[31] Bockhorn, H.; Hornung, A.; Hornung, U.; Schwaller, D. Kinetic Study on the Thermal Degradation of Polypropylene and Polyethylene. J. Anal. Appl. Pyrolysis 1999, 48, 93-109.

[32] Lattimer, R. Direct Analysis of Polypropylene Compounds by Thermal-Desorption and Pyrolysis Mass-Spectrometry. J. Anal. Appl. Pyrolysis 1993, 26, 65-92.

[33] Fayolle, B.; Audouin, L.; Verdu, J. A Critical Molar Mass Separating the Ductile and Brittle Regimes as Revealed by Thermal Oxidation in Polypropylene. Polymer 2004, 45, 4323-4330.

[34] Wong, A.; Lam, F. Study of Selected Thermal Characteristics of polypropylene/polyethylene Binary Blends using DSC and TGA. Polym. Test. 2002, 21, 691-696.

[35] Bains, M.; Balke, S.; Reck, D.; Horn, J. The Compatibility of Linear Law Density Polyethylene-Polypropylene Blends - Viscosity Ratio Plots. Polym. Eng. Sci. 1994, 34, 1260-1268.

[36] Rychlý, J.; Matisová-Rychlá, L.; Tiemblo, P.; Gomez-Elvira, J. The Effect of Physical Parameters of Isotactic Polypropylene on its Oxidisability Measured by Chemiluminescence Method. Contribution to the Spreading Phenomenon. Polym. Degrad. Stab. 2001, 71, 253-260.

[37] Ujheyliova, A.; Michlik, P.; Ryba, J.; Brejka, O.; Strecka, Z. Comparison of Structure and Properties of Fibres Prepared from Metallocene and Ziegler-Natta Pp, 2008; pp. 178.

[38] Hatanaka, T.; Mori, H.; Terano, M. Study of Thermo-Oxidative Degradation of Molten State Polypropylenes with a Variety of Tacticities. Polym. Degrad. Stab. 1999, 64, 313-319.

[39] Nakatani, H.; Suzuki, S.; Tanaka, T.; Terano, M. New Kinetic Aspects on the Mechanism of Thermal Oxidative Degradation of Polypropylenes with various Tacticities. Polymer 2005, 46, 12366-12371.

[40] Yu, Y.; Pochiraju, K. Modeling Long-Term Degradation due to Moisture and Oxygen in Polymeric Matrix Composites. Mater. Sci. Eng. A-Struct. Mater. Prop. Microstruct. Process. 2008, 498, 162-165.

[41] Iring, M.; Tudos, F.; Fodor, Z.; Kelen, T. The Thermo-Oxidative Degradation of Polyolefines .10. Correlation between the Formation of Carboxyl Groups and Scission in the Oxidation of Polyethylene in the Melt Phase. Polym. Degrad. Stab. 1980, 2, 143-153.

[42] Holmstrom, A.; Sorvik, E. Thermal-Degradation of Polyethylene in a Nitrogen Atmosphere of Low Oxygen-Content .4. Structural-Changes Occurring in Different

Types of High-Density Polyethylene. Journal of Polymer Science Part C-Polymer Symposium 1976, 33-53.

[43] Holmstrom.A; Sorvik, E. Thermal-Degradation of Polyethylene in a Nitrogen Atmosphere of Low Oxygen-Content .3. Structural-Changes Occurring in Low-Density Polyethylene at Oxygen Contents Below 1.2 Percent. J Appl Polym Sci 1974, 18, 779-804.

[44] Holmstrom.A; Sorvik, E. Thermal-Degradation of Polyethylene in a Nitrogen Atmosphere of Low Oxygen-Content .3. Structural-Changes Occurring in Low-Density Polyethylene at Oxygen Contents Below 1.2 Percent. J Appl Polym Sci 1974, 18, 3153-3178.

[45] Rideal, G.; Padget, J. Thermal-Mechanical Degradation of High-Density Polyethylene. Journal of Polymer Science Part C-Polymer Symposium 1976, 1-15.

[46] Pinheiro, L.A.; Chinelatto, M.A.; Canevarolo, S.V. Evaluation of Philips and Ziegler–Natta High-Density Polyethylene Degradation during Processing in an Internal Mixer using the Chain Scission and Branching Distribution Function Analysis. Polym. Degrad. Stab. 2006, 91, 2324-2332.

[47] Barabas, K.; Iring, M.; Fodor, Z.; Balint, G.; Tudos, F. Stabilization of Lldpe - Interactions between Stabilizers of Different Types. Magy. Kem. Foly. 1989, 95, 248-256.

[48] Goldberg, V.; Zaikov, G. Kinetics of Mechanical Degradation in Melts Under Model Conditions and during Processing of Polymers - a Review. Polym. Degrad. Stab. 1987, 19, 221-250.

[49] Witt, D.; Hogan, J. Double-Bond Isomerization and Hydrogenation in Polyethylene with Soluble Nickel Catalysts. Journal of Polymer Science Part A-1-Polymer Chemistry 1970, 8, 2689-&.

[50] Moss, S.; Zweifel, H. Degradation and Stabilization of High-Density Polyethylene during Multiple Extrusions. Polym. Degrad. Stab. 1989, 25, 217-245.

[51] Cran, M.J.; Fearon, P.K.; Billingham, N.C.; Bigger, S.W. Application of Chemiluminescence to Probe Miscibility in Metallocene-Catalyzed Polyethylene Blends. J Appl Polym Sci 2003, 89, 3006-3015.

[52] Allen, N.S.; Edge, M.; Holdsworth, D.; Rahman, A.; Catalina, F.; Fontan, E.; Escalona, A.M.; Sibon, F.F. Ageing and Spectroscopic Properties of Polyethylenes: Comparison with Metallocene Polymer. Polym. Degrad. Stab. 2000, 67, 57-67.

[53] Moghaddam, L.; Blinco, J.P.; Colwell, J.M.; Halley, P.J.; Bottle, S.E.; Fredericks, P.M.; George, G.A. Investigation of Polypropylene Degradation during Melt Processing using a Profluorescent Nitroxide Probe: A Laboratory-Scale Study. Polym. Degrad. Stab. 2011, 96, 455-461.

[54] Hinsken, H.; Moss, S.; Pauquet, J.; Zweifel, H. Degradation of Polyolefins during Melt Processing. Polym. Degrad. Stab. 1991, 34, 279-293.

[55] Hilado, C.J., 1933-. Flammability Handbook for Plastics Electronic Resource].; Technomic Pub. Co: Lancaster, Pa., 1998.

[56] Cullis, C.F.; Hirschler, M.M. The Significance of Thermoanalytical Measurements in the Assessment of Polymer Flammability. Polymer 1983, 24, 834-840.

[57] Camacho, W.; Karlsson, S. Assessment of Thermal and Thermo-Oxidative Stability of Multi-Extruded Recycled PP, HDPE and a Blend Thereof. Polym. Degrad. Stab. 2002, 78, 385-391.

[58] Dintcheva, N.; La Mantia, F.; Scaffaro, R.; Paci, M.; Acierno, D.; Camino, G. Reprocessing and Restabilization of Greenhouse Films. Polym. Degrad. Stab. 2002, 75, 459-464.

[59] González-González, V.A.; Neira-Velázquez, G.; Angulo-Sánchez, J.L. Polypropylene Chain Scissions and Molecular Weight Changes in Multiple Extrusion. Polym. Degrad. Stab. 1998, 60, 33-42.

[60] Xiang, Q.; Xanthos, M.; Mitra, S.; Patel, S.; Guo, J. Effects of Melt Reprocessing on Volatile Emissions and structural/rheological Changes of Unstabilized Polypropylene. Polym. Degrad. Stab. 2002, 77, 93-102.

[61] Lehrle, R.; Williams, R.; French, C.; Hammond, T. Thermolysis and Methanolysis of Poly(Beta-Hydroxybutyrate) - Random Scission Assessed by Statistical-Analysis of Molecular-Weight Distributions. Macromolecules 1995, 28, 4408-4414.

[62] Yamane, H.; White, J. Extrusion and Melt Spinning Characteristics of Thermally Degraded Polypropylene. Polym. Eng. Sci. 1983, 23, 516-520.

[63] Pfaendner, R. How Will Additives Shape the Future of Plastics? Polym. Degrad. Stab. 2006, 91, 2249-2256.

[64] Reingruber, E.; Buchberger, W. Analysis of Polyolefin Stabilizers and their Degradation Products. J. Sep. Sci. 2010, 33, 3463-3475.

[65] Cramer, C.J., 1961-. Essentials of Computational Chemistry : Theories and Models.; J. Wiley: Chichester, West Sussex, England ; Hoboken, NJ, 2004.

[66] Steinhauser, M.O.; Hiermaier, S. A Review of Computational Methods in Materials Science: Examples from Shock-Wave and Polymer Physics. Int. J. Mol. Sci. 2009, 10, 5135-5216.

[67] Stewart, J. Optimization of Parameters for Semiempirical Methods .1. Method. Journal of Computational Chemistry 1989, 10, 209-220.

[68] Stewart, J. Optimization of Parameters for Semiempirical Methods .2. Applications. Journal of Computational Chemistry 1989, 10, 221-264.

[69] Ridley, J.; Zerner, M. Intermediate Neglect of Differential Overlap Technique for Spectroscopy - Pyrrole and Azines. Theor. Chim. Acta 1973, 32, 111-134.

[70] Entrialgo-Castano, M.; Salvucci, A.E.; Lendlein, A.; Hofmann, D. An Atomistic Modeling and Quantum Mechanical Approach to the Hydrolytic Degradation of Aliphatic Polyesters. Macromol. Symp. 2008, 269, 47-64.

[71] Endo, K.; Masumoto, C.; Matsumoto, D.; Ida, T.; Mizuno, M.; Kato, N. Fragment Distribution of Thermal Decomposition for PS and PET with QMD Calculations by Considering the Excited and Charged Model Molecules. Appl. Surf. Sci. 2008, 255, 856-859.

[72] Hatanaka, T.; Mori, H.; Terano, M. Semiempirical Calculation on the Oxidative Degradation of Polypropylene. Polym. Degrad. Stab. 1999, 65, 271-278.

[73] Bertin, D.; Leblanc, M.; Marque, S.R.A.; Siri, D. Polypropylene Degradation: Theoretical and Experimental Investigations. Polym. Degrad. Stab. 2010, 95, 782-791.

[74] Ramachandran, K.I. Computational Chemistry and Molecular Modeling : Principles and Applications.; Springer: Berlin, 2008.

[75] Farah, K.; Mueller-Plathe, F.; Boehm, M.C. Classical Reactive Molecular Dynamics Implementations: State of the Art. Chemphyschem 2012, 13, 1127-1151.

[76] Castner, E.; Galiatsatos, V. Computer Simulation of Polymer Network Formation by Radiation Cross-Linking. Irradiation of Polymers: Fundamentals and Technological Applications 1996, 620, 96-109.

[77] Brenner, D. Empirical Potential for Hydrocarbons for use in Simulating the Chemical Vapor-Deposition of Diamond Films. Phys. Rev. B 1990, 42, 9458-9471.

[78] Nyden, M.; Noid, D. Molecular-Dynamics of Initial Events in the Thermal-Degradation of Polymers. J. Phys. Chem. 1991, 95, 940-945.

[79] Yu, J.; Sinnott, S.B.; Phillpot, S.R. Optimized Many Body Potential for Fcc Metals. Philos. Mag. Lett. 2009, 89, 136-144.

[80] Brooks, B.; Bruccoleri, R.; Olafson, B.; States, D.; Swaminathan, S.; Karplus, M. Charmm - a Program for Macromolecular Energy, Minimization, and Dynamics Calculations. J. Comput. Chem. 1983, 4, 187-217.

[81] Kaminski, G.; Friesner, R.; Tirado-Rives, J.; Jorgensen, W. Evaluation and Reparametrization of the OPLS-AA Force Field for Proteins Via Comparison with Accurate Quantum Chemical Calculations on Peptides. J Phys Chem B 2001, 105, 6474-6487.

[82] Lifson, S.; Hagler, A.; Dauber, P. Consistent Force-Field Studies of Inter-Molecular Forces in Hydrogen-Bonded Crystals .1. Carboxylic-Acids, Amides, and the C=o...H- Hydrogen-Bonds. J. Am. Chem. Soc. 1979, 101, 5111-5121.

[83] Abell, G. Empirical Chemical Pseudopotential Theory of Molecular and Metallic Bonding. Phys. Rev. B 1985, 31, 6184-6196.

[84] Tersoff, J. New Empirical-Model for the Structural-Properties of Silicon. Phys. Rev. Lett. 1986, 56, 632-635.

[85] Robertson, D.; Brenner, D.; White, C. Temperature-Dependent Fusion of Colliding C-60 Fullerenes from Molecular-Dynamics Simulations. J. Phys. Chem. 1995, 99, 15721-15724.

[86] Brenner, D.; Shenderova, O.; Harrison, J.; Stuart, S.; Ni, B.; Sinnott, S. A Second-Generation Reactive Empirical Bond Order (REBO) Potential Energy Expression for Hydrocarbons. J. Phys. -Condes. Matter 2002, 14, 783-802.

[87] Ni, B.; Lee, K.; Sinnott, S. A Reactive Empirical Bond Order (REBO) Potential for Hydrocarbon-Oxygen Interactions. J. Phys. -Condes. Matter 2004, 16, 7261-7275.

[88] Stuart, S.J.; Tutein, A.B.; Harrison, J.A. A Reactive Potential for Hydrocarbons with Intermolecular Interactions. J. Chem. Phys. 2000, 112, 6472-6486.

[89] Su, Y.; Shan, T.; Sinnott, S.B. Modification of Poly(Methyl Methacrylate) by keV Ar Deposition. Nucl. Instrum. Methods Phys. Res. Sect. B-Beam Interact. Mater. Atoms 2009, 267, 2525-2531.

[90] Delcorte, A.; Arezki, B.; Bertrand, P.; Garrison, B. Sputtering Kilodalton Fragments from Polymers. Nucl. Instrum. Methods Phys. Res. Sect. B-Beam Interact. Mater. Atoms 2002, 193, 768-774.

[91] Delcorte, A.; Bertrand, P.; Garrison, B. Collision Cascade and Sputtering Process in a Polymer. J Phys Chem B 2001, 105, 9474-9486.

[92] Elert, M.; Zybin, S.; White, C. Molecular Dynamics Modeling of Impact-Induced Shock Waves in Hydrocarbons. Shock Compression of Condensed Matter-2001, Pts 1 and 2, Proceedings 2002, 620, 1406-1409.

[93] Mattsson, T.R.; Lane, J.M.D.; Cochrane, K.R.; Desjarlais, M.P.; Thompson, A.P.; Pierce, F.; Grest, G.S. First-Principles and Classical Molecular Dynamics Simulation of Shocked Polymers. Physical Review B 2010, 81, 054103.

[94] Joseph J Végh and David,B.Graves. A Molecular Dynamics Study of H Radical Bombardment of CH 3 : Si(1 0 0)— Comparison of Simulation and Experiment. J. Phys. D 2009, 42, 222001.

[95] Polvi, J.; Nordlund, K. Irradiation Effects in High-Density Polyethylene. Nuclear Instruments and Methods in Physics Research Section B: Beam Interactions with Materials and Atoms 2013, 312, 54-59.

[96] Polvi, J.; Luukkonen, P.; Nordlund, K.; Jarvi, T.T.; Kemper, T.W.; Sinnott, S.B. Primary Radiation Defect Production in Polyethylene and Cellulose. J Phys Chem B 2012, 116, 13932-13938.

[97] Chenoweth, K.; Cheung, S.; van Duin, A.C.T.; Goddard, W.A.; Kober, E.M. Simulations on the Thermal Decomposition of a Poly(Dimethylsiloxane) Polymer using the ReaxFF Reactive Force Field. J. Am. Chem. Soc. 2005, 127, 7192-7202.

[98] Chenoweth, K.; van Duin, A.C.T.; Goddard,William A.,,III. ReaxFF Reactive Force Field for Molecular Dynamics Simulations of Hydrocarbon Oxidation. J Phys Chem A 2008, 112, 1040-1053.

[99] van Duin, A.C.T.; Zybin, S.V.; Chenoweth, K.; Zhang, L.; Han, S.; Strachan, A.; Goddard,William A.,,III. Reactive Force Fields Based on Quantum Mechanics for Applications to Materials at Extreme Conditions. Shock Compression of Condensed Matter - 2005, Pts 1 and 2 2006, 845, 581-584.

[100] Desai, T.G.; Lawson, J.W.; Keblinski, P. Modeling Initial Stage of Phenolic Pyrolysis: Graphitic Precursor Formation and Interfacial Effects. Polymer 2011, 52, 577-585.

[101] Qi, T.; Bauschlicher, C.W., Jr.; Lawson, J.W.; Desai, T.G.; Reed, E.J. Comparison of ReaxFF, DFTB, and DFT for Phenolic Pyrolysis. 1. Molecular Dynamics Simulations. Journal of Physical Chemistry a 2013, 117, 11115-11125.

[102] Papkov, D.; Beese, A.M.; Goponenko, A.; Zou, Y.; Naraghi, M.; Espinosa, H.D.; Saha, B.; Schatz, G.C.; Moravsky, A.; Loutfy, R. et al. Extraordinary Improvement of

the Graphitic Structure of Continuous Carbon Nanofibers Templated with Double Wall Carbon Nanotubes. Acs Nano 2013, 7, 126-142.

[103] Lane, J.M.D.; Grest, G.S.; Thompson, A.P.; Cochrane, K.R.; Desjarlais, M.P.; Mattsson, T.R. Shock Compression of Hydrocarbon Polymer Foam using Molecular Dynamics. Shock Compression of Condensed Matter - 2011, Pts 1 and 2 2012, 1426.

[104] Lane, J.M.D.; Grest, G.S.; Mattsson, T.R. Hot Spot and Temperature Analysis of Shocked Hydrocarbon Polymer Foams using Molecular Dynamics Simulation. Computational Materials Science 2013, 79, 873-876.

[105] An, Q.; Zybin, S.V.; Goddard,William A.,,III; Jaramillo-Botero, A.; Blanco, M.; Luo, S. Elucidation of the Dynamics for Hot-Spot Initiation at Nonuniform Interfaces of Highly Shocked Materials. Physical Review B 2011, 84, 220101.

[106] Medhekar, N.V.; Ramasubramaniam, A.; Ruoff, R.S.; Shenoy, V.B. Hydrogen Bond Networks in Graphene Oxide Composite Paper: Structure and Mechanical Properties. ACS Nano 2010, 4, 2300-2306.

[107] Marx, D. Ab Initio Molecular Dynamics : Basic Theory and Advanced Methods.; Cambridge University Press: Cambridge ;New York, 2009.

[108] Car, R.; Parrinello, M. Unified Approach for Molecular-Dynamics and Density-Functional Theory. Phys. Rev. Lett. 1985, 55, 2471-2474.

[109] Agarwal, V.; Dauenhauer, P.J.; Huber, G.W.; Auerbach, S.M. Ab Initio Dynamics of Cellulose Pyrolysis: Nascent Decomposition Pathways at 327 and 600 Degrees C. J. Am. Chem. Soc. 2012, 134, 14958-14972.

[110] Hosoya, T.; Nakao, Y.; Sato, H.; Kawamoto, H.; Sakaki, S. Thermal Degradation of Methyl Beta-D-Glucoside. A Theoretical Study of Plausible Reaction Mechanisms. J. Org. Chem. 2009, 74, 6891-6894.

[111] Zhang, M.; Geng, Z.; Yu, Y. Density Functional Theory (DFT) Study on the Dehydration of Cellulose. Energy Fuels 2011, 25, 2664-2670.

[112] Lin, Y.; Cho, J.; Tompsett, G.A.; Westmoreland, P.R.; Huber, G.W. Kinetics and Mechanism of Cellulose Pyrolysis. J. Phys. Chem. C 2009, 113, 20097-20107.

[113] Liu, D.; Nimlos, M.R.; Johnson, D.K.; Himmel, M.E.; Qian, X. Free Energy Landscape for Glucose Condensation Reactions. J Phys Chem A 2010, 114, 12936-12944.

[114] Tuzun, R.E.; Noid, D.W.; Sumpter, B.G. Molecular Dynamics Treatment of Torsional Interactions Accompanied by Dissociation. Macromolecular Theory and Simulations 1995, 4, 909-920.

[115] Nyden, M.; Gilman, J. Molecular Dynamics Simulations of the Thermal Degradation of Nano-Confined Polypropylene. Comput. Theor. Polym. Sci. 1997, 7, 191-198.

[116] Blaistenbarojas, E.; Nyden, M. Molecular-Dynamics Study of the Depolymerization Reaction in Simple Polymers. Chem. Phys. Lett. 1990, 171, 499-505.

[117] Nyden, M.; Stoliarov, S.; Westmoreland, P.; Guo, Z.; Jee, C. Applications of Reactive Molecular Dynamics to the Study of the Thermal Decomposition of Polymers and Nanoscale Structures. Materials Science and Engineering A-Structural Materials Properties Microstructure and Processing 2004, 365, 114-121.

[118] Stoliarov, S.; Westmoreland, P.; Nyden, M.; Forney, G. A Reactive Molecular Dynamics Model of Thermal Decomposition in Polymers: 1. Poly(Methyl Methacrylate). Polymer 2003, 44, 883-894.

[119] Stoliarov, S.; Lyon, R.; Nyden, M. A Reactive Molecular Dynamics Model of Thermal Decomposition in Polymers. II. Polyisobutylene. Polymer 2004, 45, 8613-8621.

[120] Jee, C.S.Y.; Guo, Z.X.; Stoliarov, S.I.; Nyden, M.R. Experimental and Molecular Dynamics Studies of the Thermal Decomposition of a Polyisobutylene Binder. Acta Materialia 2006, 54, 4803-4813.

[121] Jiang, B.; Selvan, M.E.; Keffer, D.J.; Edwards, B.J. A Reactive Molecular Dynamics Study of the Thermal Decomposition of Perfluorodimethyl Ether. J Phys Chem B 2009, 113, 13670-13677.

[122] Charlesby, A.; Pinner, S. Analysis of the Solubility Behaviour of Irradiated Polyethylene and Other Polymers. Proceedings of the Royal Society of London Series A-Mathematical and Physical Sciences 1959, 249, 367-386.

[123] Paturej, J.; Milchev, A.; Rostiashvili, V.G.; Vilgis, T.A. Thermal Degradation of Unstrained Single Polymer Chain: Non-Linear Effects at Work. J. Chem. Phys. 2011, 134, 224901.

[124] Milchev, A.; Paturej, J.; Rostiashvili, V.G.; Vilgis, T.A. Thermal Degradation of Adsorbed Bottle-Brush Macromolecules: A Molecular Dynamics Simulation. Macromolecules 2011, 44, 3981-3987.

[125] Hamerton, I.; Howlin, B.J.; Yeung, S.C. Designing Thermoplastic Oligomers with Programmed Degradation Mechanisms using a Combined Empirical and Simulation Approach. Polym. Degrad. Stab. 2013, 98, 829-838.

[126] Emsley, A.; Heywood, R. Computer Modeling of the Degradation of Linear-Polymers. Polym. Degrad. Stab. 1995, 49, 145-149.

[127] Martl, M.; Saf, R.; Hummel, K. Monte-Carlo Calculation of a Partial Reaction in Radical Cross-Linking of 1,4-Polybutadiene. Makromolekulare Chemie-Macromolecular Symposia 1990, 40, 53-60.

[128] Tobita, H. Simulation-Model for the Modification of Polymers Via Cross-Linking and Degradation. Polymer 1995, 36, 2585-2596.

[129] GUAITA, M.; CHIANTORE, O.; LUDA, M. Monte-Carlo Simulations of Polymer Degradations .2. Degradations Involving Random Chain Scissions and Volatilization of Low-Molecular-Weight Products. Macromolecules 1991, 24, 2198-2202.

[130] Guaita, M.; Chiantore, O.; Luda, M. Monte-Carlo Simulations of Polymer Degradations .1. Degradations without Volatilization. Macromolecules 1990, 23, 2087-2092.

[131] Guaita, M.; Chiantore, O. Molecular Mass Changes in the Thermal-Degradation of Poly-Alpha-Methylstyrene. Polym. Degrad. Stab. 1985, 11, 167-179.

[132] Guaita, M.; Chiantore, O.; Costa, L. Changes in Degree of Polymerization in the Thermal-Degradation of Polystyrene. Polym. Degrad. Stab. 1985, 12, 315-332.

[133] Camino, G.; Luda, M.; Costa, L.; Guaita, M. Thermal Degradation of Ethyleneurea Formaldehyde Polycondensates. Macromol. Chem. Phys. 1996, 197, 41-60.

[134] Bose, S.; Git, Y. Mathematical Modelling and Computer Simulation of Linear Polymer Degradation: Simple Scissions. Macromol. Theory Simul. 2004, 13, 453-473.

[135] Staggs, J. Modelling Random Scission of Linear Polymers. Polym. Degrad. Stab. 2002, 76, 37-44.

[136] Staggs, J. Modelling End-Chain Scission and Recombination of Linear Polymers. Polym. Degrad. Stab. 2004, 85, 759-767.

[137] Staggs, J. Discrete Bond-Weighted Random Scission of Linear Polymers. Polymer 2006, 47, 897-906.

[138] Platkowski, K.; Reichert, K. Application of Monte Carlo Methods for Modelling of Polymerization Reactions. Polymer 1999, 40, 1057-1066.

[139] Galina, H.; Lechowicz, J. An Algorithm for Monte Carlo Modeling of Degradation of Polymer Networks. Comput. Chem. 1998, 22, 39-41.

[140] Galina, H.; Lechowicz, J. Monte-Carlo Modeling of Degradation of Polymer Networks. Polym. Gels Networks 1998, 6, 103-111.

[141] Galina, H.; Lechowicz, J. Monte Carlo Modeling of Degradation of Polymer Networks: 2. Highly Branched Molecules. Polym. Gels Networks 1998, 6, 247-255.

[142] Bystritskaya, E.V.; Karpukhin, O.N.; Kutsenova, A.V. Monte Carlo Simulation of Linear Polymer Thermal Depolymerization Under Isothermal and Dynamic Modes. Int. J. Polym. Sci. 2011, 849370.

[143] Conforti, P.F.; Prasad, M.; Garrison, B.J. Simulations of Laser Ablation of Poly(Methyl Methacrylate): Fluence Versus Number of Photons. Journal of Physical Chemistry C 2007, 111, 12024-12030.

[144] Conforti, P.F.; Prasad, M.; Garrison, B.J. On the Correlation between the Photoexcitation Pathways and the Critical Energies Required for Ablation of Poly(Methyl Methacrylate): A Molecular Dynamics Study. J. Appl. Phys. 2008, 103, 103114.

[145] Conforti, P.F.; Prasad, M.; Garrison, B.J. The Impact of Point Thermal Absorbers in Ablation of Poly(Methyl Methacrylate). Applied Physics A-Materials Science & Processing 2008, 92, 1037-1041.

[146] Conforti, P.F.; Prasad, M.; Garrison, B.J. A Molecular Dynamics Study of the Effects of the Inclusion of Dopants on Ablation in Polymethyl Methacrylate. Physical Chemistry Chemical Physics 2008, 10, 6002-6008.

[147] Conforti, P.F.; Prasad, M.; Garrison, B.J. Elucidating the Thermal, Chemical, and Mechanical Mechanisms of Ultraviolet Ablation in Poly(Methyl Methacrylate) Via Molecular Dynamics Simulations. Acc. Chem. Res. 2008, 41, 915-924.

[148] Prasad, M.; Conforti, P.F.; Garrison, B.J. Interplay between Chemical, Thermal, and Mechanical Processes Occurring upon Laser Excitation of Poly(Methyl Methacrylate) and its Role in Ablation. Journal of Physical Chemistry C 2009, 113, 11491-11506.

[149] Kim, W.; Hayden, L. Fully Atomistic Modeling of an Electric Field Poled Guest-Host Nonlinear Optical Polymer. J. Chem. Phys. 1999, 111, 5212-5222.

[150] Yingling, Y.G.; Zhigilei, L.V.; Garrison, B.J. Photochemical Fragmentation Processes in Laser Ablation of Organic Solids. Nuclear Instruments & Methods in Physics Research Section B-Beam Interactions with Materials and Atoms 2001, 180, 171-175.

[151] Beste, A. ReaxFF Study of the Oxidation of Lignin Model Compounds for the most Common Linkages in Softwood in View of Carbon Fiber Production. Journal of Physical Chemistry a 2014, 118, 803-814.

[152] Plimpton, S. Fast Parallel Algorithms for Short-Range Molecular-Dynamics. J. Comput. Phys. 1995, 117, 1-19.

[153] van Duin, A.; Dasgupta, S.; Lorant, F.; Goddard, W. ReaxFF: A Reactive Force Field for Hydrocarbons. J Phys Chem A 2001, 105, 9396-9409.

[154] Http://ncsu.edu/hpc/.

[155] Humphrey, W.; Dalke, A.; Schulten, K. VMD: Visual Molecular Dynamics. Journal of Molecular Graphics & Modelling 1996, 14, 33-38.

[156] Rapoport, N.; Livanova, N.; Balogh, L.; Kelen, T. Simulation of the Durability and Approach to the Stabilization of Polyolefins Undergoing Oxidative-Degradation Under Mechanical-Stress. Int. J. Polym. Mater. 1993, 19, 101-108.

[157] Barnes, H.A.; Hutton, J.F.; Walters, K. an Introduction to Rheology, 1989.

[158] da Costa, H.M.; Ramos, V.D.; Rocha, M.C.G. Rheological Properties of Polypropylene during Multiple Extrusion. Polym. Test. 2005, 24, 86-93.

[159] Barakos, G.; Mitsoulis, E.; Tzoganakis, C.; Kajiwara, T. Rheological Characterization of Controlled-Rheology Polypropylenes using Integral Constitutive Equations. J Appl Polym Sci 1996, 59, 543-556.

[160] Fox, T.G.; Flory, P.J. 2nd-Order Transition Temperatures and Related Properties of Polystyrene .1. Influence of Molecular Weight. J. Appl. Phys. 1950, 21, 581-591.

[161] Fox, T.G.; Flory, P.J. Viscosity-Molecular Weight and Viscosity-Temperature Relationships for Polystyrene and Polyisobutylene. J. Am. Chem. Soc. 1948, 70, 2384-2395.

[162] Chenoweth, K.; Cheung, S.; van Duin, A.; Goddard, W.; Kober, E. Simulations on the Thermal Decomposition of a Poly(Dimethylsiloxane) Polymer using the ReaxFF Reactive Force Field. J. Am. Chem. Soc. 2005, 127, 7192-7202.

[163] Dasdemir, M.; Maze, B.; Anantharamaiah, N.; Pourdeyhimi, B. Influence of Polymer Type, Composition, and Interface on the Structural and Mechanical Properties of core/sheath Type Bicomponent Nonwoven Fibers. J. Mater. Sci. 2012, 47, 5955-5969.

[164] Wang, X.Y.; Gong, R.H. Thermally Bonded Nonwoven Filters Composed of Bi-Component polypropylene/polyester Fiber. II. Relationships between Fabric Area Density, Air Permeability, and Pore Size Distribution. J Appl Polym Sci 2006, 102, 2264-2275.

[165] Cho, H.H.; Kim, K.H.; Kang, Y.A.; Ito, H.; Kikutani, T. Fine Structure and Physical Properties of Poly(Ethylene Terephthalate)/polyethylene Bicomponent Fibers in High-Speed Spinning. II. Poly(Ethylene Terephthalate) sheath/polyethylene Core Fibers. J Appl Polym Sci 2000, 77, 2267-2277.

[166] Kikutani, T.; Radhakrishnan, J.; Arikawa, S.; Takaku, A.; Okui, N.; Jin, X.; Niwa, F.; Kudo, Y. High-Speed Melt Spinning of Bicomponent Fibers: Mechanism of Fiber Structure Development in Poly(Ethylene Terephthalate)/polypropylene System. J Appl Polym Sci 1996, 62, 1913-1924.

[167] Zhou, F.; Gong, R. Manufacturing Technologies of Polymeric Nanofibres and Nanofibre Yarns. Polym. Int. 2008, 57, 837-845.

[168] Rwei, S.P.; Lin, Y.T.; Su, Y.Y. Study of Self-Crimp Polyester Fibers. Polymer Engineering & Science 2005, 45, 838-845.

APPENDICES

Appendix A

The method to calculate the modulus from strain-stress curve obtained from MD simulations

To obtain the mechanical properties of polymer systems from MD simulation, a constant strain rate needed to be applied to a system. The strain rate for each system in this dissertation was set at 10^{-9} s^{-1}, which was chosen because for strain rates higher than that, an irregular spike in the stress response at low strains along with an increased temperature and additional broken bonds were observed. No or limited bond breakage are found during the formation. To reduce random and temperature-related stress fluctuations that result from applying strains at the atomistic level, the stress is averaged further over a small time interval of 0.125 ps around the desired time point of the stress calculation. The modulus is calculated from 1% strain of the 10^{-9} s^{-1} strain rate.

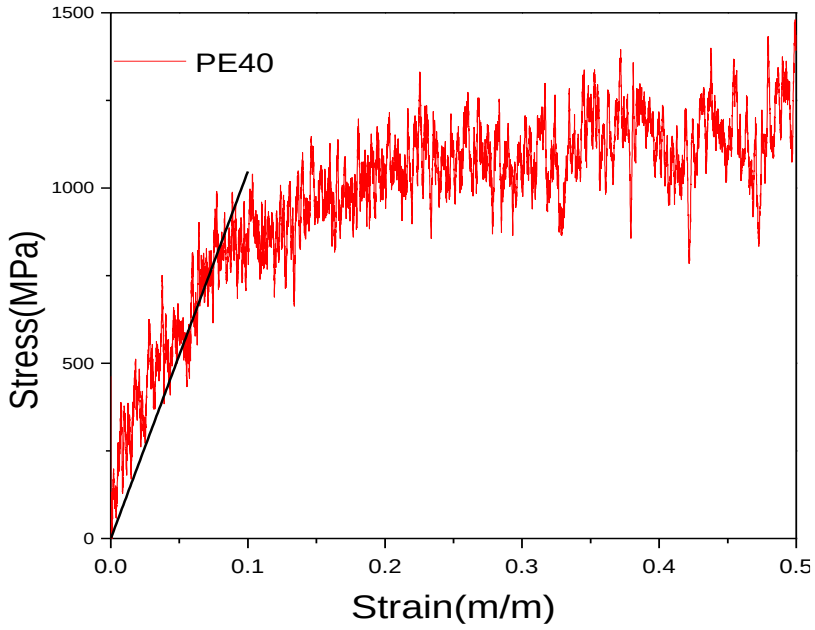

Figure A- 1: Strain-stress curve obtained from MD simulations.

Appendix B

The degradation behavior of polyethylene

Figure B-1 (a) is the shear viscosity data measured under constant temperature but increasing shear rate. It was noticeable that shear viscosities at 280 °C were higher than at 260 °C under same shear rates lower than 300 /s. Figure B-1 (b) and (c) is the shear viscosity changes measured under constant shear rate and temperature. At the fixed temperature of 200 °C and 230 °C, the shear viscosity of PE, ASPUN6850, remained relatively constant, indicating that there is no or limited degradation happening (*ie.* no or limited molecular weight changes) at both shear rates. However, the shear viscosity was slightly increased about 7% and 10% after 100 minutes at 260 °C and 280 °C, respectively, at a shear rate = 60/s. It is germane to note that the shear viscosity of ASPUN 6850 at 280 °C is higher than at 260 °C, indicating that at low shear rate, crosslinking happens during the pre-heating time. It appears that crosslinking continues as residence time increases since the shear viscosity slightly increases. Because of shear thinning at a higher shear rate of 300/s, the shear viscosity of 280 °C is lower than 260 °C. There is no obvious change of shear viscosity since the testing duration is limited to 20 minutes. However, as temperature went up to 340 °C, the decrease of shear viscosity indicates that the chain scissions start to dominate thermal degradation and cause loss of molecular weight.

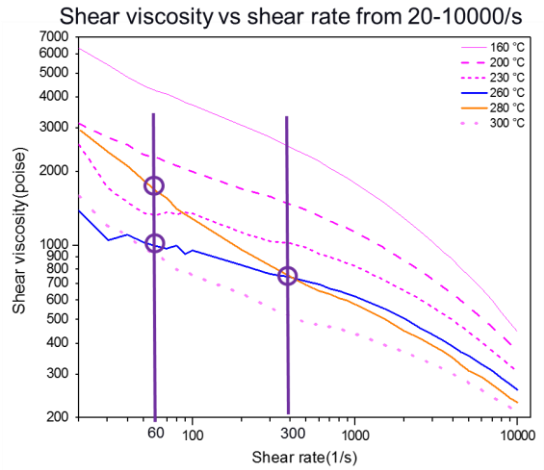

(a)

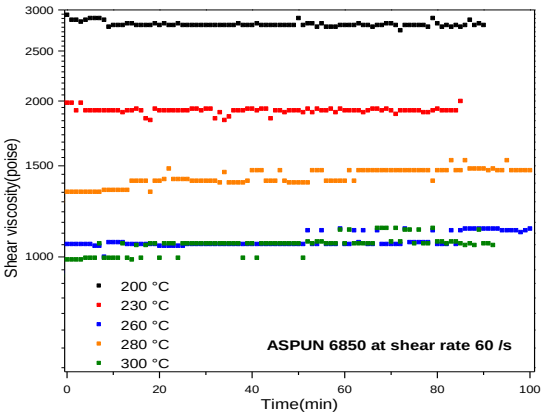

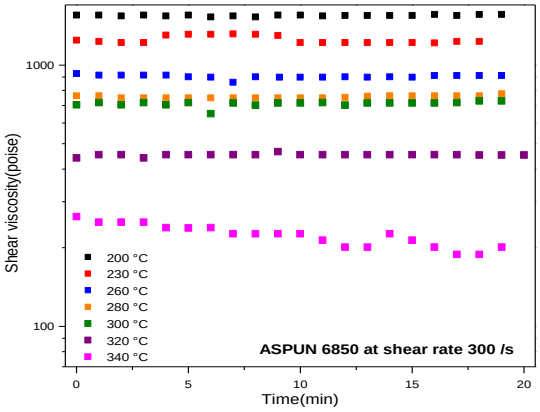

(b) (c)

Figure B- 1: (a) Shear viscosity measured from 20-10000 /s shear rate at constant temperatures, (b) degradation test at fixed shear rate for PE, ASPUN6850 at shear rate=60/s and (c) degradation test at fixed shear rate for PE, ASPUN6850 at shear rate=300/s.